Identification and Characterization of Signal Motifs that Regulate Surface Levels of Membrane Proteins

BY

JOSHUA DAVID BERNSTEIN
B.A., Yeshiva University, 2009

THESIS

Submitted as partial fulfillment of the requirements
for the degree of Doctor of Philosophy in Biochemistry and Molecular Genetics
in the Graduate College of the
University of Illinois at Chicago, 2017

Chicago, Illinois

Defense Committee:

Sojin Shikano, Chair and Advisor
Karen Colley
Jack Kaplan
Nava Segev
Constance Jeffery, Biological Sciences

Dedication

This thesis is dedicated to my lovely wife Sarah and to my children Olivia and Liam.

Acknowledgments

I would like to thank my thesis advisor, Dr. Sojin Shikano for mentoring me and allowing me to develop my skills in his laboratory under his guidance. I am grateful for the patience he had with me and his invaluable feedback in regards to my thesis. He enabled me to be an independent researcher while still providing me the needed support as a student, this is truly a unique skill that I hope to emulate one day. Additionally, I would like to thank Dr. Yukari Okamoto, who aided me in my project with her knowledge and expertise. Working beside you these past few years has been a true honor.

I would like to thank the members of my thesis committee; Dr. Jack Kaplan, Dr. Karen Colley, Dr. Nava Segev, and Dr. Constance Jeffery for the extensive amount of time you lent to me in supporting my project and bestowing upon me invaluable feedback, ideas, and advice that enabled me to strengthen my skills as an independent researcher.

Thank you to my family and friends, who have been my support system through this process, without each and every one of you I would not be submitting my dissertation today. Your love and friendship have made this journey a realty and for that I am indebted to each and every one of you.

Contribution of Authors

All the work included in this dissertation was performed under the guidance of Dr. Sojin Shikano and Dr. Yukari Okamoto. Some plasmids used in the study were constructed by the previous lab member Minjee Kim, who also performed initial testing of the yeast growth complementation. The B31 strain was provided by Dr. Hana Sychrova of the Academy of Sciences of the Czech Republic.

Table of Contents

Table of Contents (continued)

Table of Contents (continued)

List of Tables

List of Figures (continued)

List of Figures (continued)

List of Figures (continued)

LIST OF ABBVREATIONS

aa	amino acid
Ala	alanine
AF488	Alexa Fluor 488
Ab	antibody
Arg	arginine
Ba^{2+}	barium
Bip	binding immunoglobulin protein
CME	Clathrin-mediated endocytosis
CIE	Clathrin-independent endocytosis
co-IP	co-immunoprecipitation
C-terminus	carboxy-terminus
DAT	dopamine transporter
EAG1	voltage-gated mammalian neuronal K^+ channel ether à go-go 1
EE	early endosomes
EGFR	epidermal growth factor receptor
ENaC	epithelial sodium channel
ER	endoplasmic reticulum
ERAD	endoplasmic reticulum associated degradation
ERES	endoplasmic reticulum exit sites
ERGIC	endoplasmic reticulum-Golgi intermediate compartment
ERQC	endoplasmic reticulum quality control
ESCRT	endosomal sorting complexes required for transport
FACS	fluorescence-activated cell sorting
FBS	fetal bovine serum
FCM	flow cytometry
GAP	GTPase activating proteins
GEF	guanine nucleotide exchange factors
Glu	glutamate
hrs	hours
HSC70	ATPase heat shock cognate 70
Ile	isoleucine
K^+	potassium
KCNK	two-pore-domain K^+ channel
LE	late endosomes
Leu	leucine
Lys	lysine
Met	methionine
min	minute
Na+	sodium
N-terminus	amino-terminus
O/N	overnight
PCR	polymerase chain reaction
Pro	proline
RE	recycling endosomes
SD	synthetic defined
Ser	serine

LIST OF ABBVREATIONS (continued)

siRNA	small interfering RNA
SNARE	soluble N-ethylmaleimide-sensitive factor activating protein receptor
TGN	*trans*-Golgi network
TRAK2	ϒ-aminobutyric acid receptor-interacting factor 1
Trp	tryptophan
Ura	uracil
WT	wild type

SUMMARY

The cell surface density of membrane proteins dictates their corresponding cellular activity. Intracellular trafficking of membrane proteins is often dictated by distinct signal sequences on the cargo proteins. These trafficking signals often take the form of short linear amino acid motifs in the cytosolic regions of membrane proteins. Many diseases, such as cystic fibrosis, arise from defects in cell surface trafficking of membrane proteins. Therefore, identifying, characterizing, and elucidating the mechanisms of trafficking signal sequences is important for understanding normal cellular physiology, disease physiology, and the potential development of therapeutic interventions for diseases that involve trafficking defects. Still, many membrane proteins are transported throughout the cell without containing any of the characterized trafficking motifs. More systematic approaches to identifying trafficking signals would facilitate our understanding of membrane protein trafficking.

In this study we demonstrate potential use of potassium (K^+) efflux-deficient yeast for studying trafficking signals and K^+ channel functions. The *Saccharomyces cerevisiae* B31 strain (*ena1-4Δ nha1Δ*) lacking the K^+ and sodium (Na^+) efflux system has previously been reported to show sensitivity to higher external concentrations of alkali–metal–cation salts when transformed with the mammalian inward rectifying K^+ channel Kir2.1. Due to the fact that Kir2.1 activity inversely correlates with B31 growth in high K^+ media, we show that that complementation of growth of B31 expressing Kir2.1 on high K^+ media represents the trafficking of functional channel to the cell surface and suggest that this can be developed into systematic screening systems to identify either structural components of channel function or trafficking components.

We further develop and implement a novel B31 based screening system to identify *cis*-acting signal sequences that reduce the surface levels of proteins. We characterized the mechanism of action of identified hit clones and observe that the screening system was able to enrich from a random peptide

library several trafficking signal sequences that reduce the surface level of proteins. Furthermore, the trafficking motifs from the screen functioned via several distinct trafficking pathways including endocytosis, retrograde transport to the endoplasmic reticulum (ER), and degradation. While many of the motifs identified in the screening have been previously characterized, motifs potentially functioning through novel mechanisms were identified. Our newly developed B31 screening system adds a new tool for systematically studying protein trafficking motifs.

I. BACKGROUND AND SIGNIFICANCE:

Proteins are the workhorses of the cell. The human genome contains around 20,000 protein encoding genes which encodes an estimated 20,000 to 100,000 unique proteins per cell type (1). Each protein serves its specific function at its specific site/s of action within the cell. Mutations or other errors that cause the loss or functional alteration of even one protein type within the cell have the potential to cause disease (2). Similarly, mutations or other errors that cause the mislocalization of even one protein type within the cell can also cause disease. Simply put, a protein that is not localized to its correct site of action will not be able to perform its correct function within the cell, and if that protein serves an essential function disease will occur as is the case with the most common form of cystic fibrosis (3-6). As the correct trafficking of proteins throughout the cell is critical for cell function and survival, it is not surprising that cells have evolved a thorough and complex system of transporting proteins throughout the cell which is still only partially understood (7).

I.1 Pathways of vesicular membrane trafficking:

The most characterized mechanism of protein transport throughout the cell is vesicular transport (Figure 1). In vesicular protein transport, proteins are loaded into vesicles from one compartment of the cell and targeted either to another intracellular compartment within the cell, expressed on the plasma membrane or secreted from the cell. The transport vesicles often contain a protein coat which varies based on the trafficking pathway. Vesicular protein trafficking can be broadly characterized into two pathways; the exocytic and endocytic pathways. In the exocytic pathway, newly synthesized proteins are folded in the ER and are transported outward to the various intracellular compartments, to the plasma membrane, or in the case of soluble proteins, secreted from the cell. In the endocytic pathway proteins are brought from the plasma membrane to the various intracellular compartments within the cell (7).

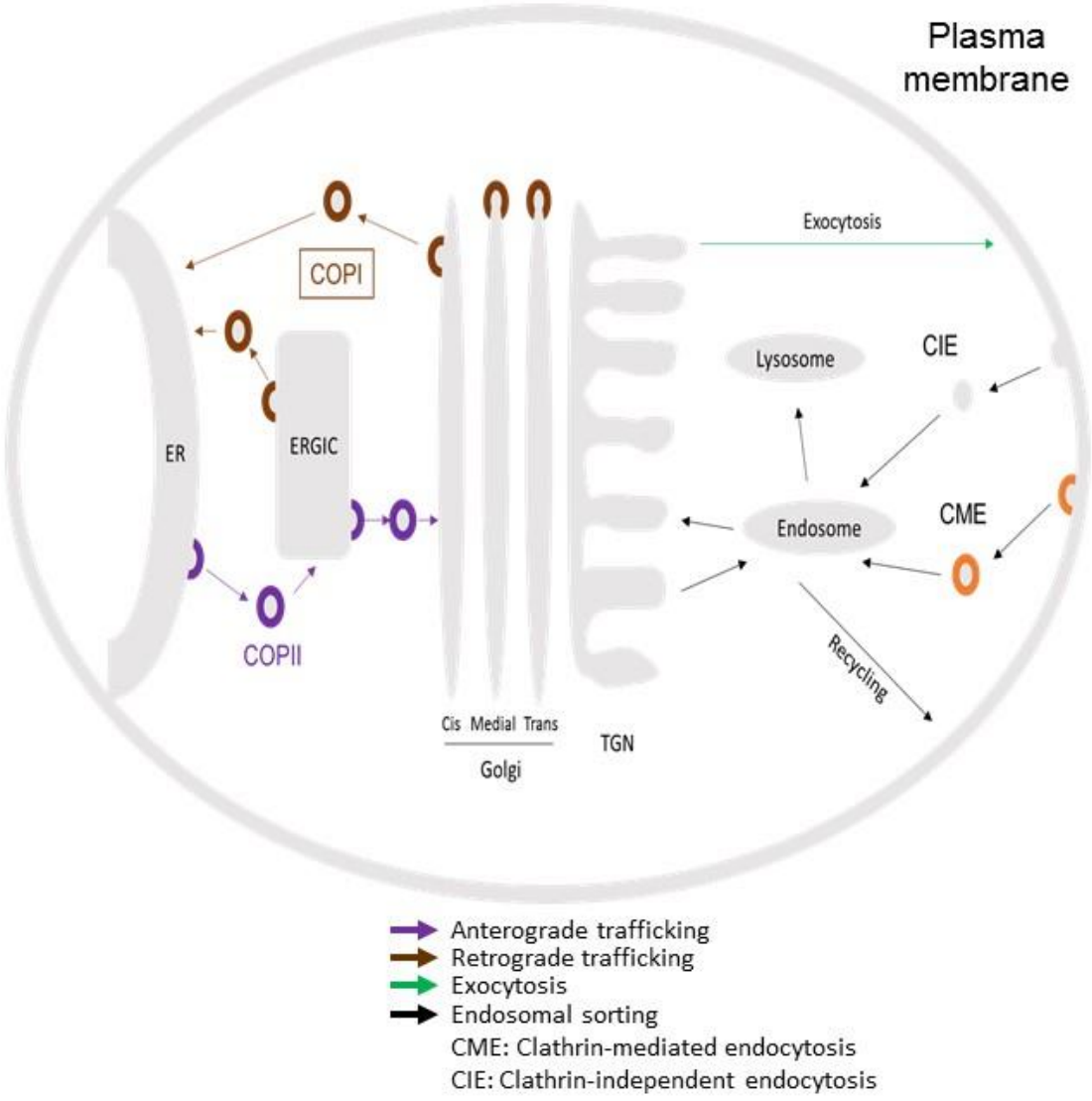

Figure 1. Vesicular protein trafficking. Overview of protein trafficking through the secretory system, including organelles, trafficking pathways, and coat proteins.

Both soluble and membrane bound proteins are transported through the cell through vesicular transport. Our laboratory takes particular interest in the trafficking of membrane bound proteins. The cell surface density of membrane proteins dictates their corresponding cellular activity (8), and many diseases, such as cystic fibrosis, arise from defects in cell surface trafficking of membrane proteins (5). This review aims to provide a background of the systems and mechanisms of vesicular trafficking focusing on the transport of membrane bound proteins.

I.1.1 The exocytic pathway:

Newly synthesized proteins are folded in the rough ER, where membrane bound proteins are inserted into the ER membrane and soluble proteins are translocated to the ER lumen (9). Protein folding in the ER is monitored by the ER quality control (ERQC) which determines whether proteins are correctly folded. Correctly folded proteins are allowed to exit the ER, whereas proteins incorrectly folded or assembled are targeted for degradation via ER-associated degradation (ERAD) (10). Proteins which have passed the ERQC checkpoints exit the ER via recruitment into the COPII-coated membrane vesicles and are transported toward the Golgi (9).

In human cells as well as other eukaryotic cells, en route to the Golgi complex, COPII coated vesicles pass through the ER-Golgi intermediate compartment (ERGIC) (11). The precise nature of the ERGIC compartment is still poorly understood, however it appears as if the ERGIC is a sorting compartment biochemically distinct from both the ER and Golgi in which further sorting of forward trafficking cargo can occur. Additionally, the ERGIC is enriched in COPI coat proteins and the components of retrograde trafficking (9). Retrograde trafficking is the reverse trafficking of proteins back toward the ER. It is necessary that proteins that function by shuttling between the ER and Golgi be retrieved back to the ER. Additionally, some proteins escape the ERQC and exit the ER as a misfolded or misassembled protein. Misfolded or misassembled proteins can have a deleterious and even disastrous effect on the cell (6),

therefore the detection and retrieval of escaped misfolded proteins is an important role of the retrograde trafficking machinery (12). Retrograde trafficking occurs in both the ERGIC and Golgi (9,13). Proteins are loaded into COPI-coated vesicles and transported back either to earlier compartments or returned all the way back to the ER (9).

Proteins traveling on the exocytic pathway are trafficked through the Golgi apparatus (11). The Golgi apparatus is a series of closely packed membrane cisterna with a defined orientation. The Golgi apparatus functions to sort and further process proteins en route to their final destinations (14). Golgi resident proteins do not progress through the Golgi but are rather maintained in the Golgi through a variety of mechanisms, many still uncharacterized (15). Additionally, as with the ERGIC, COPI-mediated retrograde trafficking occurs within the Golgi returning some proteins to the earlier compartments and the ER (9). Proteins traveling the exocytic pathway enter the *cis*-Golgi and proceed through the *medial*-Golgi then the *trans*-Golgi (9). In the Golgi, proteins simultaneously proceed through the cisterna while being further sorted, and when appropriate, undergo post-translational modifications such as protein glycosylation and sialylation. These modifications occur in an ordered sequential process (14). Post Golgi, proteins enter the *trans*-Golgi network (TGN) where proteins are sorted into distinct carriers and targeted to their intended destinations, including the plasma membrane, or secreted out (16).

I.1.2 The endocytic pathway:

Membrane bound proteins expressed on the plasma membrane, as well as nutrients and proteins outside the cell, will inevitably require internalization into the cell. Endocytosis is the process of internalization into the cell. There is not just a single pathway of endocytosis, but rather many distinct mechanisms of endocytosis operating with distinct trafficking machinery (17). All endocytic pathways require a mechanism for cargo selection, vesicle formation, vesicle budding, and vesicle fusion to the target compartment (18). Clathrin-dependent endocytosis, a system in which cargo is internalized into

the cell in clathrin-coated vesicles, was the first characterized pathway of endocytosis, and is the most well characterized pathway. However, at least eight other distinct pathways of clathrin-independent endocytosis have since been discovered (19). Some, pathways, such as caveolin-dependent endocytosis, have become better characterized in the past few years, however still many of the clathrin-independent pathways of endocytosis remain poorly understood (18).

Regardless of the endocytic pathway, proteins internalized back into the cell will require further sorting to determine their fate. This sorting typically occurs in the endosomal compartments, a series of distinct membrane bound sorting compartments that serves to sort internalized proteins, setting them on a pathway of either recycling or degradation (20,21). The endosomal network can be broadly divided into early endosomes (EE), late endosomes (LE), recycling endosomes (RE) and the lysosome. Each compartment serves a distinct function and contains a distinct population of sorting machinery as well as varies in its degree of acidification. Endocytosed vesicles typically first fuse with the EE. Proteins in the EE can be either be directly recycled back to the plasma membrane, transported back to the TGN or transported to a further endosomal compartment, either the RE or LE. Proteins in the RE are recycled back to the plasma membrane. Proteins in the LE can be sent back to the TGN or transported to the lysosome for degradation. Which pathway a particular protein takes is determined by its interactions with the sorting proteins. Changes in pH between components of the endosome (becoming more acidic in the later compartments) also play a role in sorting by inducing conformational changes in the proteins (21).

I.2 Mechanisms of vesicular protein transport

I.2.1 Vesicle formation and budding

As discussed above, proteins are transported throughout the cell in protein coated vesicles. The coat protein and vesicle composition vary based on the trafficking pathway. Proteins undergoing anterograde

trafficking from the ER towards the Golgi are transported in COPII-coated vesicles. Proteins undergoing retrograde trafficking, within the Golgi or between the Golgi, ERGIC, and ER are transported in COPI-coated vesicles (9). While there are many different mechanisms of endocytosis, in the most well characterized mechanism, clathrin-dependent endocytosis, proteins are internalized into the cell in clathrin-coated vesicles (22).

I.2.2 COPII and COPI vesicle formation and budding:

COPII and COPI are the coat proteins required for anterograde and retrograde trafficking, respectively. They are large cytosolic multi-subunit complexes that are recruited to membranes by small activated G proteins (14). Guanine nucleotide exchange factors (GEF) activate the small G proteins to their GTP-bound form, while their corresponding GTPase activating proteins (GAP) deactivate the small G proteins to their GDP-bound form. COPII-mediated anterograde trafficking always occurs at the ER exit sites (ERES). Sar1 is the small G protein that recruits COPII to the membrane, and it is activated by the Sec12 GEF. Sar1 recruits the COPII complex to the membrane in two steps, Sar1 directly binds the Sec23/Sec24 subcomplex of COPII, which in turn recruits the Sec13/31 subcomplex of COPII. These have been determined to be the minimal components required for COPII vesicle formation (9).

COPI vesicle formation can occur in multiple locations within the cell including the ERGIC, *cis*-Golgi or within the Golgi cisternae. The ADP ribosylation factor (Arf) family of proteins are the small G proteins that recruit COPI to the membrane. The specific Arf protein is dictated by the location of vesicle formation. Similarly, the specific GEF protein that activates the Arf varies based on the location of vesicle formation. The COPI coat is a heptameric complex composed of seven subunits and is recruited en bloc to the membrane (9). In both COPII- and COPI-mediated transport, the coat polymerization deforms the membrane and, after scission, the vesicle begins its transport to its destination membrane. The coat

proteins and corresponding components also play important roles in cargo selection, which will be discussed further in the next section (9).

I.2.3 Clathrin-coated vesicle formation and budding

Clathrin-mediated endocytosis is the most well characterized pathway of endocytosis. However, at least eight other distinct pathways of clathrin-independent endocytosis have since been discovered (17). Excellent reviews of our current understanding of clathrin-independent endocytosis have been written (18,19). Here, I will give an overview of clathrin-mediated endocytosis.

In clathrin-mediated endocytosis, cargo protein and extracellular fluids are brought into the cell in clathrin-coated vesicles (19). AP2 is the primary adapter protein crucial to clathrin-mediated endocytosis. AP2 is recruited to the plasma membrane by direct binding to domains in cargo proteins (discussed in the next section) as well as by binding to plasma membrane specific phosphatidylinositol-4,5-bisphosphate. AP2's interaction with the plasma membrane causes its conformational change, activating it to recruit and bind the clathrin coat. As the clathrin polymerization occurs the coated pit begins to invaginate. The invagination is thought to occur both as an effect of polymerization, as well as mediated by specific proteins known as curvature effectors. Dynamin is a GTPase motor protein that mediates vesicle scission from the plasma membrane (22).

I.2.4 Vesicle transport, tethering, and fusion to target compartment:

Post budding, all coated vesicles, whether it be COPII, COPI, or clathrin, must travel and fuse to their correct target membranes. While the trafficking machinery differs for each pathway, similar steps apply. First, after budding the vesicles must transport to the target membrane. This can occur via simple diffusion or by motor driven transport along a cytoskeleton track. Once the vesicle reaches the target membrane it will need to be tethered and ultimately fuse with the target membrane. Tethering is achieved by tethering factors, a diverse group of proteins that mediate the initial vesicle-membrane

interaction, which are recruited to the vesicle by Rab GTPase's. Tethering factors mediate the initial docking of the vesicle to the target membrane prior to fusion, which is then mediated by soluble N-ethylmaleimide-sensitive factor activating protein receptor (SNARE) proteins (23).

Before fusion can occur between the vesicle and target membrane it is necessary for the vesicle to shed its protein coat. Depending on the trafficking pathway coat shedding can occur shortly after vesicle budding or later after tethering has occurred (23). In the case of anterograde and retrograde trafficking, specific GAP proteins deactivate the Sar1/Arf1 proteins causing the depolymerization of the vesicle coat. In clathrin-coated vesicles the ATPase Heat Shock Cognate 70 (HSC70) and its cofactors mediate vesicle uncoating (24). After docking to the target membrane, membrane fusion is mediated by a family of SNARE proteins. Both the transport vesicle and the target membrane contain distinct SNARE proteins, v-SNAREs and t-SNAREs, respectively. After initial docking of the vesicle to the membrane by the tethering factors, v-SNAREs and t-SNAREs interact, bringing the two distinct membranes into proximity where the thermodynamic barrier to membrane fusion can be overcome and fusion of the vesicle to the target membrane can occur (9). The specify of the tethering factors and SNARE proteins ensures transporting vesicles dock and fuse to the correct target membrane (23).

I.2.5. Mechanisms of cargo protein selection and sorting:

Perhaps the most intriguing aspect of the protein trafficking system is the mechanisms of cargo selection and sorting. How are the cargo proteins specifically recognized and loaded into the correct coated vesicles? While there is an element of "bulk flow" of cargo loading into vesicles, that is, cargo proteins enter the vesicles as a factor of their relative concentrations, it is clear based on analysis of vesicle-cargo protein concentrations that selection and enrichment of select cargo protein is occurring (25). Much effort has been put in to elucidating the mechanisms of cargo selection into vesicles, and

indeed, it has been shown in both the exocytic and endocytic pathways that active selection of proteins into vesicles occurs (26-29).

How does cargo selection occur? Cargo selection can occur through a variety of mechanisms, in some cases cargo specific adapters recognize cargo and recruit them to the vesicles (22). In other cases, proteins require further modification, such as ubiquitination, for sorting into vesicles (30). However, the best characterized mechanism of protein selection occurs through signal sequences contained on the cargo proteins that are recognized by the protein trafficking machinery - often the coat proteins themselves or adapter complexes that interact with the coat proteins- and sorted into the correct vesicle (16,27,29,31-33). In the case of membrane bound proteins, most of these signal sequences occur in the cytosolic region of the protein (16,27,29,31-33). Soluble proteins that cannot directly interact with the cytosolic coat proteins or machinery require additional adaptor membrane proteins, e.g., ERGIC53, which binds the luminal cargo protein and also associates with cytosolic COPII complex (34). In some cases, these trafficking signals can involve the tertiary structure of the protein (35). However, the majority of the trafficking signals that have been identified are short linear amino acid motifs that occur in the cytosolic domains of membrane bound proteins (16,27,29,31-33). A selection of the most characterized motifs in membrane bound proteins is shown in Table 1.

With the best characterized trafficking motifs, the consensus sequence, interacting machinery, as well as the trafficking pathway have been elucidated (16,27,29,31-33). Structural studies have even identified the exact binding residues between the motifs and trafficking machinery of some proteins (36-38). Despite this, there is still much mystery that surrounds even the most well characterized motifs. For example, the well characterized di-leucine (di-Leu) motif [DE]XXXL[LI] can function either as an endocytosis motif or in the direct targeting of proteins from the *trans*-Golgi network to the endosome/lysosome network depending on the protein context. How the cell makes the distinction between these two pathways has yet to be fully understood (39). Additionally, there are less common

trafficking motifs whose mechanism remains still only partially understood (40,41). Our current understanding of the mechanisms of the well characterized motifs has been reviewed in detail in a number of well written articles (16,27,29,31-33).

Table 1. Select sequence signals that mediate trafficking of membrane proteins

Signal	Pathway	Membrane protein with motif	Interacting machinery	Source
DxE (di-acidic)	ER export	Kir2.1	COPII	(27)
FF-COOH (di-Ø)	ER export	ERGIC53	COPII	(27)
KKxx-COOH (di-Lys)	ER retrieval	p25	COPI	(37)
RxR (di-Arg)	ER retrieval	CTFR	COPI	(12)
YxxØ	Endocytosis	Transferrin receptor	AP2	(39)
[DE]xxxL[LI] (Di-Leu)	Endocytosis	CD3-ϒ	AP2	(39)
NPxY	Endocytosis	LDL receptor	AP2	(29)

I.3 The study of protein trafficking signals:

I.3.1 Tools and techniques for the study of protein trafficking signals:

Our current knowledge of the protein trafficking pathways and machinery are a product of a century of research. Over that time technology has improved and there is now a great toolbox of methods and techniques used to study protein trafficking. Microscopy is perhaps the oldest tool for studying protein trafficking but has evolved and now includes florescent microscopy techniques and live cell imaging. The development of *in vitro* cell-free systems to study vesicular trafficking has also been an invaluable tool to the study of protein trafficking. Additionally, the use of yeast with genetic defects in the trafficking pathways has proven to be an invaluable tool. Finally, there are a wide range of cellular, genetic and

biochemical methods for the study of protein trafficking (42). Preuss *et. al.* provides a comprehensive review on many of the techniques for studying protein trafficking pathways (42) .

We are particularly interested in identifying the trafficking signal sequences contained on the cargo proteins. Many cargo proteins are transported through the cell lacking any of the well- characterized trafficking motifs (43). The traditional and standard method for the identification of the trafficking signal sequences has been the identification and study of individual target proteins (44). First a candidate protein is identified. Historically, it is a protein in which a natural mutation changes the localization of the protein and leads to disease or a viral protein that is internalized and localized within the cell (26,29,33,39). Once the candidate is selected, genetic modification of the protein is used to determine the essential sequences involved in the trafficking of the protein. Often the sequences are confirmed by transplantation of the essential sequences onto an unrelated protein to verify the trafficking effect (26,29,33,39). Once a sequence is identified, further analysis can be done into its mechanism of action, as well as the identification of other proteins utilizing the same trafficking sequence (26,29,33,39).

I.3.2 Newer more systematic approaches for the identification of protein trafficking signals:

While the standard method of identifying protein trafficking signals through mutational analysis of single proteins has been very effective, more systematic approaches to screen for trafficking motifs adds additional tools to the study of protein trafficking signals. Recently, newer more systematic approaches have begun to be developed to identify trafficking signal sequences as well as other trafficking factors that regulate protein transport (43,45-48). The earliest of these systems are yeast based systems (45,46,48). Yeast offers a good model for studying mammalian protein trafficking mechanisms, since the basic molecular machinery for protein trafficking is well conserved between yeast and mammals. More importantly, clonal expression of library transgenes in a cell enables a systematic screening and analysis, which is not achievable in mammalian cells that will inevitably take up multiple gene clones within a cell

upon transfection of libraries. More recently systematic screening strategies for identifying trafficking factors have been developed in mammalian cells as well (43,47).

Currently, the yeast based screening systems primarily utilize mutant *Saccharomyces cerevisiae* strains that lack the K^+ uptake transporters Trk1 and Trk2, such as SGY1528 (45,46,48). SGY1528 yeast is unable to grow in low concentrations of K^+ but growth can be restored by the heterologous expression of the mammalian Kir2.1 K^+ channel (45). This complementation of growth has been utilized as the basis of many screening systems (45,46,48):

The first yeast based systematic screening system utilized a Kir2.1 protein with a di-arginine (di-Arg, RXR) type ER-retrieval signal fused to its carboxyl-terminal (C-terminal) tail (45). The di-Arg signal fused to Kir2.1 has been shown to localize Kir2.1 in the ER of both mammalian cells and yeast cells. Furthermore, when expressed in SGY1528 yeast, the di-Arg-fused Kir2.1 protein does not restore growth when plated in low K^+ media. A random peptide library was fused to the C-terminal tail of the di-Arg-fused Kir2.1 protein and expressed in SGY1528 yeast plated on low K^+ media in order to identify forward trafficking sequences that would override the di-Arg signal and restore the surface level of Kir2.1 complimenting the yeast growth on the low K^+ media. The screening identified a group of *cis*-acting sequences that specifically interact with 14-3-3 proteins and promote surface expression of membrane proteins (45).

A second yeast based screen again utilized SGY1528 yeast expressing the mammalian Kir2.1 channel. The group demonstrated that SGY1528 yeast expressing the mammalian Kir2.1 was unable to grow in media containing only 0.5 mM K^+, as this concentration of K^+ was too low for complementation of growth by the baseline Kir2.1 expression level. They transformed this Kir2.1-expressing SGY1528 cells with a human cDNA library to identify genes that increased the surface level of Kir2.1 to allow growth at

0.5 mM K^+. The screening identified the ϒ-aminobutyric acid receptor-interacting factor 1 (TRAK2) as a trafficking factor for Kir2.1 (46)

A third yeast based screen utilized YAK01, a yeast strain lacking the K^+ uptake transporters Trk1 and Trk2, and expressing the mammalian Kir2.1 channel to identify negative regulators of Kir2.1. YAK01 yeast expressing the mammalian Kir2.1 channel were mated to the yeast deletion collection to generate a library of YAK01 expressing the mammalian Kir2.1 channel with one additional nonessential gene deleted. The library was screened for increased growth on low K^+ media to identify which gene knockouts increased the surface level of Kir2.1 to allow growth. The screening identified the endosomal sorting complexes required for transport (ESCRT) as a negative regulator of the Kir2.1 channel (48).

More recently, systematic screening strategies for identifying trafficking factors have been developed in mammalian cells as well (43,47). One group developed a novel fluorescence-activated cell sorting (FACS) based screening system to screen for endocytosis signal sequences that reduced the surface level of a modified CD8 reporter protein. A random peptide library was fused to the modified C-terminal tail of CD8 and stably expressed in HeLa cells. Cells were pooled and an Ab feeding assay for endocytosis was performed. The cells in which the surface level of CD8 was reduced were isolated by FACS and the random sequence was determined by polymerase chain reaction (PCR). The screening identified sequences that were variations of the di-Leu as well as a novel internalization signal (43).

Finally, a small interfering RNA (siRNA) based screening system was developed to identify regulators of clathrin-mediated endocytosis in mammalian cells. HeLa cells stably expressing CD8 fused with either the YXXphi or FXNPXY clathrin-mediated endocytosis motif were transfected with an siRNA library. Cells were stained for surface CD8 and surface florescence measured in a microreader plate. Increased surface levels of CD8 indicated a knockdown that caused a deficiency in clathrin-mediated endocytosis. The screening identified V-ATPase as having a role in clathrin-coated vesicle formation (47).

It is clear that the systematic approaches to identifying trafficking signal sequences or other trafficking factors that regulate protein transport have thus far been successful and added to our understanding of the protein trafficking mechanisms. Each screening system has its advantages and disadvantages. The SGY1528 and YAK01 yeast based approaches have proven to be versatile and comes with all the advantages of using yeast as a model system. However, the current yeast based approaches can only identify motifs or factors that cause the increase of Kir2.1 on the yeast surface (45,46,48). The mammalian cell based systems have the advantage of being directly performed in mammalian cells, eliminating the need to perform extra steps validating the screening results in mammalian cells. However, so far mammalian cell based screening systems have only been developed for clathrin-mediated endocytosis (45,46,48). The continued development of novel systematic screening systems would both increase the tools by which we study protein trafficking and aid in the further elucidation of trafficking motifs and pathways.

I.4 Protein trafficking diseases:

Due to the essential role of protein trafficking it is not surprising that there is a long and growing list of diseases caused or impacted by protein trafficking defects. Protein trafficking defects have been implicated in cancers, neurological disorders, muscular dystrophies, blood diseases, cardiac disorders, immunodeficiency, diabetes, mental retardation, and systemic disorders (4). Howell *et. al*. has written a review covering over 50 different protein trafficking diseases (4).

Protein trafficking diseases can arise through mutations in the protein trafficking machinery such as a form of acute myeloid leukemia caused by a defect in clathrin-coated pit formation. They can also arise from the mislocalization of even one protein, such as in the case of the most common cause of cystic fibrosis (ΔF508 CTFR), in which the receptor does not traffic to the plasma membrane (4). Most protein trafficking diseases are congenital, e.g., cystic fibrosis (ΔF508), however they can also be acquired e.g.,

spontaneously acquired prion diseases (4) or pentamidine-induced long QT syndrome (49). Despite the extensive study of protein trafficking diseases, most diseases still lack a cure or sufficient treatment options (4).

Cystic fibrosis is the classic example of a protein trafficking disease. It is an autosomal recessive and lethal disease. Cystic fibrosis has systemic effects but most notably affects the cell lining of the lungs, intestine and other tissues (5). The most common form of cystic fibrosis is caused by the deletion of Phe^{508} (ΔF508) in a chloride channel, cystic fibrosis transmembrane conductance regulator (CFTR), which results in the misfolding of the channel. One study proposes that the ΔF508 mutation leads to the exposure of a di-Arg motif in the cytoplasmic region, which causes COPI-mediated retrieval of the protein to the ER (50). With the ΔF508 CFTR mutation, a very small amount protein is able to escape the retrieval mechanism and reach the cell surface. Electrophysiological studies on these membrane bound ΔF508 CFTR channels have shown that the mutant channels are still functionally active, albeit at a reduced capacity compared to the wild type channel. Cellular studies in which the ΔF508 CFTR has been either pharmacologically stabilized at the plasma membrane or forced out of the ER have shown correction of the cellular electrophysiology (5). These results demonstrate that the disease phenotype of ΔF508 cystic fibrosis is caused primarily by the defective trafficking of the CTFR channel, as opposed to the defective conductance. Current research suggests that only 10-15 % of the normal plasma membrane levels of wild type CTFR channel are necessary to avoid the disease phenotype. Even with the reduced electrophysiological capacity of the ΔF508 CFTR, it is estimated that a plasma membrane restoration of 50-60% ΔF508 CFTR compared with the normal plasma membrane levels of wild type CTFR would completely eliminate the disease phenotype (51) .

The protein trafficking machinery is also heavily implicated in viral and bacterial toxin-induced pathogenesis. To infect a cell, viral/toxin proteins must first enter a cell, then be transported to and from their sites of action. This often occurs through the hijacking of the host cell's protein trafficking

machinery. Viral attachment, cellular entry, viral protein trafficking, and cellular exit are all complimented by the cellular transport machinery. This hijacking is often mediated by the intracellular trafficking motifs contained in viral proteins that cause them to be trafficked to their site of action (33).

I.5 Goal of current study:

The correct trafficking of proteins throughout the cell is an essential process. Further delineation of the protein trafficking pathways will increase our understanding of cellular physiology, and the physiology and mechanisms of protein trafficking diseases, and, hopefully, lead to therapeutic treatments for protein trafficking diseases. The past decade has seen the development of new yeast and mammalian systematic screening approaches to studying protein trafficking. Each screening system has come with its advantages and disadvantages. All of the currently developed yeast based systems can only identify factors that cause an increase in the plasma membrane levels of a reporter membrane bound protein. The mammalian cell based screening systems currently developed can only identify factors mediating endocytosis of a membrane bound reporter protein. In this study we aim to develop a novel yeast based gain-of-function genetic screen to identify factors that reduce the surface levels of a membrane bound reporter protein. No such system has yet been developed. Such a system could potentially identify a wide range of trafficking signals functioning to regulate the surface levels of membrane proteins through many different pathways. We aim to develop and conduct said screen characterizing the mechanism of action of identified hits.

II. MATERIALS AND METHODS

Parts of this chapter have been previously published in:

Bernstein, J. D., Okamoto, Y., Kim, M., and Shikano, S. (2013) Potential use of potassium efflux-deficient yeast for studying trafficking signals and potassium channel functions. *FEBS Open Bio* 3, 196-203

II.1 Plasmids:

For B31 growth assay, mouse Kir2.1 was cloned at BamHI and NotI in pYES2met vector in which GAL1 promoter was replaced with MET25 promoter (kindly supplied by Dr. Lily Jan). The EcoRI site was added before the termination codon (this was referred to as a wild-type Kir2.1) for fusion of the exogenous trafficking motifs. The C-terminal sequences were cloned from mouse Kir6.2 (aa 355–399), human GPR15 (aa 351–360), or human sodium-dependent dopamine transporter [17] (aa 587–596) and fused to Kir2.1 at EcoRI-NotI. For GPR15 sequence, the Ser residue at 359 was mutated to Ala. Human KCNK3 and KCNK9 were also cloned in pYES2met vector. Site-directed mutagenesis was performed by overlap extension PCR. For detection of cell surface expression in HEK293 cells, Kir2.1 was tagged with hemagglutinin (HA) epitope between aa 117 and 118, rat KCNK3 was tagged with HA between aa 213 and 214, and human KCNK9 was tagged with Myc between aa 40 and 41. These tagged constructs were cloned into pCDNA3.1(+) vector (Invitrogen, Carlsbad, CA).

II.2 Yeast strains and growth conditions

The *S. cerevisiae* strain B31 (MATα ena1-4_::HIS3 nha1_::LEU2) is a derivative of W303-1A (MATa ade 2-1 can1-100 his3-11/15 leu2-3/112 mal10 trp1-1 ura3-1) [16] and was kindly provided by Dr. Hana Sychrova (Institute of Physiology AS CR, Czech Republic). Cells were grown aerobically at 30 °C on YPD (1% yeast extract, 2% bactopeptone, 2% glucose, 120 mg/L adenine hemisulfate, 1.7% agar for solid media) or YNB media (6.7 g/L yeast nitrogen base without amino acids, 2% glucose, 10 mg/L adenine hemisulfate, 0.73 g/L methionine- and uracil-dropout amino acid mixture, 1% agar for solid media). The YNB media were supplemented with the indicated amount of potassium chloride and adjusted to pH 6.5

or 7.0 by Tris–HCl.

II.3 Plasmids and yeast transformation

Yeast cells grown to early logarithmic phase in YPD media were transformed by a lithium acetate method (52) and plated on YNB plates with no additional KCl (referred to as 0 mM K^+ plate).

II.4 Growth assay of B31

For the growth assay of the K^+ channel-transformed B31 cells, the cells were taken from the isolated colonies of freshly-transformed B31 cells and adjusted to 2×10^6 cells/ml in water by using a hemocytometer. This was followed by two 10-fold serial dilutions, and 5 µl aliquots of each dilution were spotted on the YNB plates with the indicated concentrations of KCl. Plates were incubated at 30 °C, and the digital images of the cells were taken at the indicated times (usually Days 4–7).

II.5 Growth assay of KCNK9-expressing B31 in liquid media

For testing the effect of pH on B31 growth, the cells freshly transformed with pYes2met vector or WT KCNK9 were adjusted to 2×10^6 cells/ml in YNB media (400 mM KCl) with pH adjusted to 5.0, 5.5, 6.0, 6.5, or 7.0 using Tris–HCl. For testing the effect of zinc ion, the cells were adjusted as above in YNB media (400 mM KCl, pH 6.5) containing 0, 10, and 100 µM zinc chloride. Zinc chloride at higher than 100 µM caused salt precipitation and reduction of the medium pH, so was not tested. The turbidity (OD 600 nm) was measured before and after 15 hrs of culture at 30 °C. Cultures were performed in triplicate for each construct.

II.6 Antibodies (Abs)

The following Abs were used: mouse anti-HA, rabbit anti-Kir2.1, and rabbit anti-14-3-3β from Santa Cruz Biotechnologies (Dallas, TX), rabbit anti-HA from Cell Signaling Technology (Danvers, MA), mouse anti-Myc (both non-conjugated and Alexa Fluor (AF) 488-conjugated) from Millipore (Billerica, MA), rabbit

anti-β-COP from Affinity BioReagent (Golden, CO), mouse anti-GST from NeuroMab (Davis, CA), AF488-conjugated goat anti-mouse IgG from Invitrogen, horse radish peroxidase (HRP)-conjugated goat anti-mouse and goat anti-rabbit IgG from Vector laboratory (Berlingame, CA).

II.7 Cell culture and transfection

HEK293 cells were maintained in 50% DMEM/50% Ham's F-12 medium containing 10% FBS, 2 mM L-GLu, 100 U/ml penicillin, and 100 μg/ml streptomycin (complete medium). Transient transfection of plasmids was performed using Mirus TransIT-LT1 (Mirus Bio, Madison, WI) according to the manufacturer's instructions.

II.8 Flow cytometry (FCM)

Transfected HEK293 cells were collected by gentle flushing and washed with Hanks' Balanced Salt Solution supplemented with 1% BSA (staining buffer). All the Ab staining and washing thereafter were performed in the staining buffer on ice. For surface staining of HA-tagged Kir2.1 and KCNK3, the transfected cells were incubated with a mouse αHA Ab followed by a AF488-conjugated secondary Ab for 20 min on ice. For Myc-tagged KCNK9, the transfected cells were stained with AF488-conjugated mouse anti-Myc Ab. The stained cells were fixed with 1% paraformaldehyde and analyzed by Cell Lab Quanta SC (Beckman Coulter, Brea, CA). For measurement of surface fluorescence intensity, the median values were determined for the entire viable cell populations (Kir2.1 and KCNK3) or for the myc-positive population (KCNK9) by using FlowJo software (Tree Star Inc., Ashland, OR). The surface expression of the channels was shown in the histograms, except that KCNK9 expression was shown in a density plot because the percentage of KCNK9 signal-positive cells were too small (<10%) to clearly show in histograms. This may be due to the inefficient accessibility of the anti-Myc Ab to the epitope.

II.9 Protein extraction from B31 yeast cells

Proteins were extracted from B31 cells to examine the expression of Kir2.1 channels. B31 cells transformed with pYES2met vector or Kir2.1 constructs were inoculated in the methionine- and uracil-deficient YNB media with no added KCl and cultured O/N at 30 °C. The next morning the cell density was adjusted to a density of 0.3 OD_{600} in 3 ml of the same medium and cultured for 4 hrs. The proteins were extracted as described previously (53), and the samples were subjected to western blot analysis for Kir2.1 and KCNK channels.

2.10. Immunoprecipitation (IP)

The transfected HEK293 cells were washed with PBS once and lysed with lysis buffer (0.5% Igepal, 25 mM Tris, 150 mM NaCl, pH 7.5) containing protease inhibitors for 20 min at 4 °C. After centrifugation for 20 min at 11,000 x*g*, the supernatant was mixed with mouse anti-HA or mouse anti-Myc and Protein A- or Protein G-conjugated agarose beads (Invitrogen). After O/N incubation at 4 °C, the beads were washed 4 times with lysis buffer, and then the immunoprecipitated proteins were eluted by incubating the beads with 2X sample buffer.

2.11 SDS–PAGE and western blots

The protein samples resolved by 10 or 12% SDS–PAGE were transferred to nitrocellulose membranes. Transfer was confirmed by staining of the membranes with Ponceau S. The membranes were blocked with skim milk and then incubated with primary Abs for 1 hr at room temperature (RT) or O/N at 4 °C and then with corresponding secondary Abs conjugated with HRP. Blot signals were obtained using ECL substrates (Thermo Scientific) and collected by exposure to X-ray films.

2.12 Immunocytochemistry

HEK293 or HeLa cells transfected with GFP-Kir2.1 or Myc-CD8 constructs in the chamber slides were fixed with Cytofix/Cytoperm buffer (BD Biosciences) for 15 min at 4 °C and permeabilized with −20 °C

chilled 90% methanol for 5 min at RT. Cells were first stained with Abs to the intracellular markers O/N at 4 °C, followed by Cy3-labeled secondary Abs for 1 hr at 4 °C. Myc-CD8 transfected cells were then incubated with AF488-labeled anti-Myc Ab for 1 hr at 4 °C. Cells were then counterstained with Hoechst 33342 (Invitrogen) for 10 min before mounting. Images were collected with a Zeiss LSM 700 laser scanning confocal microscope using Zen software (Zeiss).

II.13 Antibody feeding assay:

HEK293 cells were transiently transfected with HA-Kir2.1 constructs or, for the AP180C inhibition assay, also co-expressing either AP180C or empty pCDNA vector. Cells were collected by gentle flushing and washed in cold complete media containing 10 mM HEPES. The transfected cells were incubated with mouse αHA Ab in cold complete media containing 10 mM HEPES for one hour at 4° C. Cells were washed three times with cold Hanks' balanced salt solution, then re-suspended in complete media containing 10 mM HEPES and transferred to tissue culture treated dishes, and the temperature was shifted to 37° C for the indicated time points to allow endocytosis to occur. Cells were immediately chilled back down to 4° C for the remainder of the staining process. Cells were stained in staining buffer containing AF488-conjugated secondary Ab for 20 min on ice. The stained cells were fixed with 1% paraformaldehyde and analyzed by FCM, and the total fluorescence signal of the analyzed cells was determined using FlowJo software.

II.14 CD8 Pulse Chase assay

HEK293 cells were transiently transfected with Myc–CD8 constructs. 24 hrs after transfection cells were washed once with PBS, then starved for 30 min at 37° C in pulse media containing Met/Cys/Glu free DMEM with 10% dialyzed FBS and L-Glu. Cells were pulsed by the addition of 100 uCI of ^{35}S-Met/Cys (TRAN^{35}S-Label MP Biomedicals) to the media for 10 min. Following the pulse, cells were washed and chased in complete DMEM/F12 + 2 mM Met + 2mM Cys for selected time points, then the media was

removed, and cells were lysed with lysis buffer (0.5% Igepal, 25 mM Tris, 150 mM NaCl, pH 7.5) containing protease inhibitors for 20 min at 4 °C. After centrifugation for 20 min at 11,000 xg, the supernatant was mixed with mouse anti-Myc and Protein A conjugated agarose beads (Invitrogen). After O/N incubation at 4 °C, the beads were washed 4 times with lysis buffer, and then the immunoprecipitated proteins were eluted by incubating the beads with 2X sample buffer. The protein samples resolved by 15% SDS–PAGE were transferred to nitrocellulose membranes and exposed by autoradiography using a Molecular Dynamics Storm 860 imager.

II.15 Peptide pulldown assay

Peptides containing an N-terminal Cys and the amino acid sequence of the extreme C-terminal tail of Kir2.1 or the hit sequences were synthesized by GenScript. Forty nmol of peptides were conjugated to Sulfo-Link resin in coupling buffer (50 mM Tris, 5 mM EDTA-Na, pH 8.5) then washed and blocked in blocking buffer (50 mM Cys in coupling buffer). Peptide conjugated resin was washed in 1 M NaCl solution and lysis buffer (0.5% Igepal, 25 mM Tris, 150 mM NaCl, pH 7.5). HEK293 cells were lysed in lysis buffer and the lysate cleared by centrifugation for 20 min at 11,000 xg. The cleared lysate was incubated with the peptide coupled resin O/N at 4 °C. Then the resin was washed and proteins eluted in 2X sample buffer. Samples were run through SDS-PAGE, and blotted for interaction with β-COP.

II.16 Development and implementation of B31 based screening system:

II.16.1 Preparation of DNA for screen:

We utilized gap repair cloning by homologous recombination in yeast to generate the B31 expressing Kir2.1 C-terminal fusion library. In gap repair cloning by homologous recombination in yeast, yeast are co-transformed with a linearized expression vector and an insert cassette that contains an insert sequence flanked with 15-50 bp regions of homology to the gene/expression vector. The linearized

vector and insert cassette undergo homologous recombination in the yeast, generating a circularized expression vector encoding the modified protein of interest.

We used a pYES2 vector in which GAL1 promoter was replaced with MET25 promoter (pYES2met). The mouse Kir2.1 gene with an EcoRI site added before the termination codon was cloned between the BamHI and NotI sites. The vector was linearized by double digestion with EcoRI an NotI then purified by separation in an agarose gel and concentrated by ethanol precipitation. To generate the insert cassette containing the sequence for the random peptide library, we ordered a polyacrylamide gel electrophoresis (PAGE) purified oligonucleotide that contained a 35 bp region of homology to the Kir2.1 C-term sequence followed by a random sequence encoding a random 4-mer or 8-mer peptide followed by a stop codon and a 35 bp region of homology to the pYES2met expression vector. The random sequence was encoded by an NNK sequence; where N could encode any nucleotide and K could encode G or T. This sequence permits the encoding of all 20 aa residues while eliminating the TAA and TGA stop codons to reduce the chances of getting a truncated peptide. We initially attempted to perform the gap repair cloning with the single stranded oligonucleotides as it has previously been reported that single stranded oligonucleotides, can induce homologues recombination in yeast (54). However, while homologous recombination occurred, we found the transformation efficiency too low, and the level of false positives due to erroneous homologous recombination too high. Therefore, we generated primers to the matching regions of the oligonucleotides and used PCR with the oligonucleotides as template DNA to generate double stranded insert DNA. The double stranded insert cassette was purified by separation in an agarose gel and concentrated by Zymo DNA Clean and Concentrated kit according to manufacturer instructions.

II.16.2 Preparation of electrocompetent B31 and transformation:

B31 was made electrocompetent and transformed by electroporation by following an established high efficiency yeast transformation protocol (55). B31 was used to inoculate a small volume of YPDA, and the culture was shaken at 30 °C O/N and grown to saturation. The O/N culture was used to inoculate a 50 ml culture in YPDA to an OD_{600} of 0.1, and cells were shaken at 30 °C and grown to an OD_{600} of 1.3-1.5. Once the cells reached the OD_{600} of 1.3-1.5, 500 µl of Tris-dithiothreitol (DTT) solution (10 mM Tris, pH 8.0, 2.5 mM DTT) was added to the culture, and the cells were grown an additional 15 min. Cells were harvested by centrifugation, the supernatant removed and the pellet was washed three times in cold electroporation buffer (10 mM Tris, pH 7.5, 270 mM sucrose, 1 mM $MgCl_2$). Cells were resuspended to a final volume of 300 µl in electroporation buffer and divided into 50 µl aliquots. 1ug of linearized vector was added to each aliquot, and insert DNA was added at a 1:1 molar ratio. The yeast-DNA mixture was incubated for 5 min on ice and then transferred to a pre-chilled 0.2 cm electroporation cuvette and electroporated with a GenePulser (BioRad) at 0.54 kV voltage and 25 uF capacitance. Cells were collected in 1 ml YPDA pre-warmed to 30 °C, then shaken at 30 °C for 1 hr. Then the cells were harvested by centrifugation and resuspended in 1 ml water for plating.

II.16.3 B31 plating and screening condition:

Serial dilutions of transformed B31 were plated on YNB with no added KCl to determine the overall transformation efficiency. 1/1000, 1/10,0000, and 1/100,000 dilutions were plated per transformation. YNB plates with 600 mM KCl added were used to screen the yeast library. A 1/10 to 1/20 volume of transformed B31 per transformation was plated per screening plate until all yeast was used. Yeast was cultured for seven days at 30 °C and then stored at 4 °C.

II.16.4 Isolation of DNA from B31

The C-terminal sequences of the Kir2.1-fusion proteins from the B31 transformants that survived the screen were identified either by colony PCR or plasmid isolation.

II.16.4 Yeast colony PCR:

Yeast colony PCR was performed using a protocol adapted from the Wittrup Lab Colony PCR Protocol (http://www.openwetware.org/wiki/Wittrup:_Yeast_colony_PCR). Yeast cells were collected by dabbing a pipette tip into a yeast colony and re-suspending cells in 20 µl water. Yeast were microwaved on high power for 30 seconds, and then 2 µl of the yeast template was added to a PCR mix containing 39.5 µl water, 5 µl 10X Thermopol reaction buffer, 1 µl dNTP (10mM), 1 µl each of forward and reverse primer (20uM) and 0.5 µl Vent DNA polymerase (2000 U/ml). PCR was run using the following conditions: Denaturing cycle: 4 min at 95 °C, Cycles 2-35: 1 min at 95 °C, 1 min at 55 °C, 1 min at 72 °C, and Final anealing cycle: 10 min at 72 °C. PCR products were purified using a Zymo DNA Clean and Concentrator Kit.

II.16.4b Yeast plasmid isolation:

Plasmids were isolated from *S. cerevisiae* with the QIAprep Spin Miniprep Kit following a Qiagen protocol (https://www.qiagen.com/gb/resources/resourcedetail?id=5b59b6b3-f11d-4215-b3f7-995a95875fc0&lang=en

II.16.5 Sequencing and transfer of hit sequences to C-terminal tail of Kir2.1 in Yeast and mammalian expression vectors:

The C-terminal Kir2.1-fusion sequences obtained from the B31 screen by either colony PCR or yeast plasmid isolation were sequenced by Sanger sequencing by the UIC genomic core facility. Colony PCR products or isolated yeast plasmids were digested with PfIMI and NotI, and cloned back into the Kir2.1 sequence in the pYES2met vector for yeast expression and the HA-tagged Kir2.1 sequence in pCDNA3.1(+) for mammalian expression.

II.16.6 Additional screening optimizations and modifications:

At times, the following optimizations and modifications were made to the B31 screening system to improve efficiency, reduce false hits, and increase the chances at successfully identifying diverse trafficking motifs.

II.16.6a The addition of multiple out of frame stop codons to library insert to prevent Kir2.1 sequence elongation.

After the initial stop codon in the insert sequence, two additional out-of-frame stop codons were added before the downstream matching region. In the event of a congeneric oligonucleotide with one or more deleted nucleotides, which eliminates the initial stop codon, translation of the Kir2.1 library would stop with the addition of only one or two amino acids.

II.16.6b Use of an NVK sequence to reduce the frequency of strong hydrophobic sequences:

The most commonly identified sequence type from the screen was sequences containing a patch of strong hydrophobic residues that both reduced the surface levels of Kir2.1 when fused to its C-terminal tail and also showed a much lower level of overall expression by western blot analysis. We experimentally determined that these sequences were acting as a substrate for ERAD. The high incidence of these sequences in the screen made identifying other types of sequence motifs very inefficient. To combat this, we performed the screen with an oligonucleotide in which the random region was encoded by an NVK sequence; where N could encode any nucleotide, V could encode A, C, or G, and K could encode G or T. This sequence still permitted the encoding of all 20 aa residues, however, it now discriminated against strong hydrophobic residues and still eliminates the TAA and TGA stop codons.

II.16.6c Redesign the insert DNA matching region upstream of the random library sequence to eliminate hydrophobic sequences on the C-terminal tail of Kir2.1:

The last two amino acids of Kir2.1 are E and I. We added an EcoRI site at the end of Kir2.1 encoding an additional E and F residues making the final four amino acid residues of our Kir2.1 construct E-I-E-F. which contains two strong hydrophobic residues. We therefore changed the matching region of the insert upstream of the base pairs encoding these residues so that after homologous recombination they would be looped out during homologous recombination.

II.16.6d Addition of N-terminal GFP tag to Kir2.1:

An additional in-frame yeast-optimized GFP was cloned to the N-terminal tail of Kir2.1 in the pYes2met vector to allow for total protein expression to be measured in yeast by FCM analysis.

II.16.6e Reduction of false positive clones due to erroneous homologous recombination by screening with additional KanMX or TrpMX selection marker:

Whenever performing gap repair cloning by homologous recombination in yeast there is a small percentage of vector plasmid that undergoes erroneous homologous recombination in which the vector recombinants with itself losing the insert sequence however maintaining the selection marker. In the B31 screening system, B31 containing plasmid that maintains the auxotrophic marker sequence but loses the Kir2.1 sequence will survive the screening condition, appearing as a false hit in the screen. To reduce the prevalence of false hits by erroneous homologous recombination we performed the gap repair cloning with two inserts; the random C-terminal insert for Kir2.1 as well as an additional marker gene; either the KanMX or TrpMX marker.

We first tested the system using the additional KanMX selection marker. We PCR amplified the KanMX cassette from the pFA6a-KanMX4 vector flanked with the NotI and XhoI restriction enzyme sites and cloned the gene in to our pYes2met-Kir2.1 immediately after the Kir2.1 stop codon generating pYes2met-Kir2.1 + KanMX. The vector was linearized by double digestion with EcoRI and EcoNI. These enzymes both linearized the vector as well as truncated the first 770 bp of the KanMX cassette

sequence. The digested vector was purified by separation in an agarose gel and concentrated by ethanol precipitation. We used PCR to amplify the truncated region of the KanMX cassette with additional base pairs beyond the EcoNI site for the matching region. The PCR-amplified fragment was purified by separation in an agarose gel and concentrated by ethanol precipitation. Finally, we used PCR to amplify and make double stranded a PAGE-purified oligionucliotide that contained a 35 bp region of homology to the Kir2.1 C-terminal sequence followed by a random sequence encoding a random 4-mer or 8-mer peptide, followed by a stop codon and a 35 bp region of homology to the KanMX cassette sequence. The double stranded insert cassette was purified by separation in an agarose gel and concentrated by Zymo DNA clean and concentrated kit.

The yeast transformation was performed as described above, however, using the digested vector and the two inserts at a 1:1:1 molar ratio. It has been reported that performing gap repair cloning by homologous recombination in yeast with two DNA inserts undergoes homologous recombination with similar efficiency as one insert (56), which was true in our hands. Under these conditions only B31 that underwent correct homologous recombination should be able to survive G418 selection, however G418 is known to be ineffective on SD media containing ammonium sulfate (57). Selection was therefore done on SE plates (57) in which ammonium sulfate is replaced with Glu, lacking Ura and Met, with G418 and 600 mM K^+ added. Despite using SE selection plates G418 selection was still partially impaired in control plates possibly due to the high KCl concentration used for the screen. We therefore replaced the KanMX cassette with a TrpMX cassette and screened on SD plates –Ura/-Met/-Trp with 600 mM K^+.

Knock out of Doa10 from B31:

We used three sequential PCR steps to both amplify the KanMX cassette and add 90 bp of homology to the 5’ untranslated region and the 3’ untranslated region of the Doa10 gene. The pFA6a-KanMX4 vector was used as the template DNA, and the PCR product was purified by separation in an agarose gel and

concentrated by ethanol precipitation. B31 was made electrocompetent as described in the B31 screening. 1 µg of the KanMX insert cassette was added to a 50 µl aliquot of electrocompetent B31. The Yeast-DNA mixture was incubated for 5 min on ice then transferred to a pre-chilled 0.2 cm electroporation cuvette and electroporated with GenePulser at 0.54 kV voltage and 25 uF capacitance. Cells were collected in 2 ml of 30 °C pre-warmed YPDA and shaken at 30 °C for 3 hrs, and then harvested by centrifugation and resuspended in 1 ml water for plating. Twenty µl were plated on a YPDA plate with 200 µg/ml G418 and cultured in 30 °C for 7 days. After 7 days the plate had grown to confluence, and the yeast were replica plated onto another YPDA plate with 200 µg/ml G418 to eliminate background growth. The replica plating grew approximately 100 individual colonies. Colony PCR was performed with primers designed upstream and downstream of the KanMX insert cassette to validate that the cassette integrated at the correct loci knocking out the Doa10 gene. The knockout of Doa10 was finally confirmed by sequencing of the colony PCR products.

III. Potential use of potassium efflux-deficient yeast for studying trafficking signals and potassium channel functions

Parts of this chapter have been previously published in:

Bernstein, J. D., Okamoto, Y., Kim, M., and Shikano, S. (2013) Potential use of potassium efflux-deficient yeast for studying trafficking signals and potassium channel functions. *FEBS Open Bio* 3, 196-203

III.1 Rationale:

Yeast offers a good model for studying mammalian protein trafficking mechanisms, since the basic molecular machinery for protein trafficking is well conserved between yeast and mammal cells. Indeed, much of our understanding of the mechanisms of protein transport in mammalian cells originated from studies performed in yeast (58). Additionally, with the ease of both deleting yeast endogenous ion channels as well as heterologously expressing ion channels, yeast has also been instrumental in studying ion channel function and trafficking (59). Recently, a system was developed in yeast using Kir2.1 as a reporter protein to screen for the identification of novel trafficking pathways that increase the surface levels of membrane proteins by complementation of growth on low K^+ media. That system utilized the SGY1528 strain of yeast that lacks K^+ uptake transporters Trk1 and Trk2 and can only grow in low K^+ media when heterologously expressing Kir2.1 on the plasma membrane (45). Screening systems utilizing SGY1528 yeast have identified both *cis* and *trans* elements that promote the surface expression of membrane proteins (45,46). However, to date, there have been no systematic yeast-based gain-of-function screening systems to identify factors that downregulate the plasma membrane levels of membrane proteins.

A previous study by Kolacna *et al*. reported that the B31 yeast strain (*ena1-4Δ nha1Δ*) lacking the K^+ and sodium (Na^+) efflux system shows sensitivity to higher external concentrations of alkali–metal–cation salts when transformed with a mammalian Kir2.1 channel (60). Due to the fact that Kir2.1 activity

inversely correlates with B31 growth in high K^+ media, we hypothesized that the complementation of growth of B31 expressing Kir2.1 on high K^+ media would reflect the trafficking of functional receptor to the cell surface. Factors that reduce either the function or surface levels of Kir2.1 - including structural determinants of the K^+ channel, or the exposure or fusion of trafficking signals known to reduce the surface levels of proteins - would allow B31 growth on high K^+ media. Finally, with the ease of clonal expression of library transgenes in yeast, we hypothesized that B31 could be used to develop a new yeast-based screening system to enable systematic identification of the sorting motifs that downregulate surface expression of membrane proteins. To achieve our goal, we examined (1) if specific mutations that disrupt functions of Kir2.1 can be represented by B31 tolerance to high K^+, (2) if other K^+ channel family members can also function in the B31 growth assay, and (3) if the activities of Kir2.1-fused trafficking signals that downregulate surface expression can be represented by B31 tolerance to high K^+.

III.2 Experimental Results:

III.2.1 B31 tolerance to high K^+ media represents the loss of Kir2.1 activity on the cell surface:

A previous study by Kolacna *et al*. reported that the B31 strain (*ena1-4Δ nha1Δ*) lacking the K^+ and Na^+ efflux system shows sensitivity to higher external concentrations of alkali–metal–cation salts when transformed with a mammalian Kir2.1 channel. Inhibition of the channel through barium (Ba^{+2}) or low pH rescued the growth of B31 cultured in high K^+ media, demonstrating that the Kir2.1 function at the plasma membrane was responsible for the growth inhibition at high K^+ (60). We expanded upon this study to explore if the natural mutants of Kir2.1 that inhibit either the function or surface trafficking of the channel would rescue the growth of B31 cultured in high K^+ media. We selected V302M and Δ314/315 mutants, which are both responsible for human Andersen–Tawil syndrome that causes periodic paralysis and ventricular arrhythmias (61). The V302M mutation is reported to disrupt K^+ ion

conduction through G-loop without reducing the cell surface expression of the channel (62), while Δ314/315 (deletion of aa 314 and 315) is known to retain the channel in the Golgi (35,61). Our flow cytometry (FCM) and western blot analyses of the transfected HEK293 cells confirmed the cell surface phenotypes of these mutant Kir2.1 channels (Fig. 2A). Slightly elevated surface expression of the V302M mutant compared with the wild-type (WT) Kir2.1 was consistent with the observations from other studies (62). On this basis, we tested the growth of B31 cells transformed with these Kir2.1 constructs. Consistent with the previous report (60), the expression of WT Kir2.1 showed a marked growth inhibition of B31 cells in high external KCl conditions such as 200 mM and higher (Fig. 2B, 2nd row). In contrast, both of the mutants V302M and Δ314/315 allowed growth of B31 at comparable levels to that of vector-transformed cells (Fig. 2B, 1st, 3rd, and 4th rows).

III.2.2 B31 growth inhibition in high K^+ media represents KCNK channel activities on cell surface:

We were curious if other K^+ channel family members can also be studied in B31 yeast. It has been reported that a voltage-gated mammalian neuronal K^+ channel ether à go-go 1 (EAG1), when lacking its intracellular amino-terminus (N-terminus), can be functionally expressed in B31 and increase the growth sensitivity to high K^+ (63). It is conceivable that a K^+ channel with high open probability at the resting membrane potential has a good chance to function in B31 cells. We tested two members of a two-pore-domain K^+ channel (KCNK) family, KCNK3 and KCNK9. Many of the KCNK family members are open channels and responsible for generating the background 'leak' K^+ current at the resting membrane potential (64). Increasingly studies have been showing critical involvement of KCNK channels in a wide range of human diseases. For instance, human genetic studies indicate an involvement of KCNK3 gene in the pathogenesis of primary hyperaldosteronism (65). KCNK9 was found to be overexpressed in various human cancers, and its overexpression was experimentally shown to be sufficient to confer a tumorigenic phenotype such as tolerance to low oxygen and low serum (66). In addition, a genetic point mutation of KCNK9 is associated with abnormal development that causes a mental retardation (67).

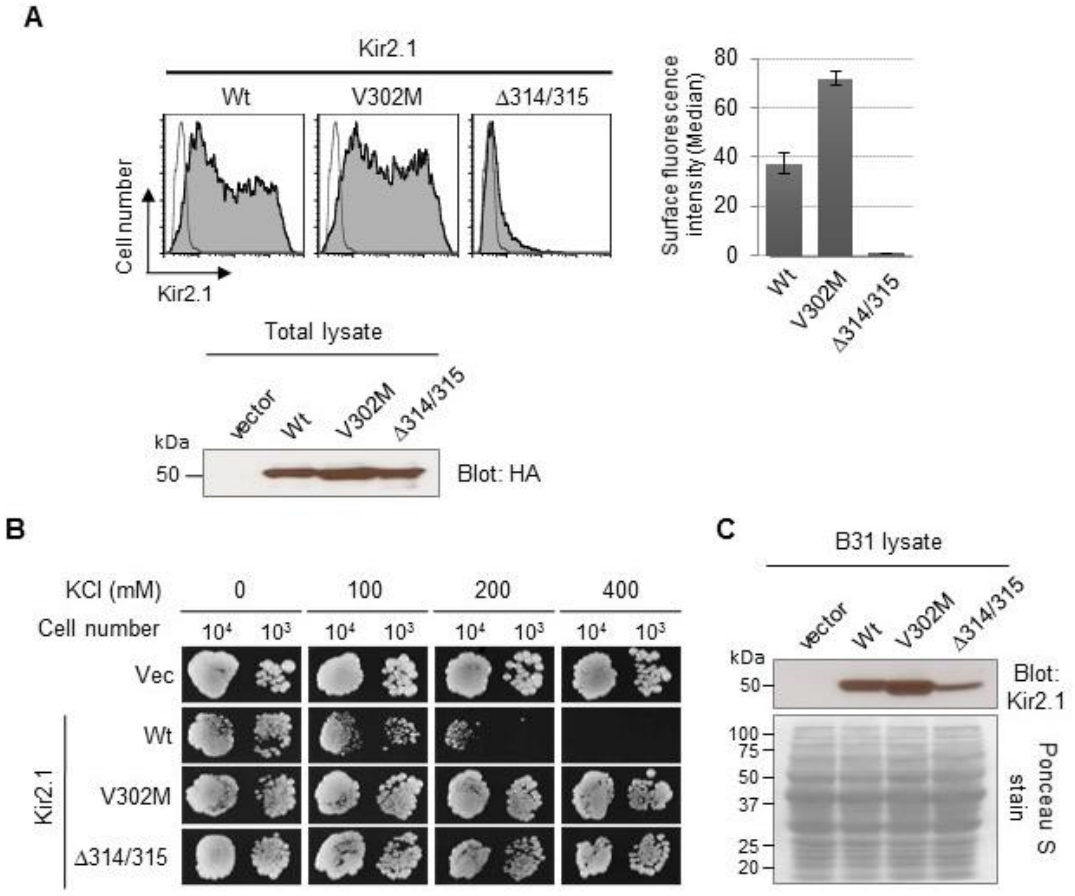

Figure 2. B31 tolerance to high K^+ media represents the loss of Kir2.1 activity on cell surface. (A) Surface expression of Kir2.1 channels. HEK293 cells were transiently transfected with HA-tagged Kir2.1 constructs or pCDNA3.1(+) vector alone. Cells stained with the HA Ab followed by Alexa Fluor 488-conjugated secondary Ab were analyzed by flow cytometry (FCM). Histograms from the representative samples are shown (left panels). The *x*-axis indicates the fluorescence intensity in a logarithmic scale and *y*-axis indicates the cell number. The histograms of Kir2.1-transfected cells (filled) were overlaid with that of vector-transfected cells (unfilled). The bar graph (right panel) shows the Median values for the total cell populations determined by FlowJo software to compare the relative surface intensity of Wt and mutant Kir2.1 channels. The values indicate average±SD of triplicate samples from the representative of three experiments. The lower panel shows the total expression levels of Kir2.1 proteins. Total lysates from HEK293 cells transfected with HA-Kir2.1 constructs were resolved by SDS–PAGE and immunoblotted for HA. (B) Growth assay of Kir2.1-expressing B31. The Kir2.1- or pYES2met vector-transformed B31 cells were plated on YNB media (pH 6.50) with the indicated concentrations of KCl and cultured at 30 °C. The images were photographed at Day 5. (C) Expression of Kir2.1 channels in B31 cells. The proteins were extracted from B31 cells transformed with pYES2met vector or the indicated Kir2.1 constructs. The samples were resolved by SDS–PAGE and immunoblotted for Kir2.1

Nevertheless, compared with other voltage-gated K^+ channel families, KCNKs are still relatively new and their biochemical properties are not fully understood.

Previous studies have reported that KCNK3 and KCNK9 channels carry a 14-3-3 protein binding motif at the extreme C-terminus (RXXSX-COOH, see Fig. 3A) (45,68). The phosphorylation-dependent 14-3-3 binding appears to occlude the overlapping di-Arg ER retention/retrieval signal that would be otherwise recognized by the COPI complex, and thus allows optimal surface trafficking of the channels. The presence and the exact penultimate position of the serine (Ser) residue (Fig. 3A underlined) in the C-terminus is critical for the 14-3-3 binding (45,68). So, we created the 14-3-3 binding-deficient KCNK channels by shifting the position of a penultimate Ser (KCNK3 Δ410) or by mutating Ser to Ala (KCNK9 S373A). These mutants and WT channels were expressed in HEK293 cells and examined for the association with 14-3-3 and COPI proteins (Fig. 3B). As expected, both KCNK3 and KCNK9 mutants lacked 14-3-3 binding but associated with more β-COP, a major binding subunit of COPI complex, than the WT channels did. The FCM analysis showed that the surface expression of these mutants were substantially lower when compared with that of WT channels (Fig. 3C). Having this, we expressed these KCNK channels in B31 for the growth test (Fig. 3D). The expression of WT KCNK3 and WT KCNK9 resulted in a marked growth inhibition of B31 cells on the high external K^+ plates, i.e., 500 mM for KCNK3 (left panels) and 600 mM for KCNK9 (right panels). In contrast, the 14-3-3-binding mutants allowed similar level of growth to that of vector-transformed cells. The expression of KCNK proteins in these B31 transformants was below detectable level by the Abs we used (data not shown). WT KCNK9 also caused substantial inhibition of B31 growth in the liquid media with high K^+, and this inhibition was sensitive to the acidic pH lower than 6.0 (Fig. 3E). This was consistent with the reported acid sensitivity of several KCNK members, including KCNK9 (64). Moreover, the growth inhibition of KCNK9-transformed B31 was attenuated by zinc ion (Fig. 3F), which has been reported to inhibit this channel in mammalian cell (69).

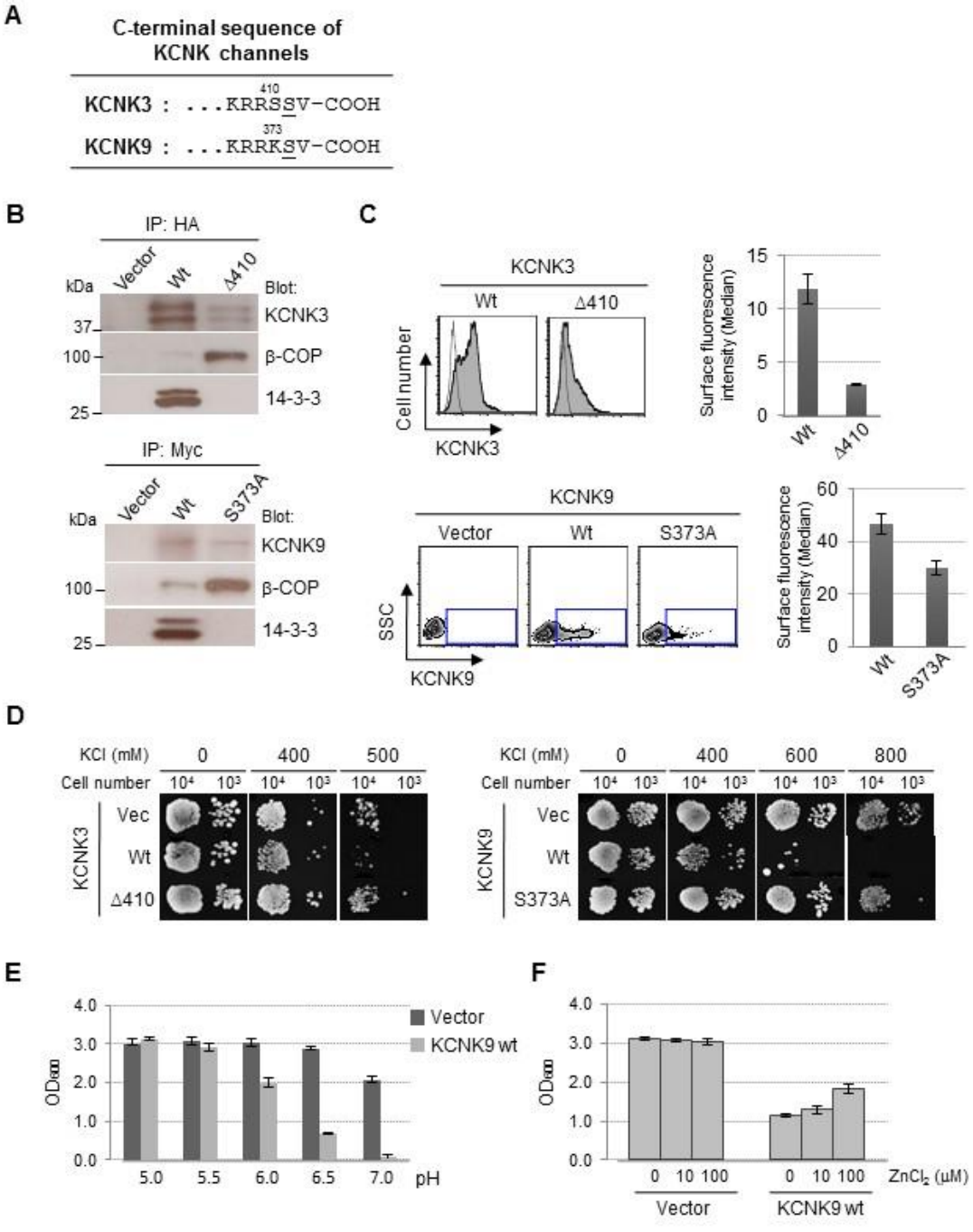
A
C-terminal sequence of KCNK channels
KCNK3 : ...KRRSSV-COOH
410
KCNK9 : ...KRRKSV-COOH
373
B
IP: HA
Vector
Wt
Δ410
kDa
Blot:
KCNK3
β-COP
14-3-3
37
100
25
IP: Myc
Vector
Wt
S373A
KCNK9
β-COP
14-3-3
C
KCNK3
Wt
Δ410
Cell number
KCNK3
Surface fluorescence intensity (Median)
KCNK9
Vector
Wt
S373A
SSC
KCNK9
D
KCl (mM)
0
400
500
Cell number
Vec
Wt
Δ410
KCNK3
KCl (mM)
0
400
600
800
Cell number
Vec
Wt
S373A
KCNK9
E
Vector
KCNK9 wt
OD600
pH
F
OD600
0 10 100
0 10 100
ZnCl2 (μM)
Vector
KCNK9 wt

Figure 3. B31 growth inhibition in high K+ media represents KCNK channel activities on cell surface. (A) Alignment of C-terminal sequences from KCNK3 and KCNK9 channels. (B) Association of COPI and 14-3-3 proteins with KCNK3 (upper panels) and KCNK9 (lower panels). HEK293 cells transfected with HA-KCNK3 or Myc-KCNK9 were lysed and immunoprecipitated with HA or Myc Abs. The eluants were resolved by SDS–PAGE and immunoblotted for the associating β-COP and 14-3-3 as well as HA (KCNK3) or Myc (KCNK9). (C) Surface expression of KCNK3 and KCNK9. HEK293 cells were transfected with HA-tagged rat KCNK3 or Myc-tagged human KCNK9 and analyzed for cell surface expression by FCM. For KCNK3 (upper panels), the expression is shown in histograms and the Median values were determined for the total cell populations as described for Fig. 1. The histograms of KCNK3-transfected cells (filled) were overlaid with that of vector-transfected cells (unfilled). For KCNK9 (lower panels), the expression is shown in density plots (see Section 2) where x-axis indicates the fluorescence intensity in a logarithmic scale and y-axis indicates the side scatter (SSC) of the cell. The Median values were determined for the cells that were positive for the KCNK9 signal (shown in squares within the density plots). The bar graphs indicate the Median values in average±SD of triplicate samples from the representative of three different experiments. (D) Growth assay of KCNK-expressing B31. The KCNK- or pYES2met vector-transformed B31 cells were plated on YNB media (pH 7.0 for KCNK3 and pH 6.50 for KCNK9) with indicated concentrations of KCl and cultured at 30 °C. The images were photographed at Day 7. (E) The effect of pH on the growth of KCNK9-expressing B31. The B31 cells transformed with vector or KCNK9 WT were grown in the liquid YNB media with indicated pH and 400 mM KCl. (F) The effect of zinc on the growth of KCNK9-expressing B31.The B31 cells transformed with vector or KCNK9 Wt were grown in the liquid YNB media with indicated concentrations of $ZnCl_2$ and 400 mM KCl at pH 6.50. In both of the pH and zinc tests, the OD at 600 nm was measured at the start of and after 15 h of culture. The values after growth of the culture were subtracted with those at the start and shown in average±SD of triplicate samples from the representative of three experiments.

III.2.3 B31 tolerance to high K^+ represents the activity of trafficking signals that downregulate surface expression of membrane proteins:

We demonstrated in III.2.1 and III.2.2 that the B31 growth inhibition on high K^+ media represents the functional levels of heterologously expressed Kir2.1 or KCNK channels on the cell surface. Factors inhibiting the K^+ channel function, such as channel inhibitors, and mutations disrupting K^+ ion conduction through the channel, as well as factors that inhibit the trafficking of the channels to the cell surface, such as the exposure of endogenous retrograde trafficking motifs or the obliteration of a Golgi exit signal, allowed for B31 growth on high K^+ media. However, the utility of K^+ transport-defective yeast does not need to be limited to the study of K^+ channel biology itself. Rather, it can be used to study the trafficking motifs that regulate the cell surface levels of membrane proteins. Indeed, a screen was conducted using SGY1528 yeast that lacks K^+ uptake transporters Trk1 and Trk2, which requires Kir2.1 surface expression to grow on low K+ media. This screen identified the C-terminal 14-3-3 binding motifs that were eventually found to promote surface expression of various membrane proteins including a G-protein coupled receptor GPR15 as well as KCNK3 and KCNK9 channels (45,70).

Since the loss of cell surface Kir2.1 or KCNK channels results in B31 survival in high K^+ media (2 and 3), we thought that B31 strain would be potentially applicable to such screening of a random peptide library that would allow identification of novel sequence motifs that downregulate surface expression of membrane proteins. To explore this possibility, we tested the signal motifs that have been reported to target intracellular compartments. These include the di-Arg (RXR) type ER retention/retrieval motifs from the C-terminus of the Kir6.2 channel (71) and a G-protein coupled receptor GPR15 (70), and also the endocytosis motif from a dopamine transporter (DAT) (72) (Fig. 4A). For the di-Arg motif from GPR15, the penultimate Ser was mutated to Ala (S359A) in order to prevent occlusion of the di-Arg motif (Arg^{352}/Arg^{354}) by 14-3-3 binding (70). The expression levels of these Kir2.1 fusions were similar in the transiently transfected HEK293 cells (Fig. 4B). As expected, the Kir2.1 fused with the RXR motifs from

Kir6.2 and $GPR15_{S359A}$ were associated with more β-COP when compared with WT Kir2.1 (Fig. 4C). The FCM analysis showed that the surface expression of all of the tested Kir2.1 fusions were significantly lower than that of WT channel (Fig. 4D). Then we addressed if these cell surface phenotypes of Kir2.1 channels are represented by the B31 growth. All of the Kir2.1 fusions allowed better growth of B31 in high K^+ media when compared with WT Kir2.1 (Fig. 4E). In B31 cells, the Kir2.1 channels fused with the RXR motif from Kir6.2 and the endocytic motif from DAT showed somewhat lower expression than the WT channel did (Fig. 4F). As mentioned for the Kir2.1 Δ314/315 mutant (Fig. 2C), we believe that this represents the enhanced susceptibility of those channels to the yeast degradation pathways due to their intracellular retention. It is of note that the RXR motif from $GPR15_{S359A}$ did not support B31 growth as efficiently as the RXR motif from Kir6.2 did (Fig. 4E), while both of these motifs seemed equally effective in retaining the Kir2.1 channel in HEK293 cells (Fig. 4D). In addition, the endocytic motif from DAT was less effective in reducing the surface expression of Kir2.1 in HEK293 cells while it allowed more B31 growth when compared with the $GPR15_{S359A}$ sequence. These observations might reflect the difference between yeast and mammalian cells in the recognition of these trafficking motifs by the cellular transport machineries. Nevertheless, our results indicate that the C-terminally transplanted signal motifs attenuated the Kir2.1 channel activity by reducing its cell surface density in B31 yeast.

Discussion:

A previous study by Kolacna *et al*. reported that the B31 yeast strain (*ena1-4Δ nha1Δ*) lacking the K^+ and Na^+ efflux system shows sensitivity to higher external concentrations of alkali–metal–cation salts when transformed with a mammalian Kir2.1 channel (60). Due to the fact that Kir2.1 activity inversely correlates with B31 growth in high K^+ media, we hypothesized that the complementation of growth of B31 expressing Kir2.1 on high K^+ media would reflect the trafficking of functional receptor to the cell surface.

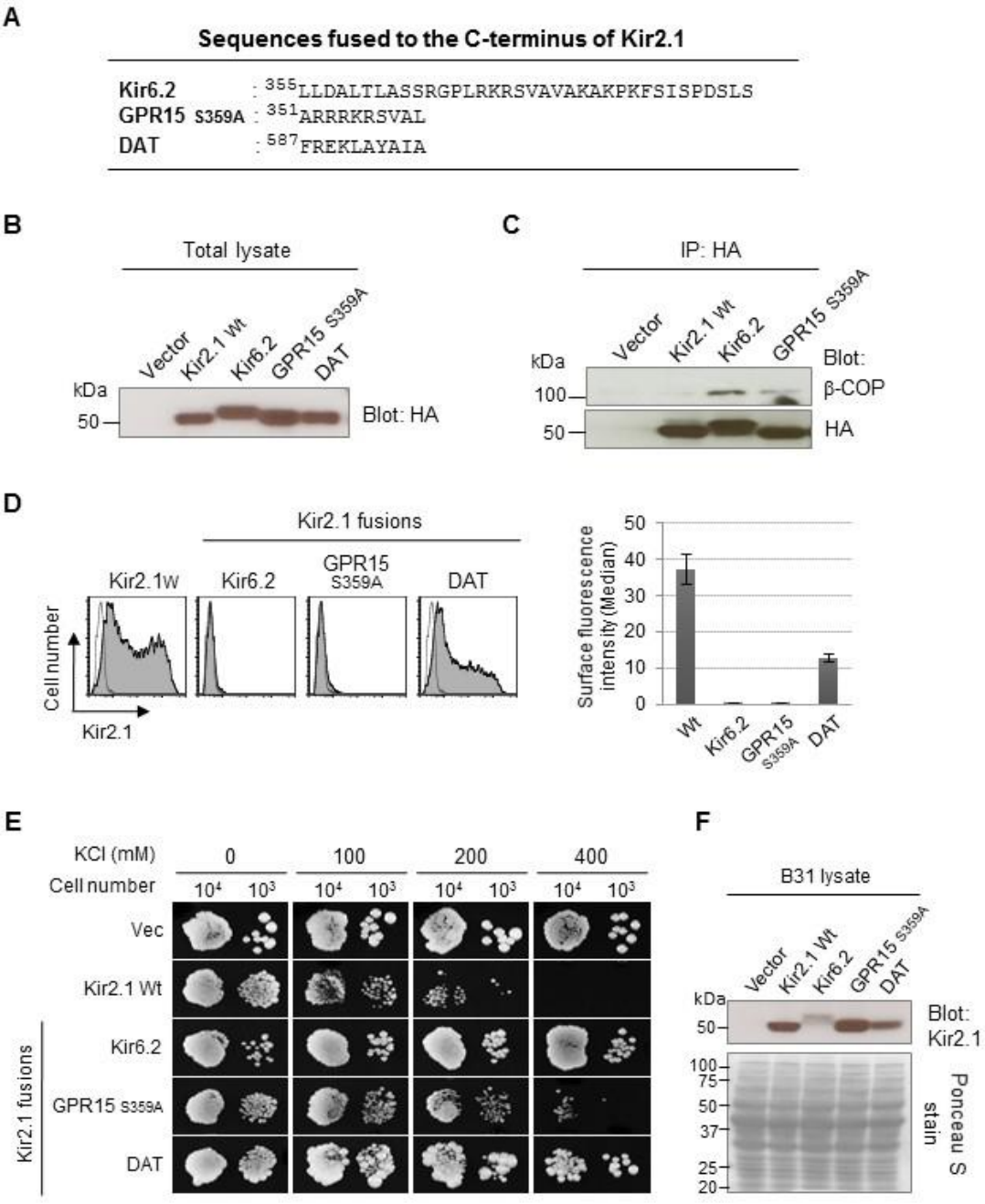
A
Sequences fused to the C-terminus of Kir2.1
Kir6.2 : 355LLDALTLASSRGPLRKRSVAVAKAKPKFSISPDSLS
GPR15 S359A : 351ARRRKRSVAL
DAT : 587FREKLAYAIA
B
Total lysate
Vector
Kir2.1 Wt
Kir6.2
GPR15 S359A
DAT
kDa
50
Blot: HA
C
IP: HA
Vector
Kir2.1 Wt
Kir6.2
GPR15 S359A
kDa
100
50
Blot:
β-COP
HA
D
Kir2.1 fusions
Kir2.1W
Kir6.2
GPR15 S359A
DAT
Cell number
Kir2.1
Surface fluorescence intensity (Median)
50
40
30
20
10
0
Wt
Kir6.2
GPR15 S359A
DAT
E
KCl (mM)
0
100
200
400
Cell number
10⁴
10³
Vec
Kir2.1 Wt
Kir6.2
GPR15 S359A
DAT
Kir2.1 fusions
F
B31 lysate
Vector
Kir2.1 Wt
Kir6.2
GPR15 S359A
DAT
kDa
50
Blot: Kir2.1
100
75
50
37
25
20
Ponceau S stain

Figure 4. B31 tolerance to high K+ represents the activity of trafficking signals that down-regulate surface expression of membrane proteins. (A) Sequences that were fused to the C-terminus of Kir2.1 channels. (B) Total expression levels of Kir2.1 fusions. Total lysates from HEK293 cells transfected with HA-Kir2.1 constructs were resolved by SDS–PAGE and immunoblotted for HA. (C) Association of COPI with Kir2.1 fusions. The Kir2.1 fusions immunoprecipitated with αHA Ab were resolved by SDS–PAGE and immunoblotted for HA (lower panel) and the associating β-COP (upper panel). (D) Surface expression of Kir2.1 fusions. HEK293 cells were transfected with HA-Kir2.1 constructs and analyzed for cell surface expression by FCM. The histograms (left panels) of Kir2.1-transfected cells (filled) were overlaid with that of vector-transfected cells (unfilled). The Median values were determined for the total cell populations and shown in average±SD of triplicate samples from the representative of three experiments (right panel). (E) Growth assay of B31 expressing Kir2.1 fusions. The Kir2.1- or pYES2met vector-transformed B31 cells were plated on YNB media (pH 6.50) with indicated concentrations of KCl and cultured at 30 °C. The images were photographed at Day 7. (F) Expression of Kir2.1 channels in B31 cells. The proteins were extracted from the B31 cells transformed with pYES2met vector or the indicated Kir2.1 constructs. The samples were resolved by SDS–PAGE and immunoblotted for Kir2.1 (upper panel). The lower panel shows the Ponceau S staining of the transfer membrane, indicating similar loading of the proteins for each sample.

As a proof of concept, we examined (1) if specific mutations that disrupt functions of Kir2.1 can be represented by B31 tolerance to high K^+, (2) if other K^+ channel family members can also function in the B31 growth assay, and (3) if the activities of Kir2.1-fused trafficking signals that downregulate surface expression can be represented by B31 tolerance to high K^+.

The fact that the natural mutants of Kir2.1 that inhibit either the ion conductance through the channel (V302M mutation) or the post-Golgi trafficking of the channel to the plasma membrane (Δ314/315 mutation) was reflected in the B31 growth in high K^+ media demonstrates the potential of B31 both as a tool for identifying the structural determinants of Kir2.1 channel functions, and for studying the trafficking of Kir2.1.

The growth phenotype of B31 in high K^+ media also reflected the surface expression of KCNK3 and KCNK9, two additional K^+ channel family members that are open channels at resting membrane potential. These results indicate that KCNK3 and KCNK9, and possibly more KCNK members, function in B31 yeast similarly to Kir2.1 to confer sensitivity to high external K^+. These channels, despite being associated with many diseases, are still not well understood. Thus, the B31 growth assay offers a valuable tool for identifying the structural determinants for the activities and cell surface expression of KCNK channels. Moreover, the restored growth of KCNK9-transformed B31 in liquid culture with zinc provides a basis for potential high-throughput screening for small molecule inhibitors of KCNK channels. Indeed, such work has been reported with the SGY1528 strain to successfully identify the inhibitors of Kir2.1 channel (73). Additionally, given the fact the exposure of the di-Arg ER retrieval motif was reflected in the B31 growth, B31 could potentially be utilized to study the trafficking of KCNK3 and KCNK9 as well.

Finally, the fact that the fusion of the previously characterized trafficking motifs known to reduce the surface levels of proteins to Kir2.1 was reflected in the growth phenotype of B31 cultured in high K^+

media demonstrates that the utility of K^+ transport-defective yeast is not limited to the study of K^+ channel biology itself, but can be used as a reporter protein to study trafficking motifs that reduce the surface levels of proteins. Furthermore, our results suggest the potential to develop B31 into a systematic screening system for identifying the *cis*-acting peptide sequences that downregulate surface trafficking of the K^+ channels and other membrane proteins in mammalian cells.

A previously developed system utilized SGY1528 yeast expressing a Kir2.1 C-terminal peptide fusion library to identify a peptide sequence that increased the surface levels of Kir2.1 on the plasma membrane (45), however to date no such gain-of-function yeast systematic screening has been developed to identify the signal sequences that reduce the surface level of proteins. The development of such a system would both increase the tools by which we study protein trafficking and aid in the further elucidation of trafficking motifs and pathways. Moreover, the fact that the B31 growth phenotype in high K^+ media reflected both the fusion of an ER retrieval motif and an endocytosis motif suggests that a B31-based screening system for novel trafficking motifs could be a robust system with the ability to identify trafficking signals that function through multiple distinct trafficking pathways (Fig. 5).

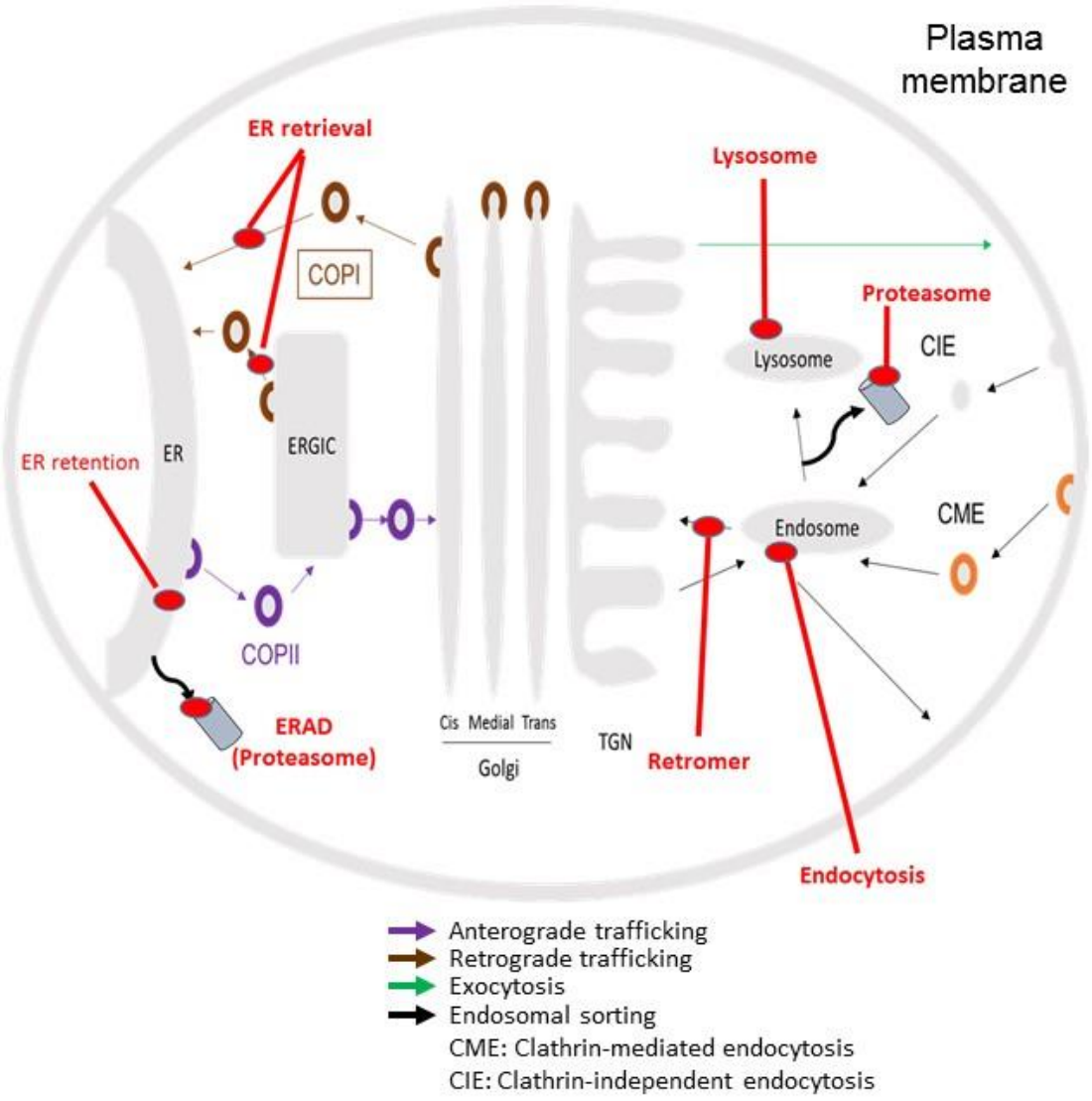

Figure 5. The B31 screening system can potentially identify trafficking motifs that reduces the surface levels of proteins through multiple trafficking pathways. Motifs that function either as an ERAD, ER retention, ER retrieval, retromer, endocytosis, lysosmal or proteasomal signal can potentially be identified through the B31 screening system.

IV. The development and use of the B31 based screening system to identify signal motifs that reduce the surface levels of membrane proteins

Parts of this chapter have been previously published in:

Bernstein, J. D., Okamoto, Y., Kim, M., and Shikano, S. (2013) Potential use of potassium efflux-deficient yeast for studying trafficking signals and potassium channel functions. *FEBS Open Bio* 3, 196-203

IV.1 Rationale:

The cell surface density of membrane proteins dictates their corresponding cellular activity. Intracellular trafficking of membrane proteins is often dictated by the distinct signal sequences on the cargo proteins (8). These trafficking signals often take the form of short linear amino acid motifs in the cytosolic regions of membrane proteins (27-29,31). Many diseases, such as cystic fibrosis, arise from defects in cell surface trafficking of membrane proteins (5). Therefore, identifying, characterizing, and elucidating the mechanisms of trafficking signal sequences is important for understanding normal cellular physiology, disease physiology, and the potential development of therapeutic interventions for diseases that involve trafficking defects. It is not surprising that membrane protein trafficking is heavily studied and many trafficking sequences have been identified and characterized (31). However, despite the progress that has been made, many membrane proteins are transported throughout the cell without containing any of the characterized trafficking motifs (43). Furthermore, there are membrane proteins that traffic through unidentified trafficking pathways (74,75). We therefore hypothesize that there are more trafficking motifs that regulate the surface expression of membrane proteins that have not yet been characterized.

The majority of the previously identified sequence motifs that direct cargo proteins to the membrane compartments have been discovered by studies on individual protein molecules. These studies typically use mutational analysis of a protein of interest to identifying mutations that alter the normal trafficking

of the protein, then hone in to identify the essential residues of the signal (44). More systematic approaches to identifying trafficking signals would facilitate our understanding of membrane protein trafficking. Indeed, recently a few yeast based systematic screening systems have been developed to study protein trafficking. These systems utilized the ability of animal K^+ channels such as Kir family channels to complement the growth of a K^+ uptake-deficient *S. cerevisiae* strain, e.g., SGY1528 that lacks major yeast K^+ uptake transporters Trk1 and Trk2 (76), in low K^+ media. For instance, Shikano *et al*. used SGY1528 cells to screen a library of Kir2.1 channels that are fused with C-terminal random 8-mer peptide sequences and identified a group of *cis*-acting sequences that specifically interact with 14-3-3 proteins and promote surface expression of membrane proteins (45). Moreover, the screening of a cDNA library transduced into the Kir2.1 channel-expressing SGY1528 cells resulted in a discovery of a *trans*-acting protein that enhances the cell surface expression of Kir2.1 (46).

A major limitation on the previously developed SGY1528 based screening systems is that they can only identify factors that increase the surface levels of membrane proteins. Currently, there has been no yeast-based gain-of-function screening system developed to identify signal motifs that downregulate plasma membrane levels of proteins. A previous study by Kolacna and coworkers reported that the B31 strain (*ena1-4Δ nha1Δ*) lacking the K^+ and Na^+ efflux system shows sensitivity to higher external concentrations of alkali–metal–cation salts when transformed with a mammalian Kir2.1 channel (60). In chapter III we expanded upon these findings and demonstrated that the ability of B31 yeast expressing the mammalian Kir2.1 channel to grow in high K^+ media could be directly related to the fusion of signal sequences known to reduce the surface levels of proteins. Now, taking advantage of this growth phenotype along with the ease of gap repair cloning by homologous recombination in yeast, combined with the use of high efficacy yeast transformation protocols, and availability of random oligonucleotides sequences, we developed a yeast-based screening system that enables systematic identification of the sorting motifs that downregulate surface expression of membrane proteins. We conducted the

screening, validated the results in yeast and mammalian cells, and then characterized the hit sequences' mechanisms of action.

The development of the B31 based screening system to identify trafficking signals that reduce the surface levels of membrane proteins

B31 expressing Kir2.1 channel is unable to grow in high K^+ media, however we demonstrated that the fusion of trafficking motifs that are known to reduce the surface levels of proteins to the C-terminal tail of Kir2.1 rescued the growth of the yeast when cultured in high K^+ media. Previous studies have demonstrated that the extreme C-terminal tail of Kir2.1 can be modified without having any effect on the function or surface transport of the protein (45,77). Dzwokai *et.al* demonstrated that the Kir2.1 C-terminal tail could be truncated up to 43 amino acid residues without a significant reduction of the function or surface levels (77). Shikano *et.al* demonstrated that when a random 10-mer amino acid peptide library was fused to the extreme C-terminal tail of Kir2.1, the large majority of sequences did not affect the channel localization (45). We therefore hypothesized that if we fused a random peptide library to the C-terminal tail of Kir2.1, expressed those constructs in B31, and cultured the yeast in high K^+ media, we would select for clones in which the surface levels of Kir2.1 are reduced. Based on this observation, we developed a B31-based screening strategy to identify signal sequences that reduce the surface levels of Kir2.1.

The technical development of the B31 screening system, including optimizations and troubleshooting, is discussed in detail in the methods section. Our strategy is illustrated in (Fig. 6) and as follows: We used PCR of random oligomers to generate double-stranded random C-terminal inserts for Kir2.1 encoded on a yeast expression vector. Utilizing a high efficiency transformation protocol, we performed gap repair cloning by homologous recombination in yeast to generate a library of Kir2.1 C-terminal fusion proteins

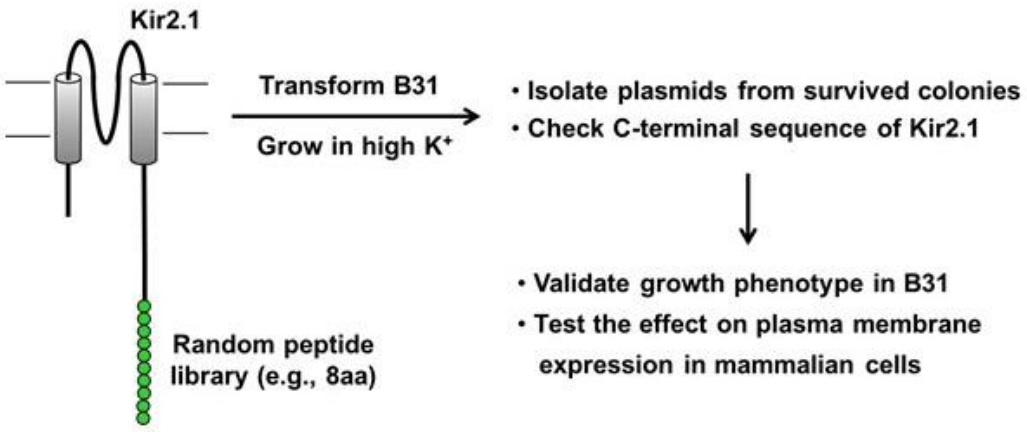

Figure 6. Strategy for the development of the B31 based screening system to identify trafficking sequences that reduce the plasma membrane levels of proteins.

in B31 yeast (Fig. 7A). The yeast was then cultured on high K^+ media (600 mM K^+) and surviving clones were

further analyzed as potential hit constructs possibly containing the trafficking motifs that reduced the surface levels of Kir2.1. We performed a series of validating assays to eliminate false positive clones, then isolated the C-terminal sequences from the surviving hit clones. True hits were defined as C-terminal hit sequences that reduced the surface levels of Kir2.1 in both yeast and mammalian cells. We assayed the true hit clones to identify their trafficking pathways and mechanisms.

IV.3 Experimental Results:

IV.3.1 B31 Screening system transformation results:

The B31 screen was performed as described in the methods section. A typical transformation yielded approximately $1x10^6$–$6x10^6$ transformants per electroporation as determined by replica plating on 0 mM K^+ -Ura/-Met SD plates. Screening was typically conducted on 600 mM K^+ SD plates, and the number of clones varied based on the level of screen optimization. The optimized B31 screen yielded 2000 hit clones per $1x10^6$ transformants (number varies a lot by conditions). Through a series of validation assays, false positive sequences were eliminated. Colony PCR was performed to isolate hit sequences, which where sequenced by Sanger sequencing. C-terminal sequences that reduced the surface levels of Kir2.1 in yeast and mammalian cells were further analyzed to determine their mechanisms.

IV.3.2 B31 Screening system - elimination of false positive clones and hit sequence validation

IV.3.2a Elimination of false positive clones due to erroneous homologous recombination:

Whenever performing gap repair cloning by homologous recombination in yeast there is a small percentage of vector plasmid that undergoes erroneous homologous recombination in which the vector recombines with itself, losing the insert sequence but maintaining the selection marker (55). In the B31

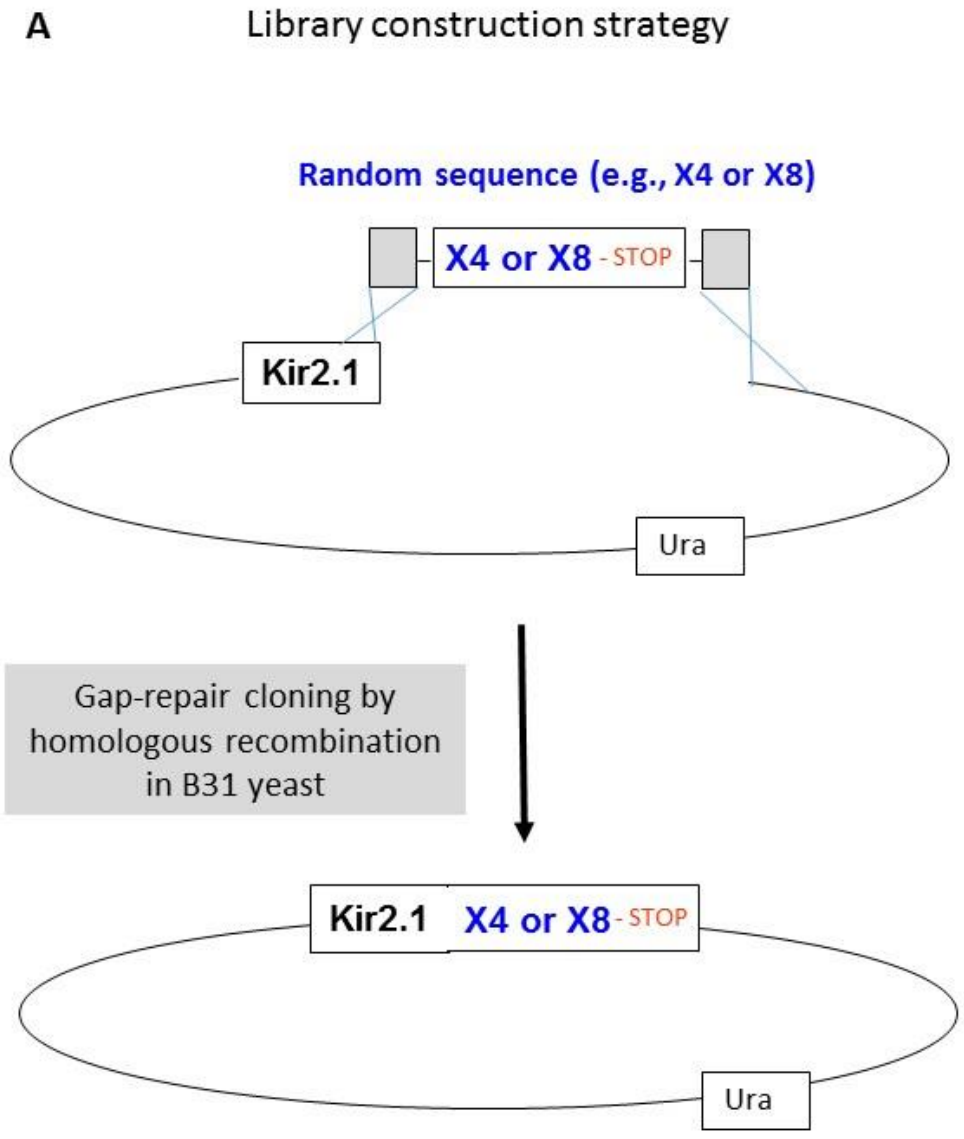
A
Library construction strategy
Random sequence (e.g., X4 or X8)
X4 or X8 - STOP
Kir2.1
Ura
Gap-repair cloning by homologous recombination in B31 yeast
Kir2.1
X4 or X8 - STOP
Ura

B Library construction strategy with selected optimizations

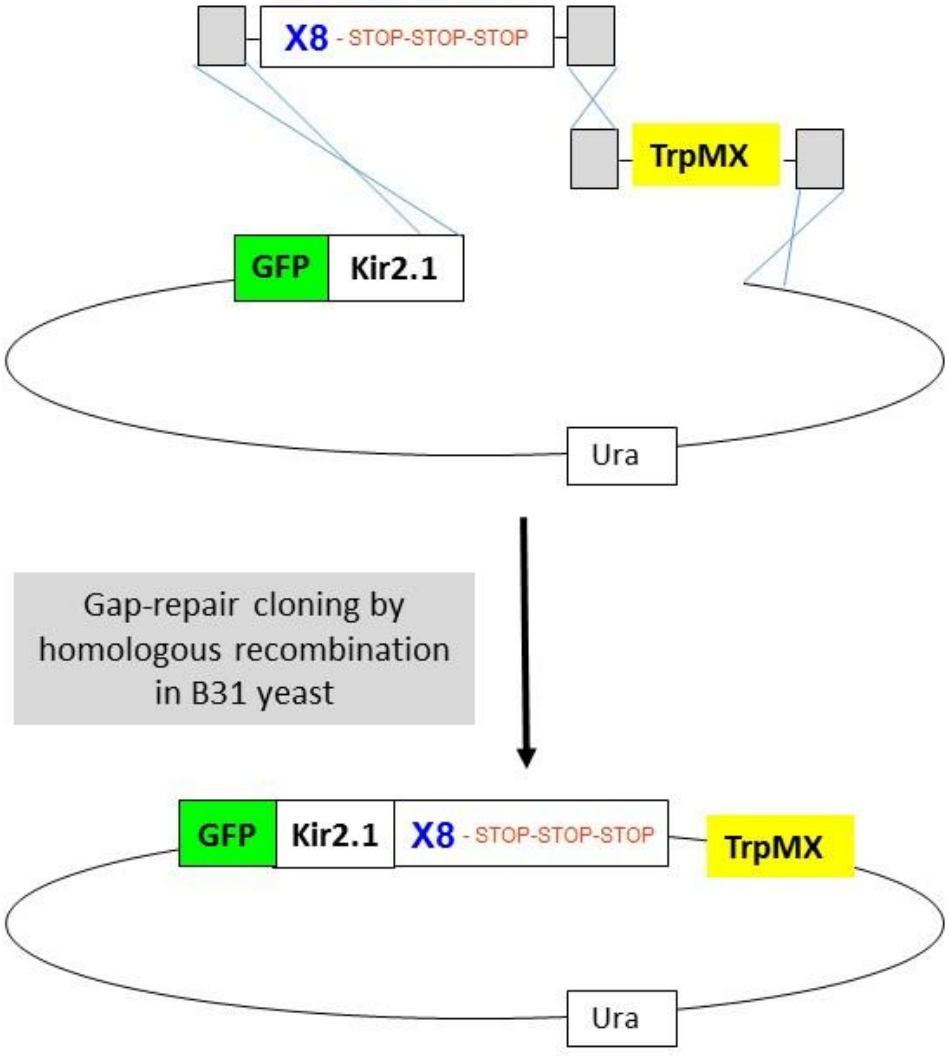

Figure 7. B31 Screening system library construction strategy. (A) General library construction strategy. Utilizing Gap-repair cloning by homologous recombination in B31 yeast, B31 were co-transformed with a linearized yeast expression vector encoding the Kir2.1 sequence along with an insert cassette containing a random sequence encoding the peptide library flanked by regions of homology to the Kir2.1 sequence and yeast expression vector. DNA undergoes homologous recombination in the yeast generating the Kir2.1- C-terminal random peptide library. (B) Library construction strategy with selected optimizations. Optimizations to the homologous recombination strategy to reduce the false positive clones include the use of GFP tagged Kir2.1, additional out of frame stop codons in the insert cassette, and the addition of an additional insert containing the TrpMx auxotrophic marker.

screening system, B31 containing plasmid that maintains the auxotrophic marker sequence but loses the Kir2.1 sequence will survive the screening condition, appearing as a false hit in the screen. With this type of plasmid, colony PCR and sequencing could not be performed as the primer sites were typically eliminated. Plasmid isolation from the yeast would typically produce an incorrect sized plasmid that could not be digested with our usual subcloning enzyme sites.

In later, more optimized versions of the screen we were able to reduce the prevalence of false hits by erroneous homologous recombination by performing the gap repair cloning with two inserts; the random C-terminal insert for Kir2.1 and TrpMX, an additional yeast auxotrophic marker. Correctly recombined plasmid would now encode for the Kir2.1 random peptide library, as well as the Ura and Trp auxotrophic markers. Screening was done on SD plates –Ura/-Met/-Trp. Plasmids which underwent erroneous homologous recombination would now typically lack the TrpMX cassette and would be screened out on the selection plates (Fig 7B).

IV.3.2b Elimination of false positive clones due to elongation sequences:

We utilized PCR of random oligonucleotide sequences to generate the inserts for the Kir2.1 random peptide library. A weakness of oligonucleotides, and particularly oligonucleotides containing random sequences is the presence, although low, of congeneric species, containing one or more deleted nucleotide from the oligonucleotide sequence (78). In the B31 screening system congenic oligonucleotides, with even a single nucleotide deleted from the library coding sequence, would result in a frame shift mutation of the C-terminal tail of Kir2.1, eliminating the terminal stop codon and extending the Kir2.1 C-terminal tail until the next random stop codon generated within the vector sequence, adding many amino acid residues. The elongated sequences could be isolated by colony PCR and sequenced. These Kir2.1 C-terminal elongation clones typically showed no visible expression by total lysate blot indicating either failure of translation or rapid degradation of elongated Kir2.1.

In later, more optimized versions of the screen we were able to reduce the prevalence of false hits by elongation sequences by the addition of out of frame stop codons within the oligonucleotide after the terminal stop codon. In the event of a congenic oligonucleotide, the initial stop codon/s would be eliminated, however major elongation would be stopped by the additional out of frame stop codons. In the later more optimized screenings false positive clones due to elongation sequences were virtually eliminated (Fig 7B).

IV.3.2c Validation of identified sequences by retransformation in B31 and further elimination of false positive clones:

Hit sequences were obtained by colony PCR of the Kir2.1 C-terminal tail from the B31 yeast then cloned back into the C-terminal of Kir2.1 in the pYES2met yeast expression vector. B31 was retransformed to express the fusion Kir2.1 hit constructs. The yeast was then re-plated on high K^+ plates to verify that the B31 growth phenotype was a direct result of the identified sequence (representative sequences shown in Fig. 8). If the B31 retransformed with the fusion Kir2.1 hit sequence did not grow on the high K^+ media equal or greater that of the screening condition, the sequence was considered a false positive sequence. B31 retransformed with the fusion Kir2.1 hit sequence which grew on the high K^+ were transferred to the C-terminal of HA tagged Kir2.1 in the pCDNA3.1 mammalian expression vector.

IV.3.2d Validation of fusion Kir2.1 hit sequence function and surface reduction in mammalian cells:

As we demonstrated previously, B31 expressing Kir2.1 channel can grow on high K^+ media either if the Kir2.1 channel surface level is reduced or if the ion conductance through the channel is inhibited. Previous studies on the Kir2.1 channel demonstrated that the manipulation of the extreme C-terminal tail of Kir2.1 is not expected to affect the ion channel function (45,77), however it was necessary to eliminate this possibility. Additionally, it is possible that the surface reduction phenotype observed in the B31 was due to yeast specific mechanisms. To determine the effect of the C-terminal hit sequences

A

Representative hit sequences from B31 screening

A19:	EIEFLVDA.	J55:	LPLIDMT.
E3:	LGILIVIIR.	K20:	PPSYYSCQ.
E6:	IRLRRRLRRIR.	A8:	EIEFLIHF.
J77:	VCRRRRVGNNK.	A9:	EIEFLVSW.
J47:	VSSLLPLL.		

B

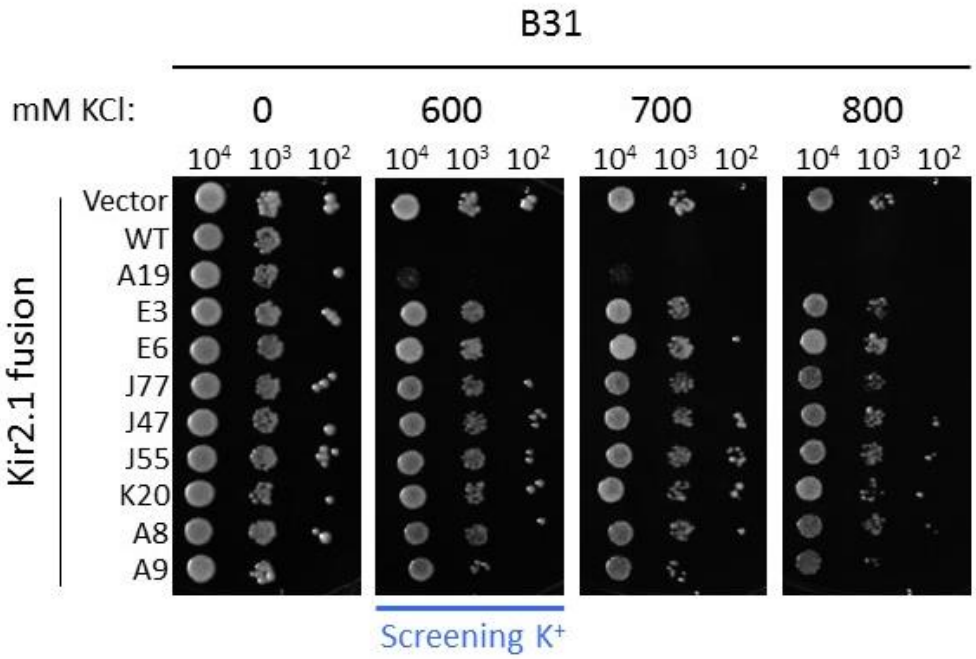

C

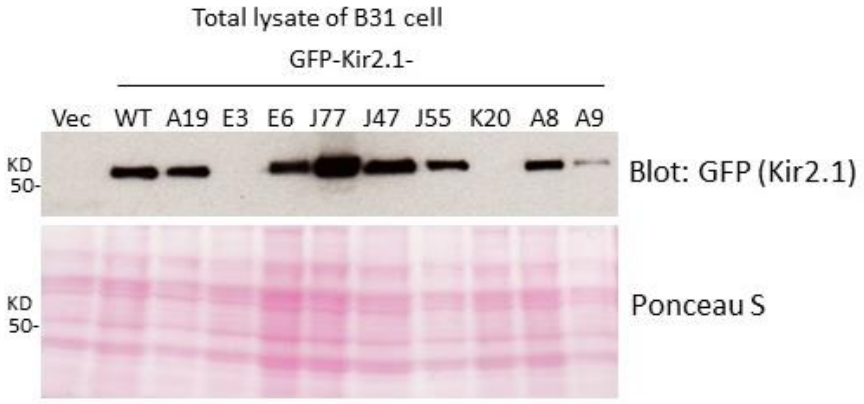

Figure 8. B31 screening identifies Kir2.1-fused C-terminal sequences that restore B31 growth in high K^+ media. (A) Representative C-terminal hit sequences obtained from the B31 screen. (B) Validation of the hit sequences in B31 yeast. Growth phenotype of B31 was examined by re-transforming B31 cells with isolated Kir2.1-fusion plasmids. The Kir2.1- or pYES2met vector-transformed B31 cells were plated on YNB media (pH 6.50) with indicated concentrations of KCl and cultured at 30 °C. The images were photographed at Day 4. Note that A19 sequence was isolated from a relatively weakly growing colony on the original 600 mM K^+ screen plate in the original screen (C) *Top*, Total lysates from B31 cells transfected with GFP-tagged Kir2.1 fusion constructs were resolved by SDS–PAGE and immunoblotted for GFP. *Bottom*, a Ponceau S-stained transfer membrane.

on the surface levels of Kir2.1 in mammalian cells, HEK293 cells were transiently transfected with the fusion Kir2.1 hit sequences. The surface levels of the Kir2.1 fusion proteins were measured by FCM

analysis, and the total expression level of the proteins was measured by western blotting of the total cell lysate (Fig. 9). Figure 9 shows the effects of representative hit sequences on the surface levels of Kir2.1 in mammalian cells. Clone A19 is an example of a sequence that rescued B31 growth in high K^+ media (albeit weakly) but did not reduce the surface levels of Kir2.1 in mammalian cells. The other representative hit sequences shown all reduced the surface levels of Kir2.1 in mammalian cells.

IV.4 Characterization of representative hit clone sequences identified in B31 screening system:

IV.4.1 Representative hit sequence E3 is a substrate for ERAD:

The most commonly identified sequence type from the screen was sequences containing a patch of strong hydrophobic residues represented by clone E3 (LGILIVIIR). These sequences strongly reduced the surface levels of Kir2.1 when fused to its C-terminal tail, but also showed a much lower level of overall expression by western blot analysis (Fig. 9). There are a few possibilities as to why we would see a reduction in overall expression of the protein on the western blot. One possibility is a problem with the protein translation, alternatively the protein could be undergoing rapid degradation (79). Within the cell, protein degradation can occur through multiple mechanisms including proteasomal degradation and lysosomal degradation, additionally proteins can be targeted through different pathways (80). A major pathway of proteasomal degradation is the ER-associated degradation (ERAD) pathway. Proteins folded in the ER are monitored by the ERQC which determines whether proteins are correctly folded. Correctly folded proteins are allowed to exit the ER, whereas proteins incorrectly folded or assembled are targeted for degradation via ERAD. It has been shown that within the ERQC an exposed region of hydrophobicity within a protein is often recognized as a sign of protein misfolding, targeting the protein for degradation (10). Being that clone E3, and the clone E3-like sequences all contain a strong patch of

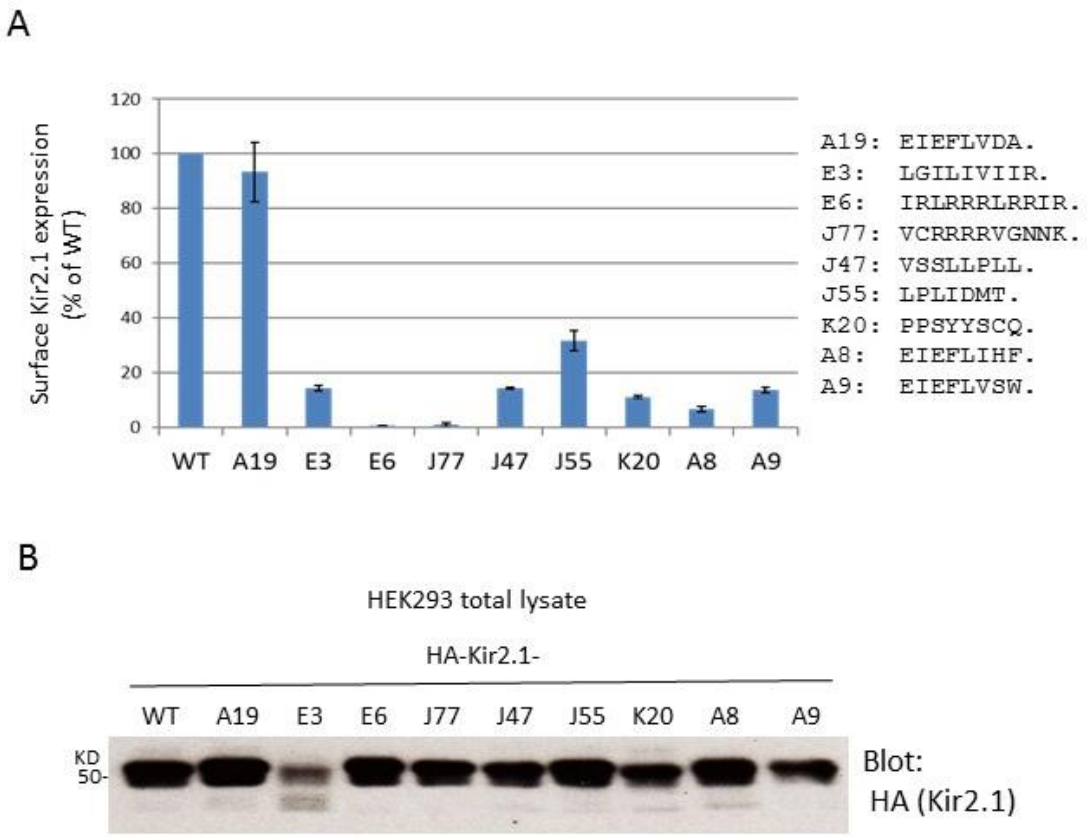

Figure 9. The fusion of the hit sequences obtained from the B31 screen reduce the surface levels of Kir2.1 in mammalian cells. (A) Surface expression levels of Kir2.1 fusion proteins. HEK293 cells were transiently transfected with HA-tagged Kir2.1 constructs and analyzed for cell surface expression by FCM. The median values were determined for the viable cell populations and normalized to the average median value of WT. Results are shown in average±SD of triplicate samples from the representative of three experiments. (C) Total lysates from HEK293 cells transfected with HA-Kir2.1 fusion constructs were resolved by SDS–PAGE and immunoblotted for HA.

hydrophobic residues we hypothesized that the loss of protein expression observed, and subsequent loss of Kir2.1 surface levels was a result of ERAD.

The ERAD ubiquitin E3 ligases have been best characterized in yeast. In yeast there are two major ERAD E3 ligase complexes whose function is based on where the misfolded region of the protein occurs. The HRD1 complex recognizes protein misfolds in the luminal and transmembrane domains of proteins. The Doa10 complex recognizes misfolds in the cytosolic domains of proteins (81) (Fig. 10). Being that our peptide library is on the cytosolic tail of Kir2.1 we figured Doa10 would be the likely candidate E3 ligase responsible for ERAD of Kir2.1-hit constructs from our screen. We knocked out Doa10 gene from B31, generating B31 *Δdoa10*. We expressed Kir2.1 fused to sequence E3 as well as other hits obtained from the screening in B31 *Δdoa10* and compared the growth phenotype in high K^+ with B31 (Fig. 11) expressing the same constructs. B31 *Δdoa10* expressing Kir2.1- E3 growth was eliminated at 500 mM K^+ whereas in B31 Kir2.1-E3 allowed growth to 800 mM K^+. Other clones, not suspected to undergo ERAD grew to similar levels of K^+ in both B31 and B31 *Δdoa10* (Fig. 11). These results indicate that sequence E3, which contains a strong hydrophobic patch and causes the degradation of Kir2.1 and subsequent reduction on the cell surface, are recognized by the components of ERCQ and send the protein to ERAD.

We next tested the transplant-ability of hit sequence E3. We transplanted sequence E3 to the extreme C-terminal tail of CD8, a dimeric Type I transmembrane protein, then transiently transfected HEK293 cells and analyzed the surface levels of the proteins by FCM and the total expression by western blot analysis (Fig. 12). Similar to Kir2.1, CD8 fused to E3 sequence appeared degraded on the total lysate blot and subsequently showed reduced surface levels of the protein. This was consistent with the previous reports of exposed hydrophobicity as a substrate for ERAD (10) (Fig. 13).

IV.4.2 Representative hit sequences E6 and J77 function as a di-Arg type ER retrieval sequences:

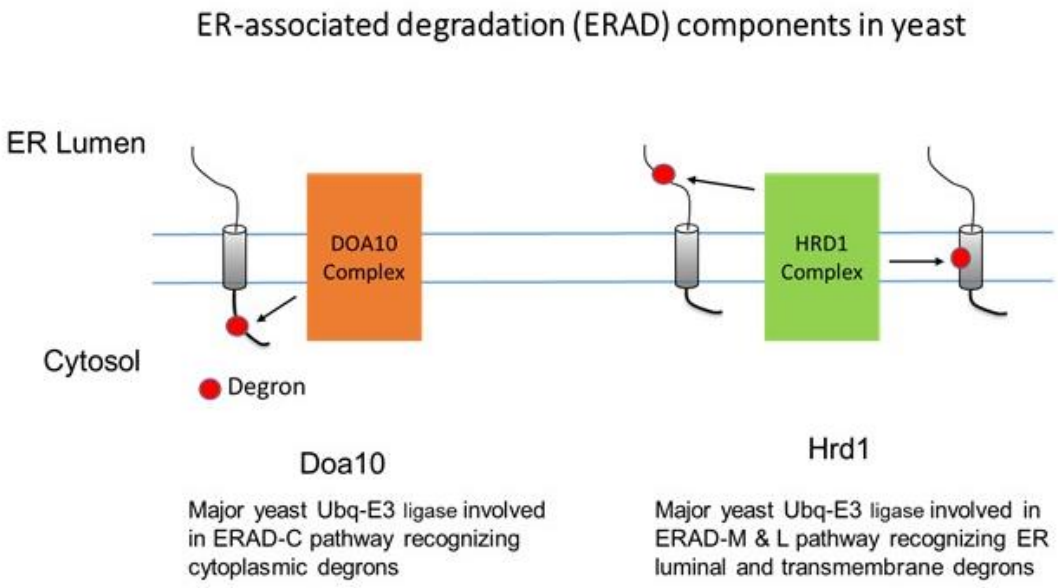

Figure 10. ER-associated degradation (ERAD) components in yeast. The major yeast ubiquition-E3 ligases have been characterized. The Doa10 complex is the major yeast ubiquition-E3 ligase recognizing cytoplasmic degrons. The HRD1 complex is the major yeast ubiquition-E3 ligase recognizing luminal and transmembrane degrons.

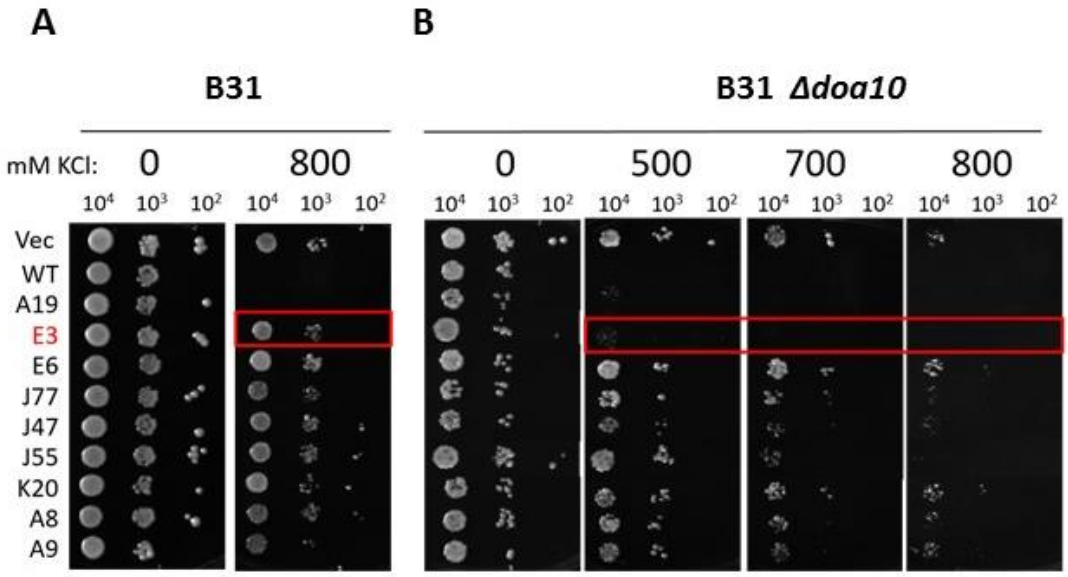

Figure 11. Deletion of Doa10 gene in B31 inhibits B31 growth in high K^+ media when expressing Kir2.1-E3 but not when expressing Kir2.1 fused to other hit sequences. (A) B31 expressing Kir2.1-Hit constructs. B31 expressing Kir2.1 fused to hit sequences are able to grow when cultured in 800 mM potassium. (B) B31 *Δdoa10* expressing Kir2.1-Hit constructs. B31 *Δdoa10* expressing Kir2.1-E3's growth is obliterated when cultured at 500 mM potassium, whereas B31 *Δdoa10* expressing Kir2.1 fused to other hit constructs continue to grow to a potassium range of 700-800 mM potassium.

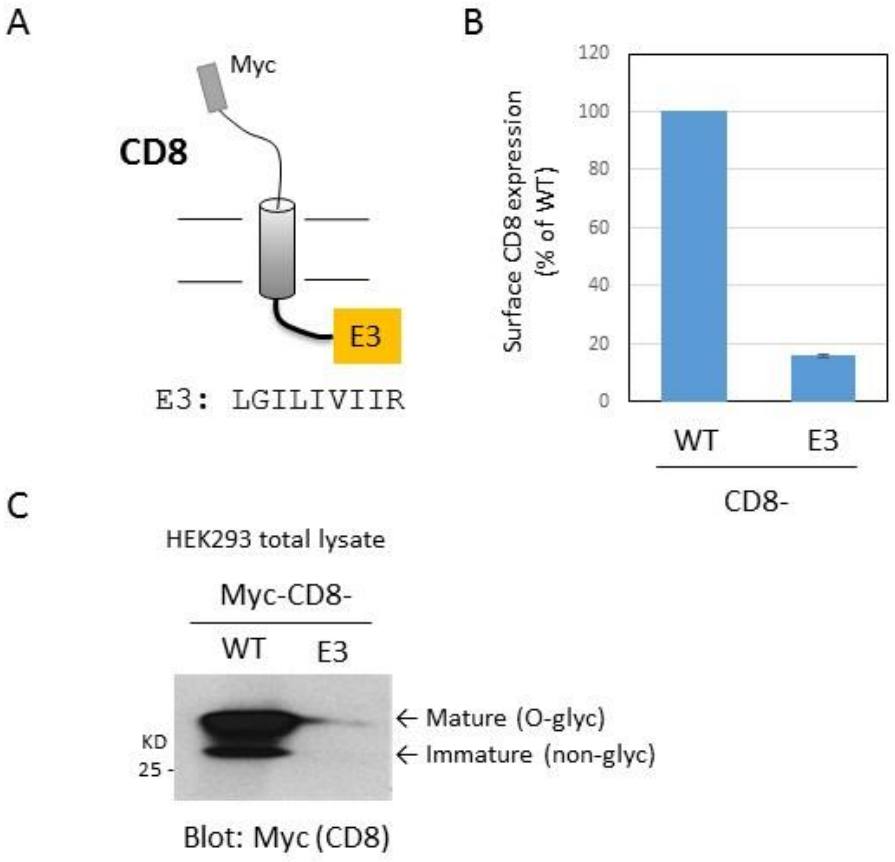

Figure 12. Hit sequence E3 transplanted to the C-Terminal tail of CD8 reduces the surface level and total expression level of CD8. (A) A diagram of CD8, a type 1 transmembrane protein, fused with E3 sequence (B) Surface expression of CD8-E3 fusion. HEK293 cells were transiently transfected with Myc-tagged CD8 constructs and analyzed for cell surface expression by FCM. The median values were determined for the total viable cell populations and normalized to the average median value of WT. Results shown in average±SD of triplicate samples from the representative of three experiments. (B) Total lysates from HEK293 cells transfected with Myc-CD8 fusion constructs were resolved by SDS–PAGE and immunoblotted for Myc.

Role of sequence E3 in down-regulating surface expression of Kir2.1 and CD8

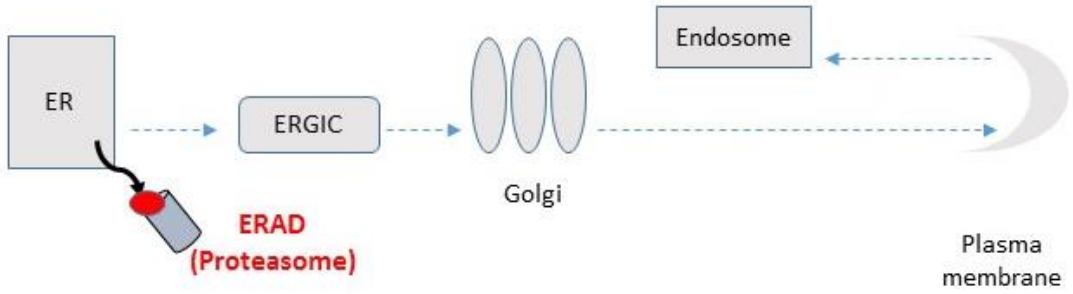

Figure 13. Hit sequence E3 fused to the extreme C-terminal tail of both Kir2.1 and CD8 functions as a substrate for ERAD.

The next category of hit sequences that we observed were sequences enriched with Arg residues represented by clones E6 (IRLRRRLRRIR) and J77 (VCRRRRVGNNK). These signals reduced the surface levels of Kir2.1 but still showed expression comparable to WT by western blot analysis (Fig. 9). These Arg rich motifs all contained the consensus motif for the di-Arg (RXR) ER retrieval motif. Additionally, the majority of these sequences contained a strong hydrophobic residue such as Leu directly upstream the di-Arg motif, which has been shown to strengthen the retrieval of proteins bearing the di-Arg motif (82).

The di-Arg motif is found on plasma membrane proteins that consist of multimeric subunits. Being that the motif is found on proteins destined to leave the ER, the di-Arg motif is understood to be a quality control signal. In order for a protein bearing the di-Arg motif to be trafficked to the plasma membrane, it must mask its di-Arg signal, which commonly occurs through proper protein folding, proper multimeric assembly, or masking by another protein. An exposed di-Arg signal indicates to the cell that the protein has escaped the ER without proper folding and/or assembly, and is thus returned to the ER for correction (12). In order to function as an ER retrieval signal the di-Arg motif must be located at least 32 Å away from the membrane region (83). Beyond this requirement the di-Arg motif is not site specific and can cause ER localization when the signal is exposed on essentially any cytoplasmic region, including intracellular loops of the multi-span membrane proteins (12). The motif is recognized by COPI, specifically residues on the β-COP and δ-COP subunits, and the cargo proteins are packaged into COPI coated vesicles and retrogradely transported to the ER (38).

We therefore explored whether these Arg rich hit sequences represented by clones E6 and J77 were functioning as a di-Arg type ER retrieval signal. The essential residues of the di-Arg are the two Arg residues, which must be separated by one amino acid (83). Mutations changing or eliminating the essential Arg residues obliterates the trafficking sequence function (12). We therefore wished to explore whether obliterating the essential Arg residues within our hit sequences would restore the surface level

of Kir2.1 bearing the mutated motif. Sequence E6 contains many Arg residues, and eliminating all combinations of di-Arg signals would be difficult without drastically altering the sequence. With sequence J77 however, elimination of the essential residues of the di-Arg motif could be achieved by mutating the 4^{th} and 5^{th} amino acids of the sequence. We generated Kir2.1 fused to the mutated J77 sequence and compared the surface levels by FCM analysis. Whereas Kir2.1-J77 shows reduced surface expression compared to Kir2.1-WT, Kir2.1-J77-R4/R5A has the surface level substantially restored (Fig. 14).

Next, we used immunocytochemistry to examine the steady-state localization of Kir2.1-J77 compared to Kir2.1-WT. If the Arg rich hit sequences are functioning as a di-Arg ER retrieval signal, we would expect to see a steady-state localization of Kir2.1 fused to E6 or J77 in the ER. We transiently transfected HEK293 cells with GFP-tagged Kir2.1-WT and Kir2.1-J77. The cells were fixed and permeablized, then immunostained for binding immunoglobulin protein (Bip), an ER luminal chaperone protein. Cells were examined under a laser scanning confocal microscope for co-localization (Fig. 15). The GFP-Kir2.1-WT staining pattern resembles a typical surface stain with little colocalization with Bip (Fig. 15, upper panels). GFP-Kir2.1-J77 loses its surface stain and rather shows co-localization with Bip indicating a steady-state localization in the ER consistent with the di-Arg ER retrieval motif (Fig. 15, lower panels).

The di-Arg motif has been shown to directly interact with COPI and direct cargo to undergo COPI mediated ER retrieval (38) Therefore, we next looked to see if Kir2.1-E6 showed enriched interaction with COPI. To test the interaction, we performed a co-IP experiment. HEK293 cells were transiently transfected with Kir2.1-WT and hit constructs. Cells were lysed and Kir2.1 was precipitated, then probed for interaction with endogenous COPI. Kir2.1-E6 showed increased interaction with COPI, similar to Kir2.1 fused to an RXR control sequence, whereas Kir2.1-WT and other Kir2.1 hit constructs do not (Fig. 16). These results are once again consistent with a di-Arg ER retrieval motif.

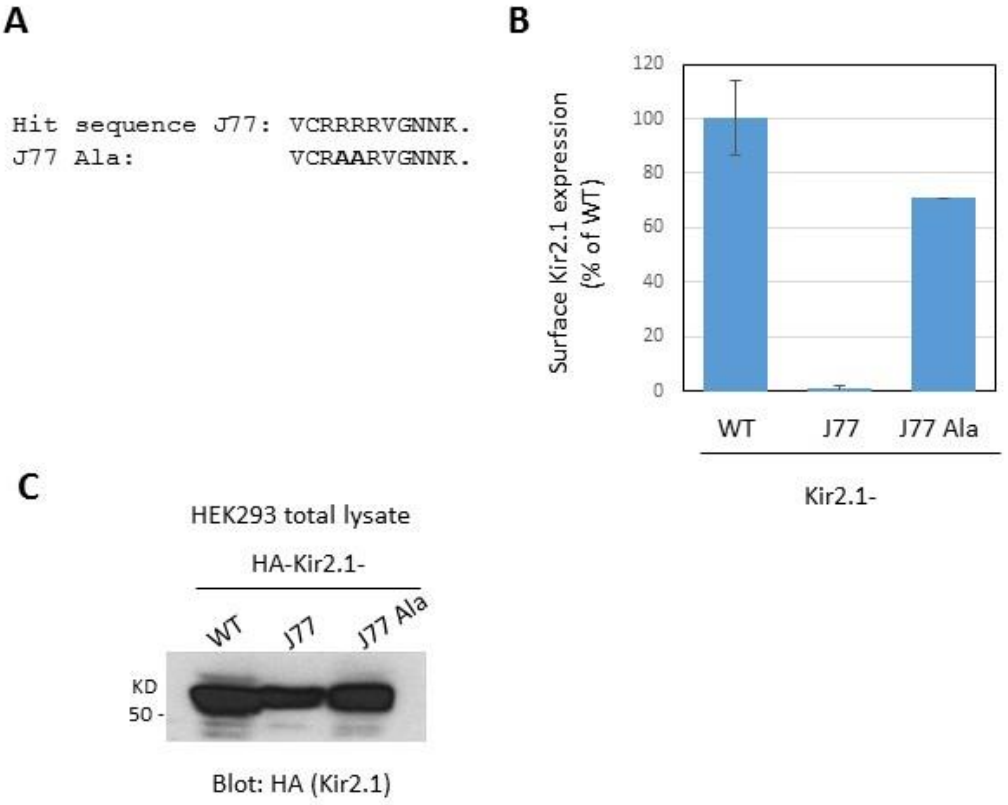

Figure 14. Obliteration of the di-Arg signals from hit sequence J77 restores the surface level of Kir2.1. (A) Amino acid sequences of parental hit sequence J77 and J77 Ala in which the di-Arg motif has been obliterated by mutating R4 and R5 to Ala. B) Surface expression of Kir2.1 fusions. HEK293 cells were transiently transfected with HA-Kir2.1 constructs and analyzed for cell surface expression by FCM. The median values were determined for the total cell populations and normalized to the average median value of WT. (C) Total lysates from HEK293 cells transfected with HA-Kir2.1 fusion constructs were resolved by SDS–PAGE and immunoblotted for HA.

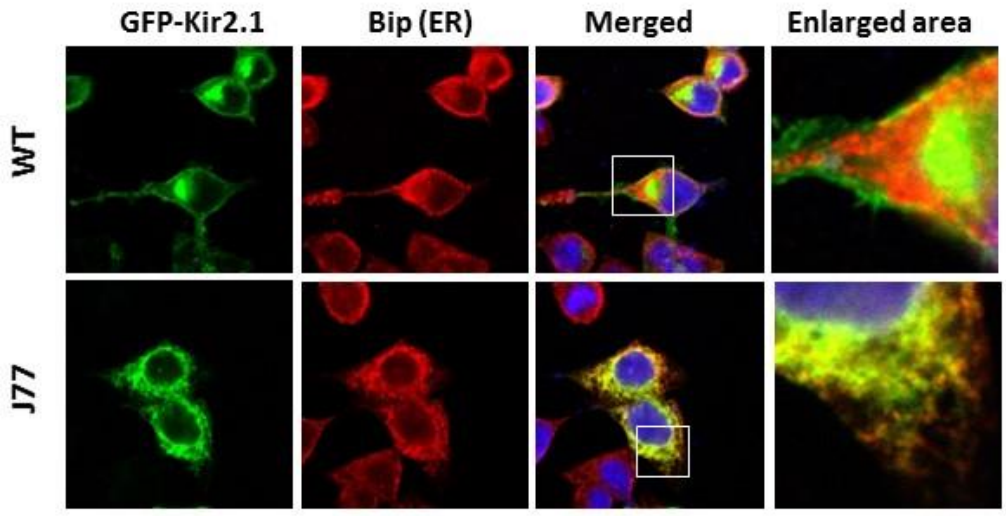

Figure 15. Kir2.1 fused to J77 shows co-localization with the ER marker Bip. HEK293 cells expressing either GFP-tagged Kir2.1-WT (upper panels) or GFP tagged Kir2.1-J77 (lower panels) were fixed and permeabilized, then stained for an ER marker Bip followed by Cy3-labeled secondary antibody. Images were collected with a Zeiss LSM 700 laser scanning confocal microscope. Kir2.1-WT shows a cell surface as well as an intracellular staining likely reflecting Golgi, which does not co-localize with Bip signal. Kir2.1-J77 is not present on the cell surface but rather shows co-localization with the Bip.

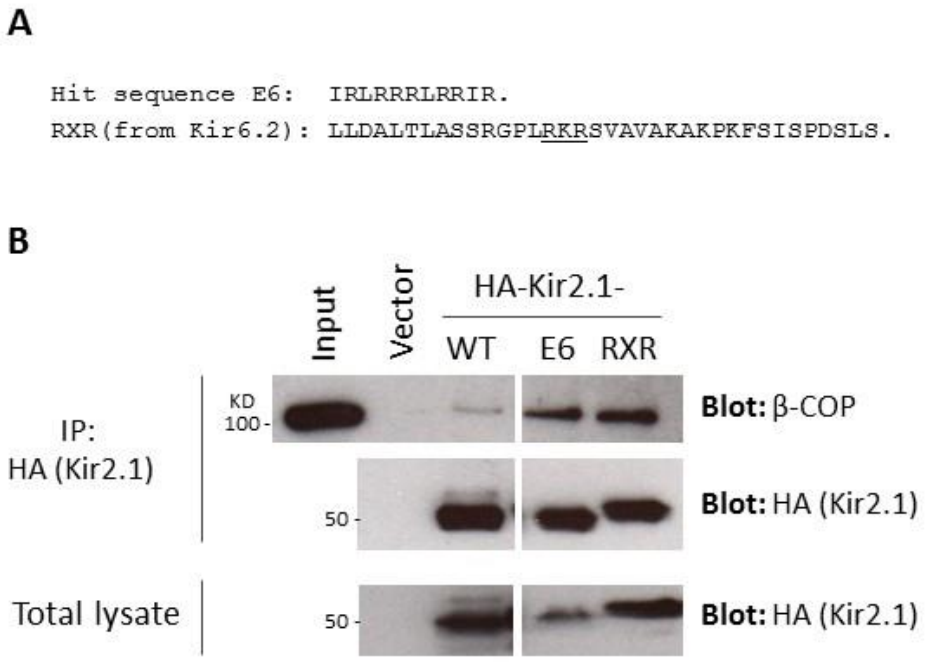

Figure 16. Kir2.1-E6 shows enriched interaction with COPI compared to Kir2.1-WT. (A) Amino acid sequence of hit sequence E6 and a positive control RXR motif from Kir6.2 C-terminal tail. (B) Association of COPI with Kir2.1-E6. Kir2.1 fused E6 and RXR control immunoprecipitated with HA Ab were resolved by SDS–PAGE and immunoblotted for HA (bottom two panels) and the associating β-COP (upper panel). Samples were run through a single gel and the gap between WT and E6 indicates the lanes not shown.

We next tested the translatability of hit sequences E6 and J77. A feature of trafficking sequences is that they are often autonomous signals that will function when transplanted to different protein contexts. However, trafficking signals can also be context dependent, so a transplanted signal sequence may not work in every protein context (83). We transplanted sequence E6 and J77 to the extreme C-terminal tail of CD8 then transiently transfected HEK293 cells and analyzed the surface levels of the proteins by FCM

and the total expression by western blot analysis. Both CD8-E6 and CD8-J77 showed extremely lower surface expression compared to CD8-WT (Fig. 17A).

CD8 undergoes heavy O-glycosylation in the Golgi, and this modification can be detected by western blot analysis. CD8 that has trafficked through the Golgi will appear as a slower migrating mature O-glycosylated band on a total lysate blot. In the western blot analysis of the total cell lysate, CD8-WT ran primarily in its mature O-glycosylated form, indicative of protein which has reached or passed the *trans*-Golgi, whereas CD8-E6 and CD8-J77 ran primarily as a faster migrating immature band indicative of CD8 which has not been transported through the *trans*-Golgi (Fig. 17B). Both the reduced surface levels and immature glycosylation pattern of CD8-E6 and CD8-J77 in the total lysate blot are consistent with CD8 bearing an exposed di-Arg ER retrieval motif.

We used immunocytochemistry to examine the steady-state localization of CD8-J77 compared to CD8-WT. Myc-tagged CD8-WT and CD8-J77 were transiently transfected into HEK293 cells. The cells were fixed and permeablized, then co-immunostained for Myc (CD8) and ER marker protein Bip. Myc-CD8-WT staining pattern resembles a typical surface stain with little co-localization with Bip (Fig. 18, upper panels). Myc-CD8-J77 loses its surface stain and rather shows co-localization with Bip, indicating a steady-state localization in the ER consistent with the di-Arg ER retrieval motif (Fig. 18, lower panels).

Finally, ideally, we would have wanted to test the interaction of our CD8-fused Arg rich hit clones with COPI, however due to technical difficulties, we were not able to see reliable COPI binding of even

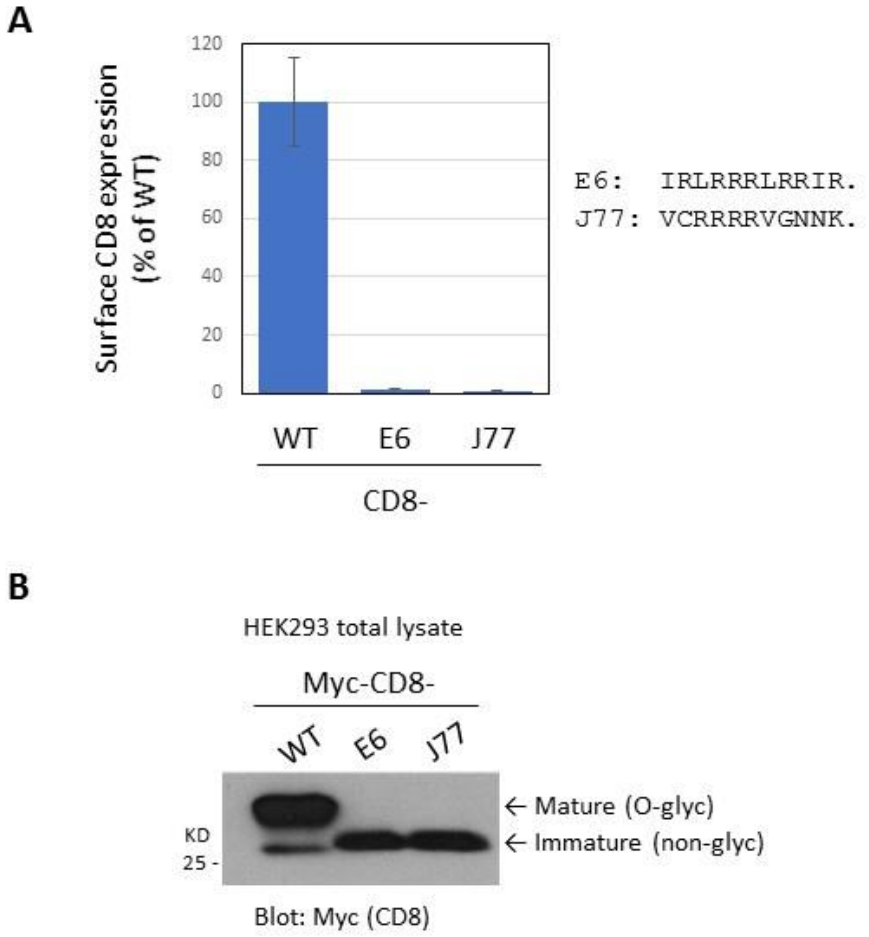

Figure 17. Hit Sequences E6 and J77 transplanted to the C-terminal tail of CD8 reduces the surface level of CD8. (A) Surface expression of CD8 fusions. HEK293 cells were transiently transfected with Myc-CD8 constructs and analyzed for cell surface expression by FCM. The median values were determined for the total viable cell populations and normalized to the average median value of WT. Results shown in average±SD. of triplicate samples from the representative of three experiments. (B) Total lysates from HEK293 cells transfected with Myc-CD8 fusion constructs were resolved by SDS–PAGE and immunoblotted for Myc.

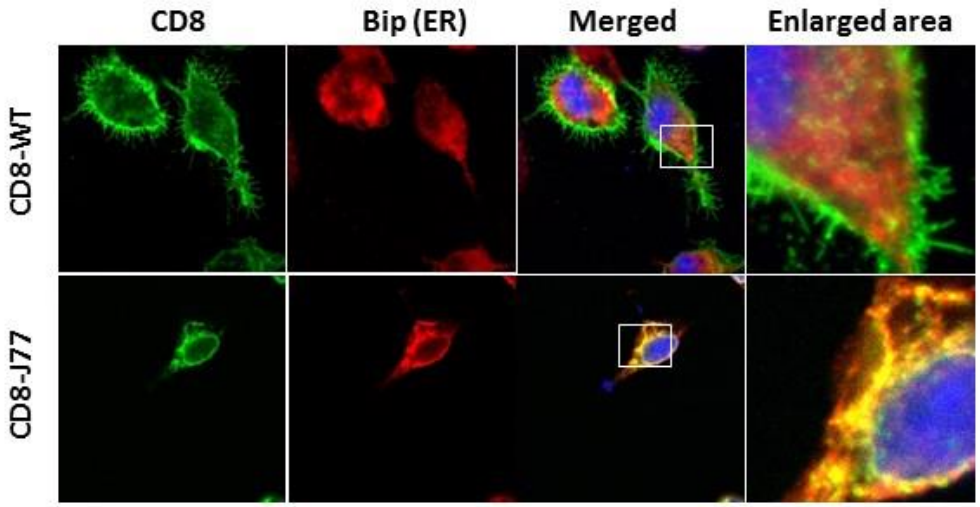

Figure 18. CD8 fused to J77 shows co-localization with the ER marker Bip. HEK293 cells expressing either Myc-CD8-WT (upper panels) or Myc-CD8-J77 (lower panels) were fixed and permeabilized, then stained for an ER marker Bip followed by Cy3-labeled secondary antibody. CD8 was stained with anti-Myc antibody followed by AF488-labeled secondary antibody. Images were collected with a Zeiss LSM 700 laser scanning confocal microscope. CD8-WT is primarily expressed on the cell surface and does not co-localize with Bip (upper panels). CD8-J77 is not present on the cell surface but rather shows co-localization with Bip (lower panels).

control CD8 constructs. We therefore utilized a pulse-chase metabolic labeling assay developed by Jackson and coworkers to visualize CD8 undergoing ER retrieval (84). They observed that while CD8 fused to C-terminal di-Lys motifs (KKXX-COOH or KXKXX-COOH) do not travel through the Golgi and therefore do not achieve full maturation, being that they are retrieved from the early Golgi, they obtain some exposure to the earliest glycosyltranferases, which slightly increases the electrophoretic mobility of CD8. This slight maturation of CD8 is not observable in a steady-state blot but can be visualized via pulse chase assay (84).

We therefore performed the pulse chase assay on CD8-WT and CD8-J77, as well as CD8 fused with the di-Lys motif of yeast WBP1 protein (LETFKKTN-COOH) as a control construct based on the previous report (84). HEK293 cells were transiently transfected with CD8-WT and fusion constructs. 24 hrs after transfection cells were pulse labeled for 10 min with ^{35}S-Met and ^{35}S-Cys at 37 ° C then chased for 2, 6, and 23 hrs. CD8 proteins collected by immunoprecipitation were resolved by SDS-PAGE and analyzed by autoradiography using the phosphor screen imager. CD8-WT shows rapid maturation already at 2 hrs of chase. CD8-J77 never fully matures but shows a slight increase in size at the 2, 6 and 23 hrs time points similar to CD8-KKTN, which is consistent with the idea that it cycles between the ER and *cis*-Golgi (Fig. 19). We therefore conclude that sequences E6 and J77 are functioning as di-Arg ER retrieval signals in both the context of Kir2.1 and CD8 localizing the proteins to the ER (fig. 20).

IV.4.3 Representative hit sequences A8, A9, J47 and J55 are enriched with Leu residues

The next category of hit sequences that we observed were sequences that contained two adjacent Leu's (or a Leu followed by Ile), which are the critical residues of the di-Leu endocytosis/sorting motif. There are two well characterized di-Leu motifs [DE]XXXL[LI] and DXXLL. The functional requirements for the DXXLL signal are strict, any mutation in the D, LL, or spacing of the D and LL obliterates the function of the signal (39) and our screening did not produce such a signal. The [DE]XXXL[LI] motif is more flexible

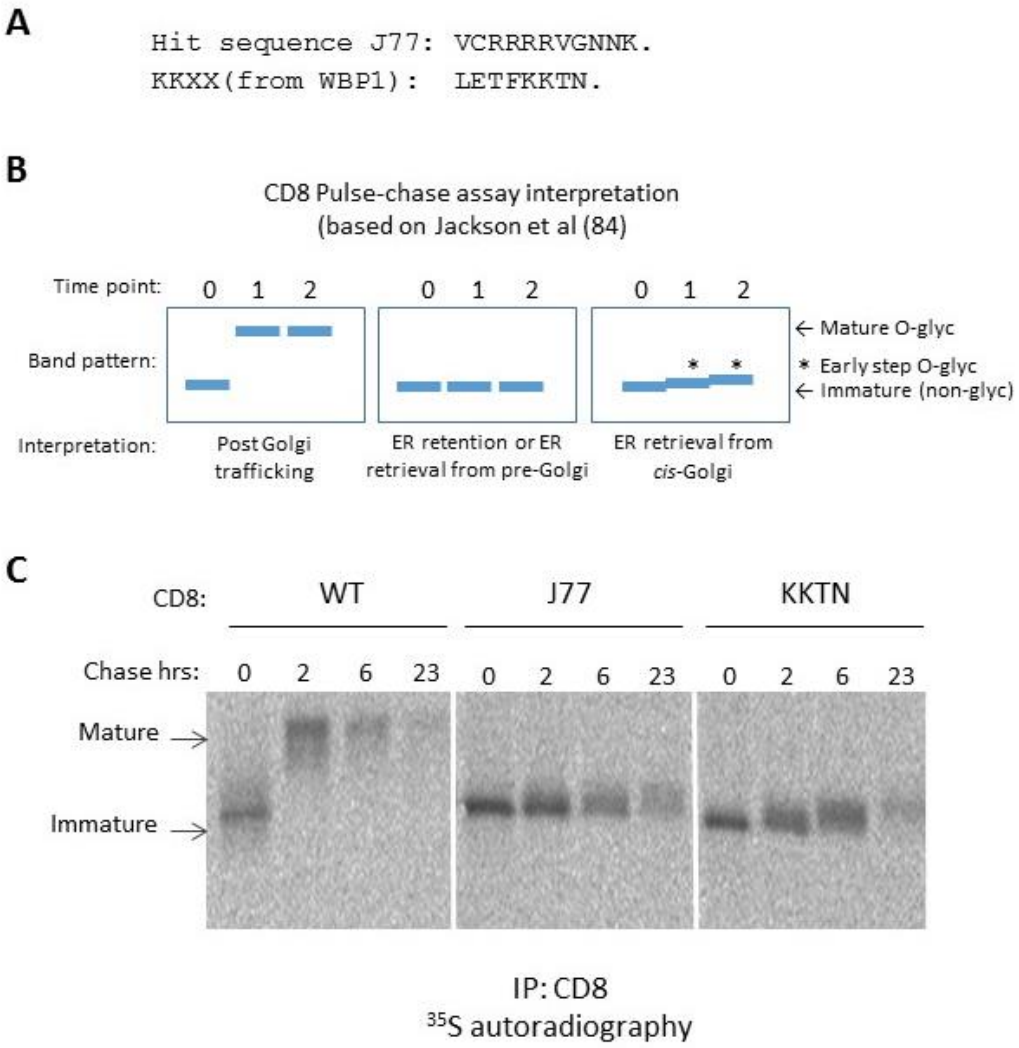

Figure 19. Pulse-chase analysis of CD8-J77 shows a glycosylation pattern consistent with CD8 undergoing ER retrieval. (A) Amino acid sequence of hit sequence J77 and a control C-termina di-Lys motif from yeast WBP1 protein. (B) A diagram of a pulse-chase analysis of CD8 O-glycosylation. The left panel depicts a CD8 blot pattern for WT which has undergone post-Golgi trafficking and runs as a fully mature band. The middle panel depicts CD8 showing no signs of O-glycosylation which indicates either being retained in the ER or retrieved to the ER from membrane compartments where cargo is not exposed to the O-glycosylation enzymes. The right panel depicts CD8 undergoing retrieval from the *cis*-Golgi in which CD8 has brief exposure to the early step O-glycosylation enzymes, and shows slight maturation over time without reaching full maturation. (C) HEK293 cells expressing CD8 constructs were pulse labeled for 10 min using 100 uCi of ^{35}S-Met/Cys at 37° C then chased for 2, 6, and 23 hrs. CD8 was collected by immunoprecipitation on beads and then resolved by SDS-PAGE followed by autoradiography using a Molecular Dynamics Storm 860 imager. CD8-WT (left panel), which is robustly expressed on the cell surface, rapidly becomes the fully mature band whereas CD8-J77 (middle panel) displays a slight maturation over time similar to CD8-KKTN (right panel), consistent with CD8 undergoing ER retrieval from cis-Golgi.

Role of sequences E6 and J77 in down-regulating surface expression of Kir2.1 and CD8

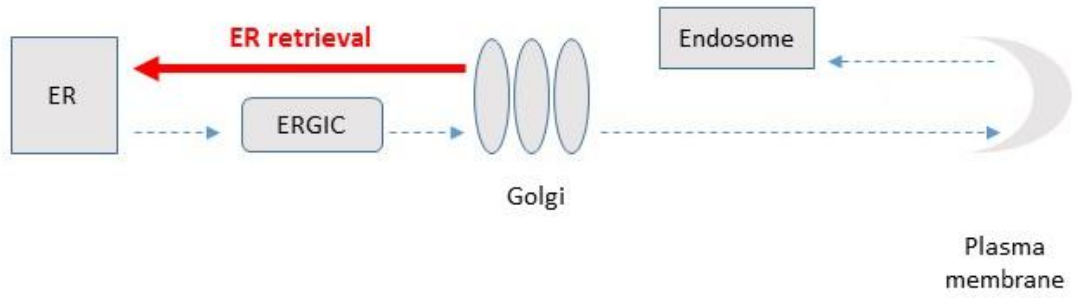

Figure 20. Hit sequence E6 and J77 fused to the extreme C-terminal tail of both Kir2.1 and CD8 functions as an ER retrieval signal.

where only the two Leu are the critical residues, with the upstream acidic residues enhancing the effect (39). Additionally, it has been shown that a Pro residue immediately upstream the di-Leu signal or additional acidic residues downstream the di-Leu signal also enhances the signal (43). Sequences A8 (EIEFLIHF), A9 (EIEFLVSW), J47 (VSSLLPLL), and J55 (LPLIDMT) all contain the residues consistent with the [DE]XXXL[LI] di-Leu motif.

IV.4.3a A8, A9, J47 and J55 reduce the surface levels of CD8 when transplanted to its C-terminal tail, but by potentially distinct mechanisms

We first wanted to determine if the hit sequences would function when transplanted to CD8. In addition to the translatability of the hit sequences, due to CD8 undergoing O-glycosylation in the Golgi, western blot analysis of CD8 constructs will give an indication of the protein localization/trafficking. If the CD8 fused hits are reduced from the cell surface as a function of enriched endocytosis, they will have nonetheless passed through the Golgi and appear on the western blot as primarily a larger mature band. If, however CD8 trafficking is disrupted at pre-Golgi step the protein will appear as an immature band.

We transplanted sequences A8, A9, J47 and J55 to the C-terminal tail of CD8 and transiently transfected HEK293 cells to examine their surface expression and total protein expression. All four hit sequences functioned to reduce the surface levels of CD8 compared to CD8-WT as measured by FCM (Fig. 21B). Upon visualization of the western blot bands, whereas CD8 fused to J47 and J55 ran as a mature O-glycosylated band, as we would expect if the CD8 surface levels were being reduced as a function of endocytosis, CD8 fused to A8 and A9 ran primarily as an immature band, which suggested that those constructs have not passed through Golgi (Fig. 21C). In light of CD8 fused to A8 and A9's O-glycosylation pattern on western blot we further explored whether the hit sequences A8 and A9 could be functioning through a mechanism of ER retrieval or retention in both the context of Kir2.1 and CD8.

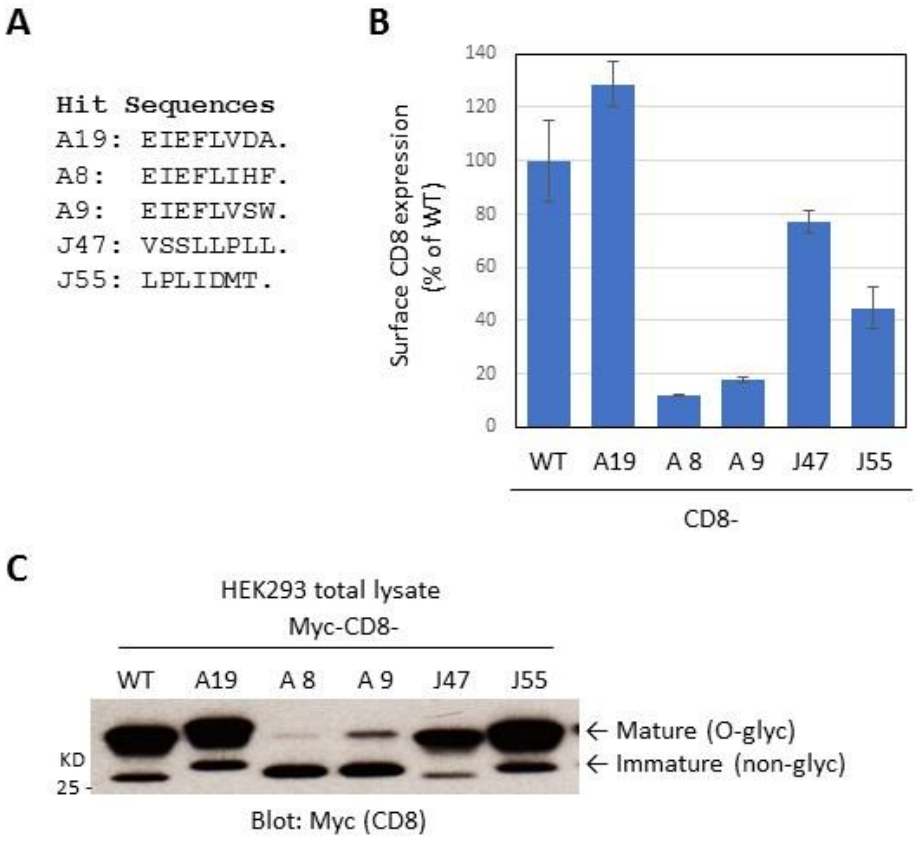

Figure 21. Leu rich hit sequences reduce the surface level of CD8 when transplanted to its C-terminus (A) Amino acid sequence of hit sequences. (B) Surface expression of CD8 fusions. HEK293 cells were transiently transfected with Myc-CD8 constructs and analyzed for cell surface expression by FCM. The median values were determined for the total viable cell populations and normalized to the average median value of WT. Results shown in average±SD. of triplicate samples from the representative of three experiments. (C) Total lysates from HEK293 cells transfected with Myc-CD8 fusion constructs were resolved by SDS–PAGE and immunoblotted for Myc.

IV.4.3b Kir2.1 fused A8 and A9 bind COPI in co-IP assay

To date, COPI-mediated retrograde transport is the only established pathway for the ER retrieval of membrane proteins (85), although there is a less well characterized Rab6-dependent COPI-independent retrograde transport pathway for certain bacterial toxins (86). We therefore decided to test if Kir2.1

fused to A8 and A9 interact with COPI by co-IP assay. HEK293 cells were transfected with Kir2.1 constructs, and the immunoprecipitated Kir2.1 proteins were probed for the co-precipitating endogenous βCOP. Interestingly, Kir2.1 fused to sequences A8 and A9 as well as J77 (our positive control for di-Arg ER-retrieval signal) showed enriched interaction with COPI compared to Kir2.1-WT. Kir2.1-A19 (a negative control signal), and Kir2.1-J47 (a Leu rich motif that reduces the surface levels of both Kir2.1 and CD8, but ran as a CD8 mature band via western blot), showed similar COPI interaction to Kir2.1-WT (Fig. 22).

IV.4.3c Synthetic peptide sequence A8 binds COPI in peptide pulldown assay

To test if this COPI association is a direct effect of these hit sequences, we performed an *in vitro* pull-down assay using synthetic peptides encoding the C-terminal sequence of A8. The peptides covalently coupled to the resin were incubated with HEK293 cell lysate, and the bound proteins were probed for COPI. Consistent with the co-IP results, sequence A8, as well the E6 di-Arg sequence, showed strong binding to COPI while WT Kir2.1 endogenous C-terminal sequence and A19 sequence did not (Fig. 23). These results raised an intriguing possibility that hydrophobic sequences such as A8 and A9 represent a novel COPI-binding motif that function for the ER retrieval in the context of Kir2.1 protein.

IV.4.3d CD8 fused to sequence A8 appears to be either retained in the ER or rapidly retrieved from the early pre-Golgi compartments by pulse-chase analysis

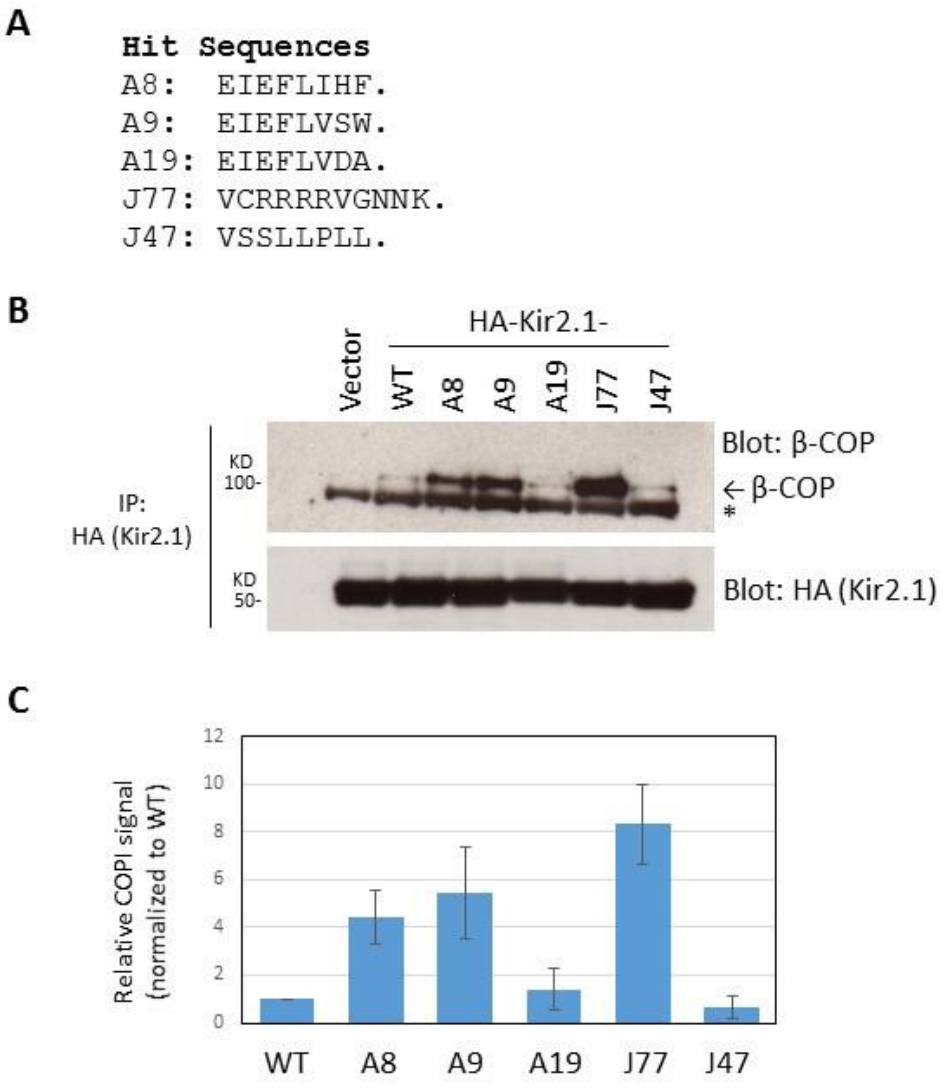

Figure 22. Kir2.1-A8 and A9 show enriched interaction with COPI compared to Kir2.1-WT. (A) Amino acid sequence of hit sequences of hit constructs (B) Association of COPI with Kir2.1-fused hit sequences. Kir2.1 with hit sequences were immunoprecipitated with αHA Ab, resolved by SDS–PAGE, and immunoblotted for HA (bottom two panels) and the associating β-COP (upper panel). Kir2.1-A8 and A9 show enriched interaction with COPI similar to Kir2.1-J77 (di-Arg control) whereas other constructs do not. * denotes the cross-reacting IgG band of HA Ab. (C) The β-COP bands from three experiments were normalized to the Kir2.1 bands and quantified using the Image Studio Lite software (LI-COR)

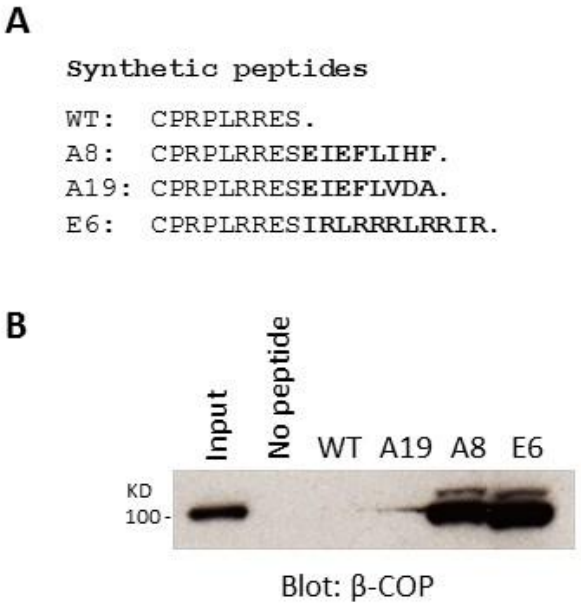

Figure 23. Synthetic peptides encoding the A8 sequence pull-down COPI in an *in vitro* peptide pulldown assay (A) Amino acid sequence of synthetic peptides. (B) Synthetic peptides containing the amino acid sequences of hit constructs were conjugated to sulfo-link resin and incubated with the total lysate of HEK293 cells. Pulled down proteins were eluted, and samples were run through SDS-PAGE and blotted for interaction with β-COP. The peptides encoding the Kir2.1-WT extreme C-terminal tail and the A19 sequence (negative control) do not pull-down COPI. The peptide encoding sequence A8 pulls down COPI similar to the sequence E6 (di-Arg positive control)

Ideally we would have wanted to test the interaction of CD8 fused to A8 and A9 with COPI, however due to technical difficulties, we were not able to see reliable COPI binding of even control CD8 constructs fused with RXR motif (data not shown). We therefore again utilized the pulse-chase assay developed by Jackson and coworkers to visualize CD8 undergoing ER retrieval (84). They observed that while CD8 fused to di-Lys motifs do not travel through the Golgi and therefore do not achieve full maturation, they are retrieved from the early Golgi where they obtain some exposure to the earliest glycosyltransferases

that modify CD8 and slightly decrease its mobility on the gel (relative to unmodified). This slight maturation is difficult to observe in a steady-state blot but can be visualized via pulse-chase assay (84).

We therefore performed the pulse-chase assay on CD8 fused to A8 together with CD8-WT and controls for the ER retrieval motifs CD8-J77 (di-Arg motif) and CD8-KKTN (di-Lys motif). CD8-WT shows rapid maturation already at 2 hrs of chase. CD8-J77, as well as the CD8-KKTN control, never fully matures but shows a slight increase in size at the 2, 6 and 23 hrs time points, the pattern which was previously characterized as a sign of CD8 ER retrieval ((84) and Fig. 24). CD8 fused with A8, however did not show any maturation over the course of the 23 hrs (Fig. 24). These results suggest that rather than undergoing ER retrieval, CD8 fused to A8 is retained in the ER. However, it is impossible to completely rule out if CD8-A8 is functioning through a retrieval mechanism via this pulse-chase assay, since ER retrieval can occur in multiple steps of forward trafficking, including from the ERGIC prior to the protein reaching the Golgi (13). If CD8-A8 is undergoing rapid retrieval from the earlier trafficking step such as ERGIC, it might not gain the exposure to the glycosyltransferases. Furthermore, if CD8-A8 is truly retained in the ER it remains to be determined whether the retention is achieved by direct recognition of signal A8 or by sequence A8 causing CD8 protein misfolding or misassembly (Fig. 25).

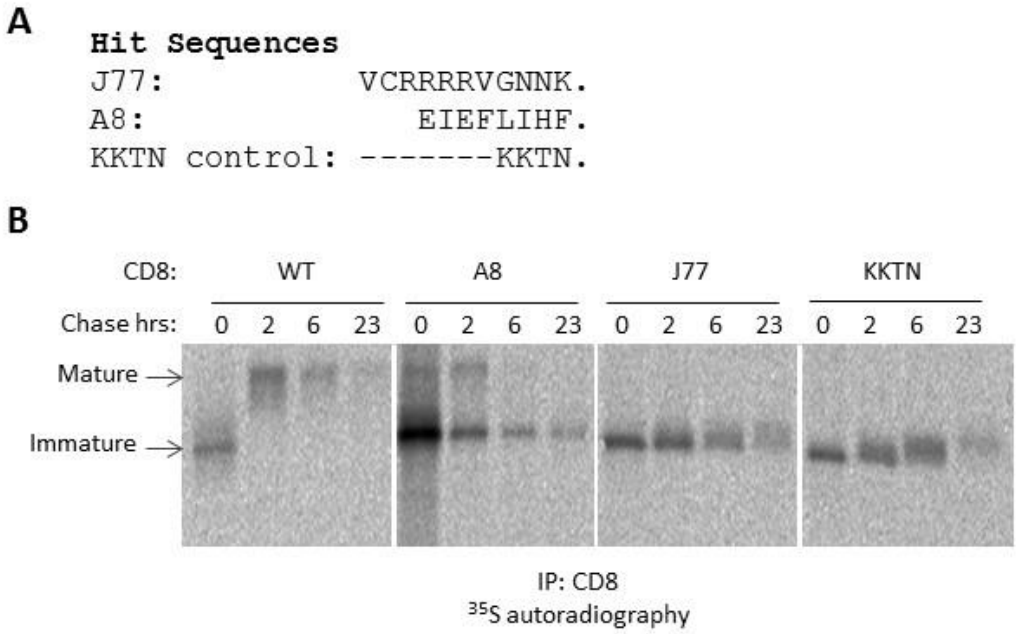

Figure 24. Pulse-chase analysis of CD8-A8 shows a glycosylation pattern consistent with CD8 retained in the ER (A) Amino acid sequence of hit sequences and a control KKXX motif. (B) HEK293 cells expressing CD8 constructs were pulse labeled for 10 min using 100 uCi of ^{35}S-Met/Cys at 37° C then chased for 2, 6, and 23 hrs. CD8 was collected by immunoprecipitation on beads and then resolved by SDS-PAGE followed by autoradiography. CD8-WT (left panel), which is robustly expressed on the cell surface, rapidly becomes the fully mature band. As we previously showed, CD8-J77 and CD8-KKTN (right two panels) display a slight maturation over time consistent with CD8 undergoing ER retrieval. However CD8-A8 (second panel from the left) shows no maturation over time, indicative of a protein either retained in the ER or rapidly retrieved to the ER prior to any exposure to the O-glycosylation enzymes in the *cis*-Golgi.

Role of sequences A8 and A9 in down-regulating surface expression CD8

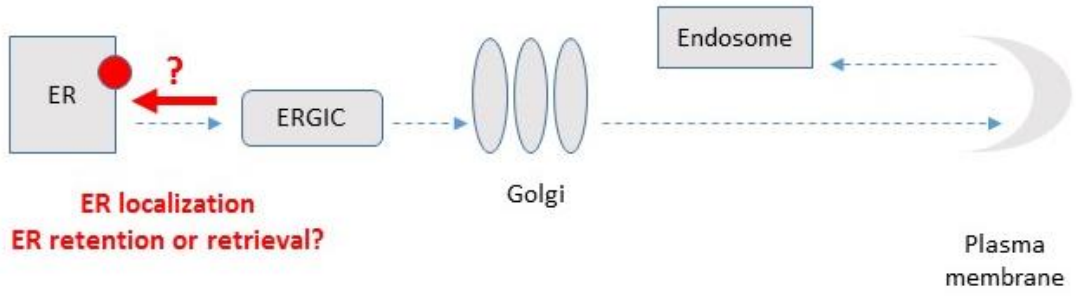

Figure 25. Hit sequences A8 and A9, fused to the extreme C-terminal tail of CD8 localized the protein to the ER. CD8-A8 does not reach the Golgi, therefore the localization is either a result of ER retention or retrieval from an early compartment such as the ERGIC.

IV.4.3e Kir2.1-A8 does not appear localized to the ER by immunocytochemical analysis

Being that both the steady-state blot and pulse-chase analysis clearly indicated ER localization for CD8-A8, combined with the fact that Kir2.1-A8 showed COPI interaction by our co-IP assay, we wanted to determine if Kir2.1-A8 was localized to the ER. We used immunocytochemistry to explore this possibility. We transiently transfected GFP-tagged Kir2.1-WT, Kir2.1-A8, and Kir2.1 fused to a di-Arg control into HeLa cells. The cells were fixed and permeablized, then immunostained for an ER luminal marker Bip. Cells were examined under a laser scanning confocal microscope for co-localization (Fig. 26). Both Kir2.1-WT and Kir2.1-A8 typically did not show increased co-localization with Bip (Fig. 26, top and middle panels) whereas the Kir2.1 fused to the di-Arg control was more clearly co-localized with Bip (Fig. 26, Bottom panels). These results suggest that despite Kir2.1 binding to COPI in the co-IP and peptide pull-down assays ER-retrieval does not appear to be the major mechanism responsible for the reduced surface expression in the context of Kir2.1. The functional role, if any, of COPI binding on Kir2.1-A8 and A9 requires further investigation.

IV.4.3f A8, A9, J47 and J55 increase endocytosis in Kir2.1

Considering the sequence A8, J47 and J55 meet the criteria of the di-Leu motif, and sequence A9 could be functioning as an atypical di-Leu, we suspected that the surface reduction of Kir2.1 could be mediated by this motif. The di-Leu motifs have been best characterized as an endocytosis motif, causing the rapid internalization of proteins bearing the motif to the endosomes. The di-Leu motif can also function to directly target proteins from the TGN to the intracellular compartments such as the endosomes and lysosomes (39).

To test if sequences A8, A9, J47 and J55 function as an endocytosis motif when fused to Kir2.1, we performed a FCM-based Ab feeding assay. Kir2.1 proteins expressed in HEK293 cells were labeled with primary anti-HA epitope Ab at 4 °C, where endocytosis is inhibited. Cells were then warmed to an

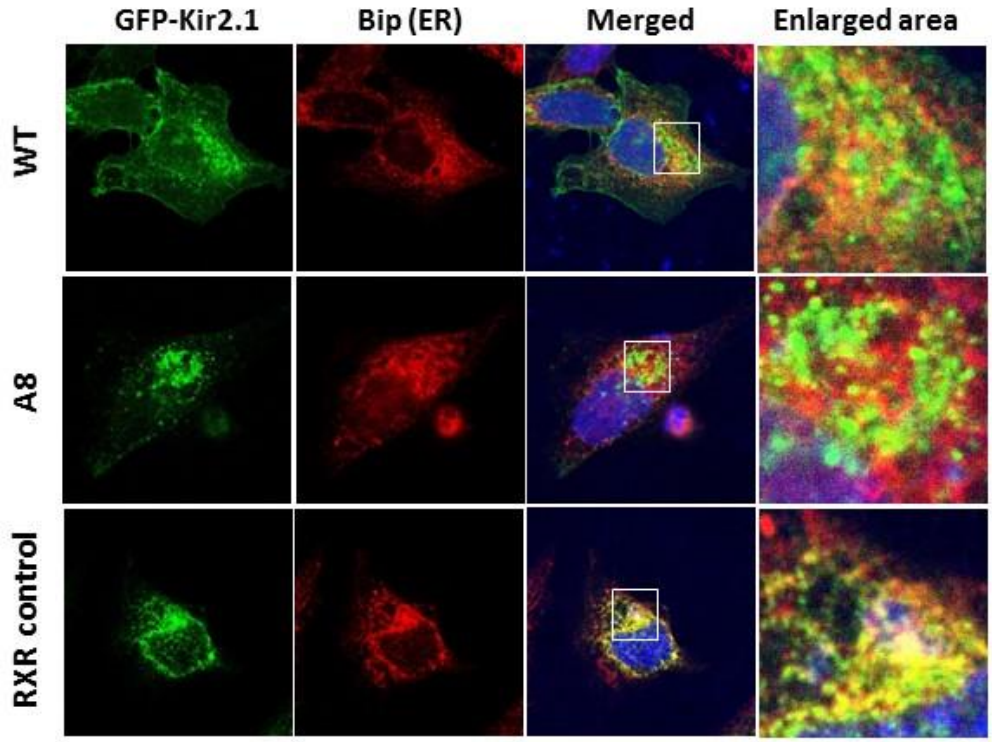

Figure 26. Kir2.1-A8 does not appear co-localized with the ER marker Bip. HeLa cells expressing either GFP-tagged Kir2.1-WT (upper panels), Kir2.1-A8 (middle panels) or Kir2.1-RXR control, were fixed and permeabilized, then stained for Bip followed by Cy3-labeled secondary antibody. Images were collected with a laser scanning confocal microscope. Kir2.1-WT does not co-localize with Bip, rather it is present on the cell surface (upper panels). Kir2.1-J77 shows no signal on the cell surface but rather shows co-localization with Bip (lower panels). Kir2.1-A8 (middle panels) is not co-localized with Bip, suggesting the surface reduction of Kir2.1-A8 is not mediated through ER retrieval/retention.

endocytosis permitting temperature, 37 °C, for various time periods, then cooled back down to 4 °C and stained with a fluorescently tagged secondary Ab at 4 °C. The Kir2.1 fusions remaining on the cell surface were analyzed by FCM. The fusion of the hit sequences A8, A9, J47, and J55 all significantly increased the rate of Kir2.1 endocytosis (Fig. 27), indicating that these hit sequences function to reduce the surface levels of Kir2.1 by promoting endocytosis.

IV.4.3g Kir2.1 fused A8, A9, J47 and J55 undergo clathrin-mediated endocytosis

The di-Leu motif has been characterized to function by promoting clathrin-mediated endocytosis (39). We were curious whether Kir2.1 fused to our hit sequences functioned this mechanism. To explore this possibility, we utilized AP180C, a C-terminal clathrin binding domain of another essential clathrin adapter protein AP180 that specifically disrupts clathrin-mediated endocytosis (87) to test if the hit Kir2.1 constructs were internalized via the clathrin-mediated pathway.

To determine if our Kir2.1 peptide fusions were undergoing clathrin-mediated endocytosis we co-expressed our Kir2.1 fusion constructs with either empty vector (pCDNA3.1) or AP180C in HEK293 cells to see if the disruption of clathrin-mediated endocytosis would increase the steady-state surface levels of Kir2.1 fusion protein. The Kir2.1 fusion constructs all showed increased presence on the cell surface when co-transfected with AP180C compared to empty vector, consistent with the proteins constitutively undergoing clathrin-mediated endocytosis (Fig. 28B). On the other hand, Kir2.1-WT showed reduced rather than increased surface expression when co-expressed with AP180C compared to empty vector (Fig. 28B), which would suggest clathrin-independent endocytosis, which is inconsistent with the previous reports (88). However, examination of the total expression levels by western blot analysis revealed that co-expression of Kir2.1 with AP180C substantially reduced the overall Kir2.1 protein expression level compared to the co-expression with empty vector pCDNA3.1 in both WT and Kir2.1 peptide fusions (Fig. 28C). We do not have good explanation for this reduced expression of Kir2.1 by

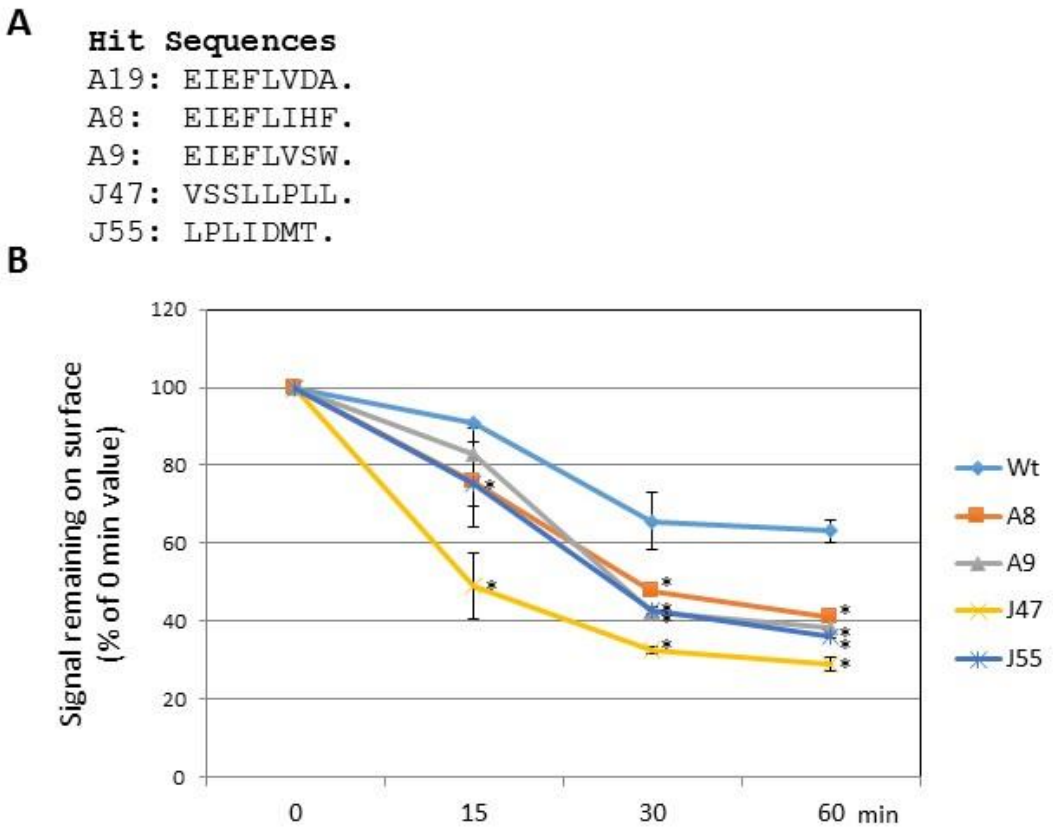

Figure 27. Kir2.1 fused to hit sequences A8, A9, J47, and J55 show enhanced endocytosis compared to Kir2.1-WT. (A) Amino acid sequence of hit sequences. (B) Endocytosis of Kir2.1-WT and fusion constructs. Kir2.1 expressed in HEK293 cells were labeled with a primary anti-HA epitope antibody at 4 °C where endocytosis is inhibited. Cells were then warmed to an endocytosis permitting temperature, 37 °C, for various time periods, then cooled back down to 4°C and stained with fluorescently tagged secondary antibody at 4°C. The Kir2.1 fusions remaining on the cell surface were analyzed by FCM. Values are average±SD from a representative experiment. * indicates significant difference ($P<0.05$) from WT values at each time point.

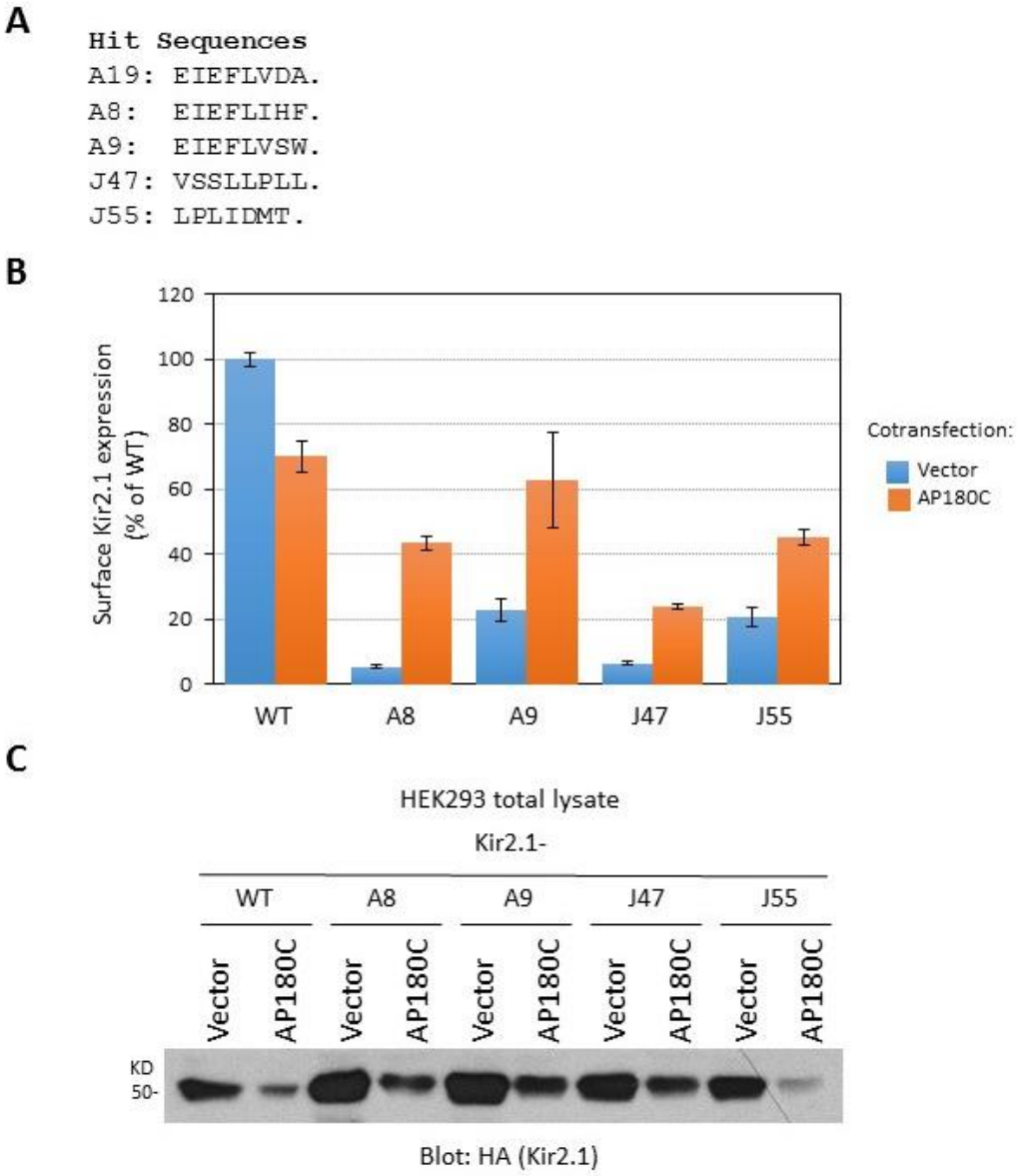

Figure 28. Kir2.1 fused to A8, A9, J47, and J55 are sensitive to AP180C, an inhibitor of clathrin-mediated endocytosis, causing an increase in their surface levels despite a decrease in overall expression level. (A) Amino acid sequence of hit sequences. (B) Surface levels of Kir2.1-WT and Kir2.1 fusion constructs when co-expressed with AP180C. HEK293 cells were co-transfected with HA-Kir2.1 constructs and either empty vector (pCDNA3.1) or AP180C. Kir2.1 cell surface expression was analyzed by FCM. The median values were determined for the total viable cell populations and normalized to the average value of WT. Results shown in average±SD. of triplicate samples from the representative of three experiments. (C) Total lysates from HEK293 co-transfected with HA-Kir2.1 constructs and either empty vector or AP180C were resolved by SDS–PAGE and immunoblotted for HA.

AP180C co-transfection, although differential transcriptional competition between the plasmid vectors might be a possible reason. Nonetheless, the relatively slow rate of endocytosis of Kir2.1-WT, combined with the reduced total expression level of Kir2.1 when co-transfected with AP180C could explain our WT result, whereas for the rapidly internalizing Kir2.1 fusion proteins (A8, A9, J47, J55) the disruption of clathrin-mediated endocytosis probably overcame the loss of total protein expression and increased the steady-state surface expression level.

To more clearly determine the clathrin dependency, we used an Ab feeding assay to test if the internalization of Kir2.1 proteins is regulated by the presence of AP180C. In the Ab feeding assay each sample is normalized to its pre-internalization value, eliminating the effect of the relative protein

expression level on the data. We co-expressed our Kir2.1 fusion constructs with either empty vector or AP180C and performed the previously described Ab feeding assay. At 30 min after shifting to the endocytosis permitting temperature 37 °C, Kir2.1-WT co-expressed with AP180C showed significantly 7hyureduced endocytosis when compared to co-transfection with empty vector, a result consistent with Kir2.1-WT undergoing a clathrin-mediated endocytosis (Fig. 29). All the tested Kir2.1 fusion proteins also showed significantly reduced endocytosis when co-expressed with AP180C, consistent with our steady-state result. Combined, our data suggest that as previously reported Kir2.1-WT undergoes a constitutive clathrin-mediated endocytosis (88) and fusion of hit sequences A8, A9, J47, and J55 to Kir2.1 all increased the rate of clathrin-mediated endocytosis (fig. 30).

IV.4.3h The Leu residues of A8, A9, J47 and J55 are critical to the Kir2.1 surface reduction phenotype, however an additional hydrophobic residue is also contributing to the A8 and A9 effect

Finally, to determine if the enriched clathrin-mediated endocytosis of the Kir2.1 fusion proteins was mediated through di-Leu motifs found in the hit sequences, we generated Ala mutants by replacing the Leu and adjacent residues. We expressed these constructs in HEK293 cells and used FCM analysis to

A

```
Hit Sequences
A19: EIEFLVDA.
A8:  EIEFLIHF.
A9:  EIEFLVSW.
J47: VSSLLPLL.
J55: LPLIDMT.
```

B

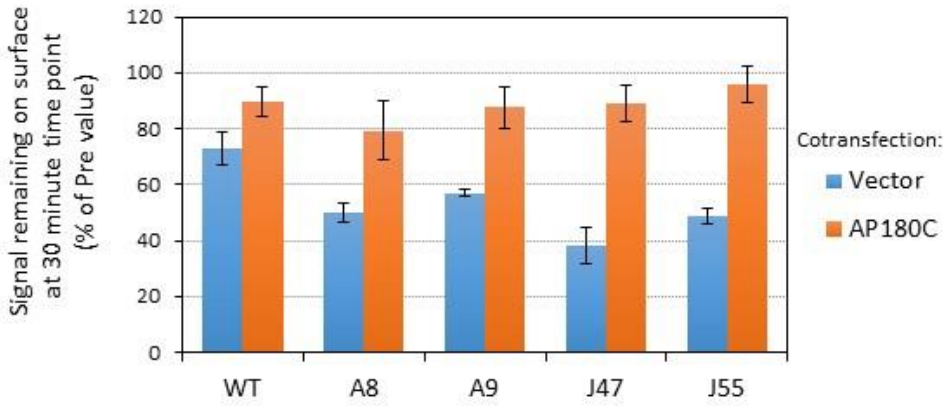

Figure 29. Kir2.1-WT and Kir2.1 fused A8, A9, J47, and J55 show sensitivity to AP180C, the inhibitor of clathrin-mediated endocytosis (A) Amino acid sequence of hit sequences. (B) Endocytosis of Kir2.1-WT and Kir2.1 fused A8, A9, J47 and J55 are sensitive to AP180C. HEK293 cells co-expressing Kir2.1 constructs and either empty vector or AP180C were labeled with primary anti-HA epitope antibody at 4 °C, where endocytosis is inhibited. Cells were then warmed to an endocytosis permitting temperature, 37 °C, for 30 min, then cooled back down to 4°C and stained with fluorescently tagged secondary antibody at 4°C. The Kir2.1 fusions remaining on the cell surface were analyzed by FCM. All the constructs Kir2.1-WT and the fusions, showed sensitivity to AP180C, with less protein endocytosed from the cell surface.

Role of sequences A8, A9, J47 and J55 in down-regulating surface expression of Kir2.1

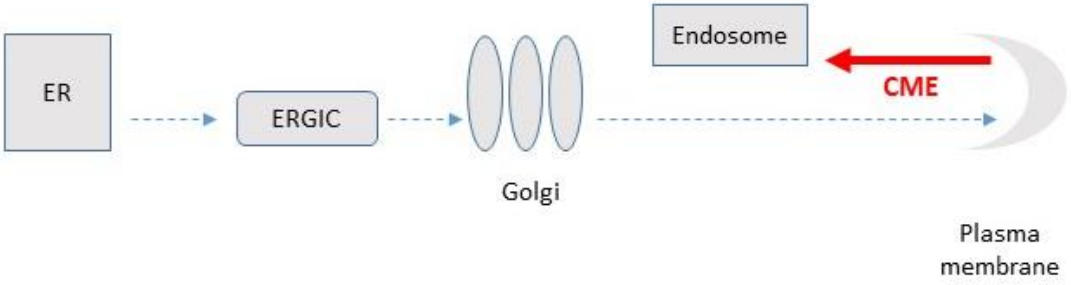

Figure 30. Hit sequences A8, A9, J47 and J55 fused to the extreme C-terminal tail of Kir2.1 promotes the clathrin-mediated endocytosis of the channel.

analyze the surface levels of the mutated hit constructs, and checked the total expression levels by western blot analysis of the total cell lysates. For Kir2.1-A8, we generated mutants making a single Ala replacement of each of the residues of the hit sequence. FCM analysis showed that mutating either of the residues comprising the di-Leu motif, L5 and I6, caused a partial surface restoration of the protein (Fig. 31A). The final C-terminal hydrophobic residue, F8, also caused the partial restoration whereas no other substitutions caused an increase of the protein on the cell surface (Fig. 31A). We generated the single Ala replacements of the last four residues of Kir2.1-A9, similar to Kir2.1-A8. Both elimination of the residues of the atypical di-Leu motif, L5 and V6, as well as the final C-terminal hydrophobic residue, W8, caused the partial restoration of the surface levels of the protein (Fig. 31C). These results were surprising in that if Kir2.1-A8 and A9 are acting as the established di-Leu signals, we would expect to see a full restoration of the surface level by replacing any of the essential Leu residues. Additionally, downstream hydrophobic residues have not been characterized to enrich the effect of the di-Leu motif, yet in both Kir2.1-A8 and A9, replacing the final hydrophobic residue with Ala caused the partial restoration of the surface levels. These results could suggest either that in the context of Kir2.1, sequence A8 and A9 could be functioning through a novel mechanism. It is also possible that the downstream hydrophobic residue enhances the effect of the di-Leu motif.

We also generated the Ala mutants of Kir2.1-J47. This sequence contained two di-Leu signals and to obliterate all potential di-Leu motifs it was necessary to mutate three Leu residues to Ala per mutant. We also generated a mutant changing all four Leu residues to Ala. Interpretation of the results was made difficult by the fact that some of the mutants did not express well as measured by the total lysate blot (Fig. 31F). Kir2.1-J47-L5/7/8/A, and Kir2.1-J47-L4/5/7/8/A had reduced total expression level and thus reduced surface levels (Fig. 31, E and F). Kir2.1-J47-L4/7/8A showed a partial restoration of the surface levels. Kir2.1-J47-L4/5/7A and Kir2.1-J47-L4/5/8/A had the majority of the protein restored to the surface (Fig. 31E).

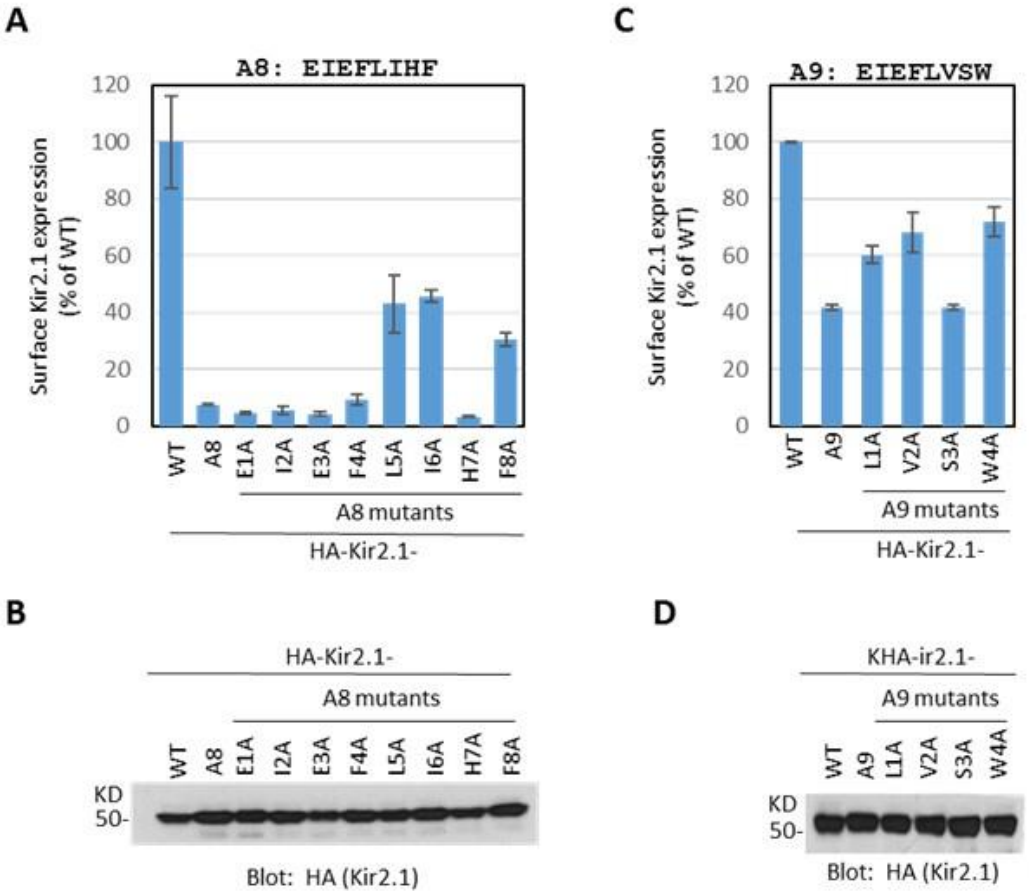
A
A8: EIEFLIHF
Surface Kir2.1 expression (% of WT)
120
100
80
60
40
20
0
WT
A8
E1A
I2A
E3A
F4A
L5A
I6A
H7A
F8A
A8 mutants
HA-Kir2.1-
C
A9: EIEFLVSW
Surface Kir2.1 expression (% of WT)
WT
A9
L1A
V2A
S3A
W4A
A9 mutants
HA-Kir2.1-
B
HA-Kir2.1-
A8 mutants
KD
50-
Blot: HA (Kir2.1)
D
KHA-ir2.1-
A9 mutants
KD
50-
Blot: HA (Kir2.1)

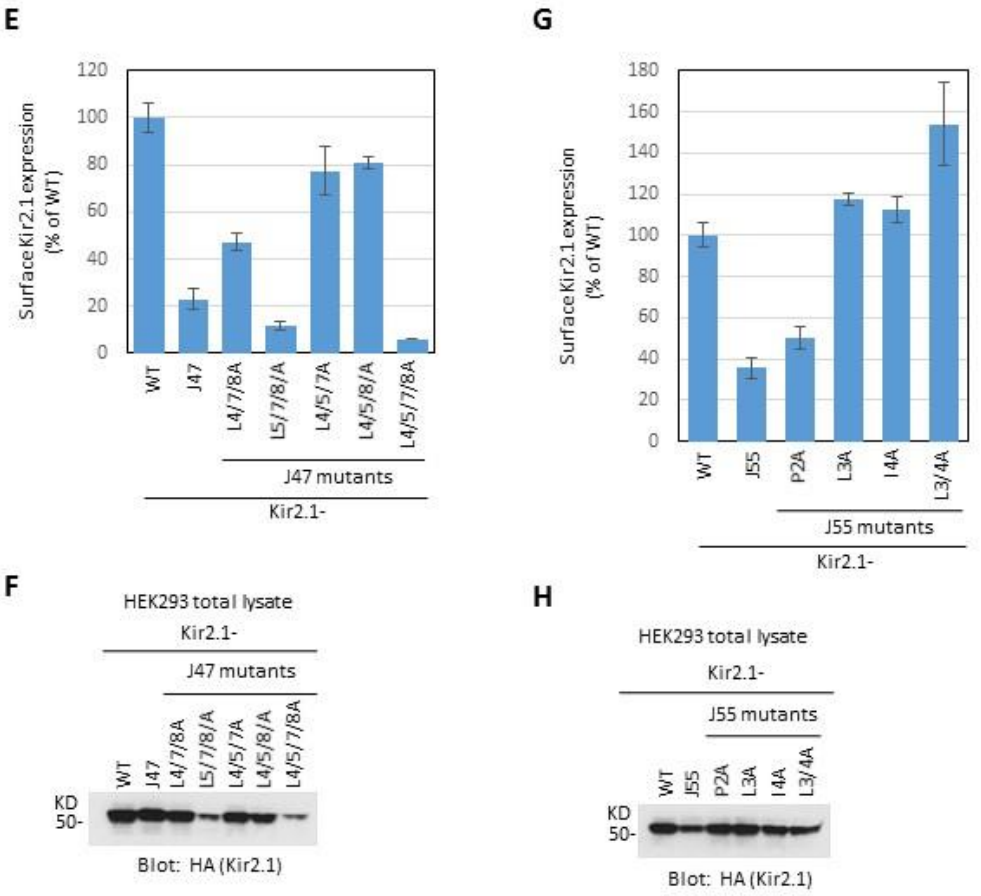

Figure 31. Surface levels of Kir2.1 fused A8, A9, J47, and J55 Ala mutations. (A, C, E, G) Surface expression of Kir2.1 fusions. HEK293 cells were transiently transfected with HA-Kir2.1 constructs and analyzed for cell surface expression of Kir2.1 fusion peptides by FCM. The median values were determined for the total cell populations and normalized to the average median value of WT. (B, D, F, H) Total lysates from HEK293 cells transfected with HA-Kir2.1 fusion constructs were resolved by SDS–PAGE and immunoblotted for HA. (A) Cell surface levels of Kir2.1-A8 Ala mutants. (B) Total expression level of Kir2.1-A8 Ala mutants. (C) Cell surface levels of Kir2.1-A9 Ala mutants. (D) Total expression level of Kir2.1-A9 Ala mutants. (E) Cell surface levels of Kir2.1-J47 Ala mutants. (F) Total expression level of Kir2.1-J47 Ala mutants. (G) Cell surface levels of Kir2.1-J55 Ala mutants. (H) Total expression level of Kir2.1-J55 Ala mutants.

Ala mutation of Kir2.1-J55 showed the clear dependence on the di-Leu motif. Mutation of L3 or I4 to Ala caused the protein surface restoration to the level of Kir2.1-WT. Double mutation of L3/4A expressed higher on the surface than Kir2.1-WT, though for an unknown reason. Since a Pro residue preceding the di-Leu motif has been characterized to enhance the signal (43) we also mutated P2 to Ala. However, this mutation did not show an effect on the surface restoration (Fig. 31G). Combined, our results suggest that in each of the hit clones the di-Leu residues are critical for the enriched endocytosis. However, it is still not clear if the Kir2.1-fused hit sequences are functioning as the classic di-Leu motif. While Kir2.1-J55 appears likely to be functioning as a classic di-Leu motif, with Kir2.1-A8 and A9, the involvement of the additional downstream hydrophobic residue as well as the only partial surface restoration by mutations could suggest that A8 and A9 sequences may be a novel type of endocytosis motif.

IV.4.4 Hit sequence K20 functions as a PPxY Ubiquitin-ligase binding motif:

We obtained one sequence from the screen, clone K20 (PPSYYSCQ) that contained a PPXY consensus sequence known to bind to the WW domains of WW domain-containing proteins. There are many characterized proteins that contain WW domains that function to mediate protein-protein interactions involved in a wide array of cellular processes, including transcription, apoptosis, cellular differentiation, RNA splicing, and ubiquitination (89). Ubiquitination is the process most relevant to protein trafficking (89). Protein ubiquitination within the protein trafficking system was first and is most well characterized in its role in protein degradation via the proteasome. In this system, proteins are covalently tagged with chains of ubiquitin moieties, which signal the protein for degradation in the proteasome (90). Proteasomal degradation is typically understood to be instrumental in cellular housekeeping, eliminating excess, misfolded, or misassembled proteins from the cell (90). ERAD, which eliminates the erroneous proteins in the ER, functions through the ubiquitin proteasome system. However, ubiquitin has since been characterized to play many additional roles in protein trafficking (91). These roles include acting as signals for endosomal sorting and lysosomal degradation through its interaction with the

Endosomal Sorting Complexes Required for Transport (ESCRT) machinery. Ubiquitination of proteins can also act as a trafficking signal that induces endocytosis of plasma membrane proteins (91).

Ubiquitin as a trafficking signal for endocytosis has now been characterized in many membrane proteins in both yeast and mammalian cells. In mammalian cells the roll of ubiquitin in the trafficking of membrane proteins has perhaps best been characterized in the epidermal growth factor receptor (EGFR) and the epithelial sodium channel (ENaC). ENaC endocytosis is specifically dependent on the ubiquitination of its PPXY domain (92). ENaC ubiquitination is mediated through the binding of Nedd4-2, a WW domain-containing E3 ubiquitin ligase, to PPXY motifs in the C-terminal tail of ENaC. Ubiquitination of ENaC when located in the the plasma membrane induces endocytosis into the early endosomes where ubiquitinated ENaC proceeds to the lysosome for degradation. Alternatively, some ENaC can be deubiquitinated in the endosome and recycled back to the plasma membrane (30). Currently the mechanism of ENaC endocytosis remains controversial (92). Some studies have shown ENaC to be undergoing clathrin-mediated endocytosis (93), whereas other studies contend the channel undergoes caveolin-dependent endocytosis (94). It seems the exact experimental conditions can affect the mechanisms by which ENaC is endocytosed as there is often conflicting data between studies using transfected or untransfected cells (95). Additionally, the processes of ENaC endocytic sorting, recycling, and degradation remain only partially understood (95).

FCM analysis of Kir2.1-K20 showed a reduction of the surface level of the fusion protein compared to WT, and the total lysate blot showed a reduction in the total expression level of the protein (Fig. 9), probably suggesting degradation. However, B31 *Δdoa10* expressing Kir2.1-K20 did not show a change in the K^+ sensitivity compared to B31, indicating that the degradation of Kir2.1-K20 was likely not mediated by ERAD (Fig. 11). In light of the apparent PPXY domain contained in sequence K20 we first tested whether Kir2.1-K20 was functioning in a PPXY-dependent manner and causing the ubiquitination of the channel.

First, in order to determine if the PPXY motif is the functional motif contained within the K20 sequence, we generated Kir2.1-K20 mutants where the essential residues of the PPXY motif P1, P2, and Y3 (PPSYYSCQ) were mutated to Ala, respectively. We compared the surface levels of Kir2.1-WT, Kir2.1 fused to K20 and the K20 Ala mutants by FCM analysis. While the K20 Ala mutants resulted in a partial restoration of the surface levels of Kir2.1 compared to Kir2.1-K20, the surface levels of the mutant K20 were still below the Kir2.1-WT levels (Fig. 32).

Reviewing the literature, we found that, in the context of poly(A)-binding protein-interacting protein 1 (Paip1), the PPXY motif was shown to partially function even with a single Pro residue. The functional motif of Paip1 was found to be PEFYPSGY requiring only the PXXY motif, indicating that the PPXY motif could function as a degenerate sequence (96). With our hit sequence K20, generating Ala mutations of P1, P2 Y3 all resulted in a PXXY sequence, and this could have partially functioned as a WW binding motif. We therefore generated a double Ala mutant of K20, mutating P1 and P2 to Ala (AASYYSCQ), and examined the surface expression level. The double Ala mutation of K20 restored the surface level of Kir2.1 even beyond that of Kir2.1-WT. (Fig. 32). While we do not have a good explanation for why the double mutant surpasses WT, our results suggest that the PPXY motif is the functional requirement of the K20 hit sequence.

Being that the PPXY motif is known to mediate ubiquitination of proteins, we tested whether sequence K20 was causing increased ubiquitination of Kir2.1 by a co-IP experiment. HEK293 cells were transiently co-transfected with HA-Kir2.1 constructs and a construct encoding Myc-tagged ubiquitin, and the immunoprecipitated Kir2.1 proteins were probed for association with ubiquitin. Kir2.1-K20 showed increased ubiquitination compared to Kir2.1-WT and other Kir2.1 hit clones (Fig. 33).

Since Kir2.1-K20 was insensitive to the disruption of an ERAD machinery Doa10 in yeast, we looked to explore whether degradation of Kir2.1-K20 involves endocytosis as has been reported for ENaC (92). We

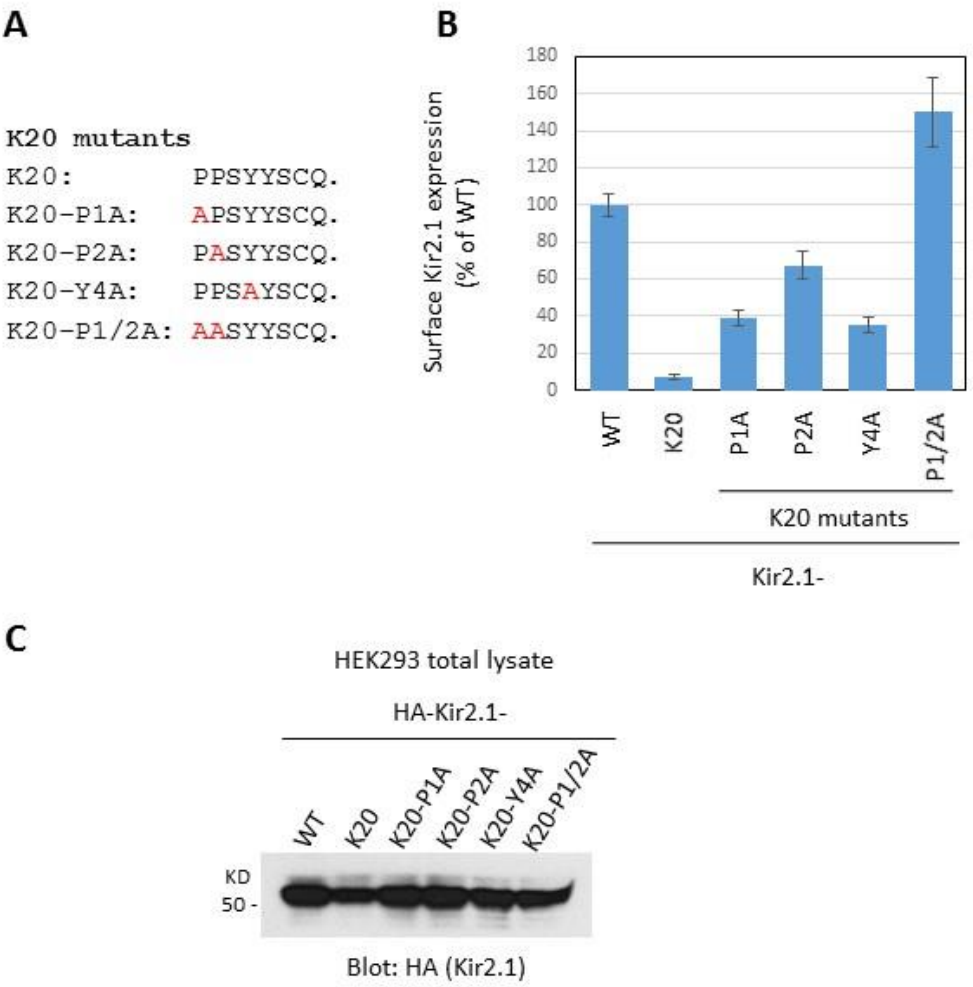

Figure 32. Ala mutation scanning of the PPxY residues from hit sequence restores the surface level of Kir2.1. (A) Amino acid sequence of parental hit sequence K20 and K20 Ala mutants of the PPXY motif. (B) Surface expression of Kir2.1-K20 fusions. HEK293 cells were transiently transfected with HA-Kir2.1 constructs and analyzed for cell surface expression by FCM. The median values were determined for the total viable cell populations and normalized to the average median value of WT. (C) Total lysates from HEK293 cells transfected with HA-Kir2.1 fusion constructs were resolved by SDS–PAGE and immunoblotted for HA.

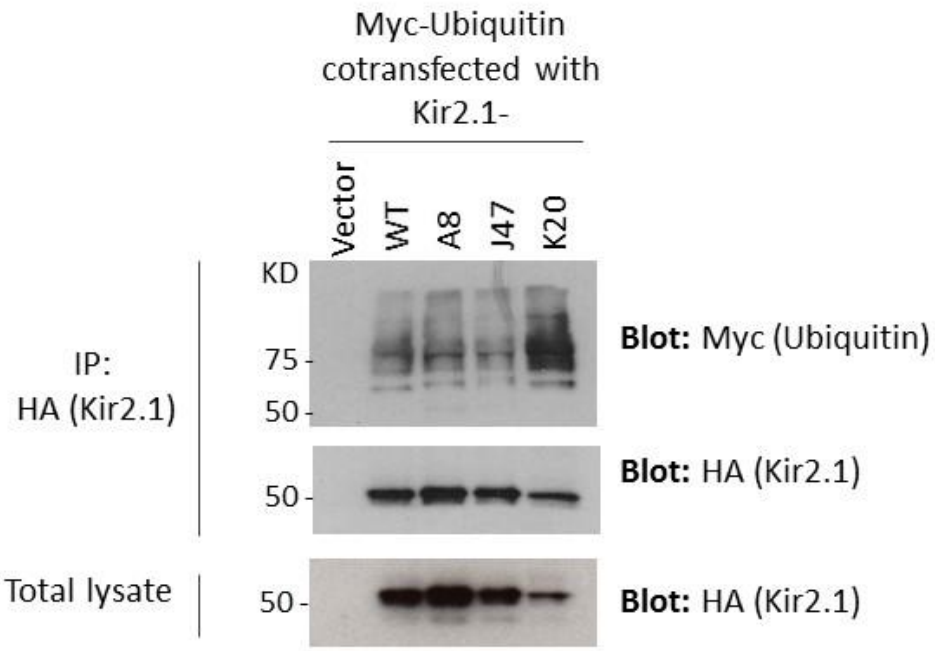

Figure 33. Kir2.1-K20 shows enriched ubiquitination compared with Kir2.1-WT and Kir2.1 fused to other hit constructs. HEK293 cells were co-transfected with HA-Kir2.1 hit constructs and a construct encoding Myc-tagged ubiquitin. The immunoprecipitated HA-Kir2.1 proteins were resolved by SDS-PAGE and blotted for HA (top) and Myc (middle). Total lysate proteins were blotted for HA (bottom).

first tested whether Kir2.1-K20 was inducing endocytosis by our previously described Ab feeding assay. We also explored Kir2.1-K20's sensitivity to AP180C in HEK293 cells by examining both the steady-state levels of Kir2.1 as well as the rate of endocytosis when co-expressed with AP180C (Fig. 34). Our Ab feeding assay did not show an increase in the endocytosis of Kir2.1-K20 when compared with Kir2.1-WT (Fig. 34A), however, interestingly, unlike Kir2.1-WT, the endocytosis of Kir2.1-K20 appeared insensitive to AP180C inhibition as measured by both steady-state surface levels (Fig. 34B) as well as the endocytosis rate of Kir2.1-K20 determined by the Ab feeding assay (Fig. 34C). These results suggest that while sequence K20 did not increase the endocytosis rate itself, it could be altering the path of internalization from clathrin-mediated to clathrin-independent endocytosis. Additionally, being that fusion of sequence K20 did not increase the rate of endocytosis, endocytosis alone cannot explain the reduced steady-state surface level of Kir2.1-K20. We speculate that Kir2.1-K20 at the plasma membrane recruits a WW domain-containing ubiquitin E3 ligase that ubiquitinates the channel, and this leads to the clathrin-independent endocytosis and the subsequent proteasomal or lysosomal degradation (Fig. 35). The switching of the endocytosis pathway from the clathrin-mediated to the clathrin-independent one by PPXY motif is a novel finding but warrants further investigation if this effect is specific to Kir2.1 or applies to other membrane proteins.

IV.4.5 Discussion:

The correct trafficking of proteins throughout the cell is critical for cell function and survival. Elucidating the mechanisms, machineries and pathways of protein transport throughout the cell provides valuable knowledge of cellular physiology, cellular disease, and potential therapeutics for diseases caused by trafficking defects. Our laboratory takes particular interest in the trafficking of membrane bound proteins. The cell surface density of membrane proteins dictates their corresponding cellular activity (8), and many diseases, such as cystic fibrosis, arise from defects in cell surface trafficking of membrane proteins (5).

A

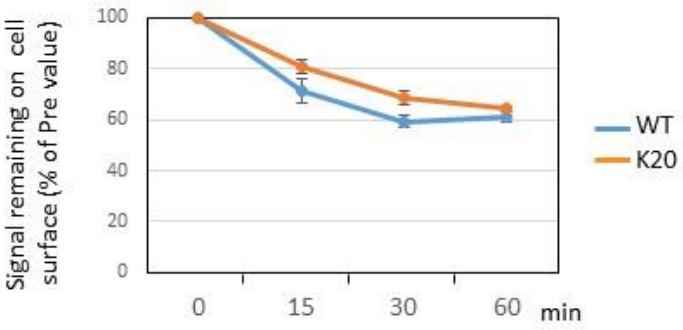
Signal remaining on cell surface (% of Pre value)
100
80
60
40
20
0
0
15
30
60
min
WT
K20

B

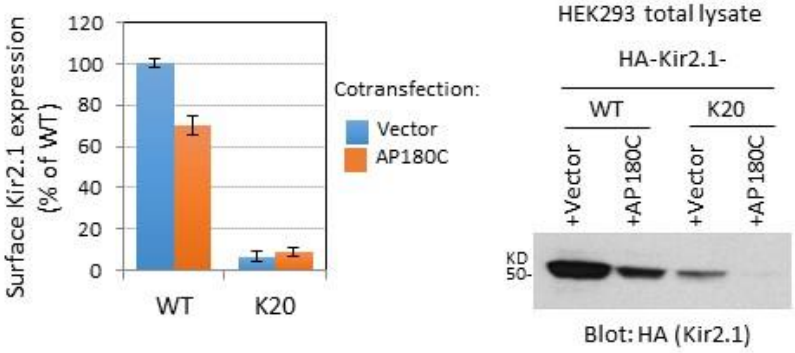
Surface Kir2.1 expression (% of WT)
120
100
80
60
40
20
0
WT
K20
Cotransfection:
Vector
AP180C
HEK293 total lysate
HA-Kir2.1-
WT
K20
+Vector
+AP180C
+Vector
+AP180C
KD
50-
Blot: HA (Kir2.1)

C

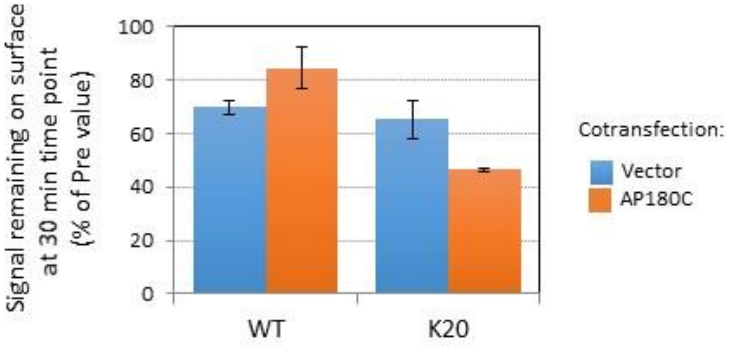
Signal remaining on surface at 30 min time point (% of Pre value)
100
80
60
40
20
0
WT
K20
Cotransfection:
Vector
AP180C

Figure 34. Kir2.1 fused K20 does not exhibit an increase of endocytosis compared to WT, however Kir2.1-K20 appears insensitive to AP180C inhibition. (A) Endocytosis of Kir2.1-WT and Kir2.1-K20. Kir2.1 expressed in HEK293 cells were labeled with primary anti-HA epitope antibody at 4 °C, where endocytosis is inhibited. Cells were then warmed to an endocytosis permitting temperature 37 °C for various time periods, then cooled back down to 4°C and stained with fluorescently tagged secondary antibody at 4°C. The Kir2.1 signals remaining on the cell surface were analyzed by FCM. The total florescent values were determined for the total viable cell populations and normalized to the average value of the pre-internalization samples. Results shown in average±SD of triplicate samples from the representative of three experiments. The fusion of hit sequence K20 did not effect the Kir2.1 endocytosis rate. (B) Surface levels of Kir2.1-WT and Kir2.1 fusion constructs when co-expressed with AP180C. HEK293 cells were co-transfected with HA-Kir2.1 constructs and either empty vector (pCDNA3.1) or AP180C. Kir2.1 cell surface expression was analyzed by FCM. The median values were determined for the total cell populations and normalized to the average median value of WT. Results shown in average ±s.d. of triplicate samples from the representative of three experiments. (C) Total lysates from HEK293 co-transfected with HA-Kir2.1 constructs and either empty vector (pCDNA3.1) or AP180C were resolved by SDS–PAGE and immunoblotted for HA. (D) HEK293 cells co-expressing Kir2.1 constructs and either empty vector (pCDNA3.1) or AP180C were labeled with primary anti-HA epitope antibody at 4 °C where endocytosis is inhibited. Cells were then warmed to an endocytosis permitting temperature 37 °C for 30 min, then cooled back down to 4°C and stained with fluorescently tagged secondary antibody at 4°C. The Kir2.1 signal remaining on the cell surface were analyzed by FCM. The total florescent values were determined for the total viable cell populations and normalized to the average value of the pre-internalization samples. Results shown as average±SD of triplicate samples from the representative of three experiments

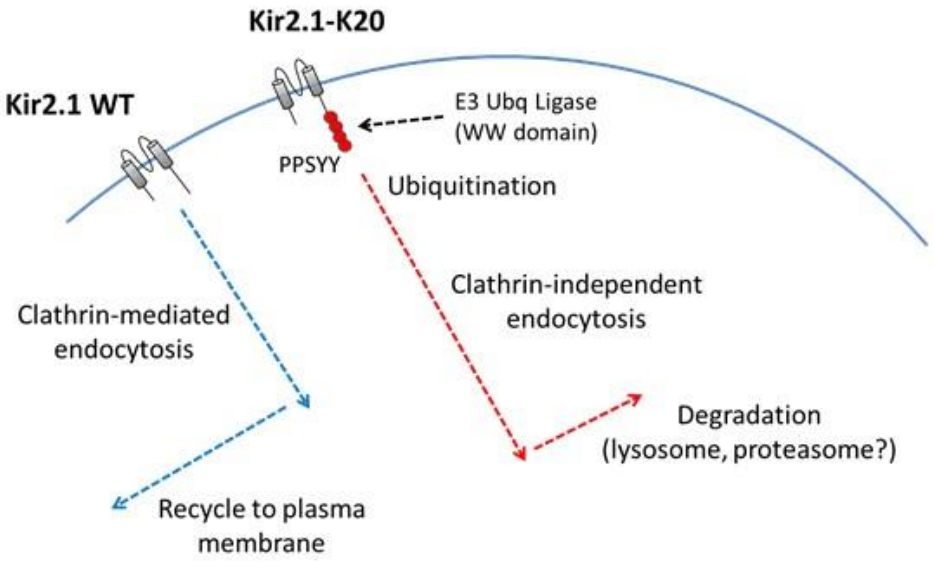

Figure 35. Hypothetical model of Kir2.1-K20. Fusion of K20 to Kir2.1 causes the ubiquitination of the channel and the switch from CDE to CIE. While the mechanism of endocytosis changes, the rate remains the same so the switch in endocytic pathways cannot explain the Kir2.1 surface reduction phenotype. We hypothesize that post endocytosis Kir2.1-K20 is targeted for degradation whereas Kir2.1-WT may undergo more recycling to the plasma membrane.

Intracellular trafficking of membrane proteins is often dictated by the distinct signal motifs on the cargo proteins (27-29,31). These signals are recognized by the protein trafficking machinery, sorted into the correct coated vesicles, and transported down the appropriate pathways to their final destinations (27-29,31). Despite the fact that many trafficking sequences have been identified and characterized, many membrane proteins are transported throughout the cell without containing any of the well-characterized trafficking motifs (43). Our goal was to develop a novel systematic approach to identify trafficking signal sequences that reduce the surface levels of membrane bound proteins.

We observed a previous study by Kolacna and coworkers that reported that the B31 yeast strain lacking the K^+ and Na^+ efflux system shows sensitivity to higher external concentrations of alkali–metal–cation salts when transformed with a mammalian Kir2.1 channel (60). Due to the fact that Kir2.1 activity inversely correlates with B31 growth in high K^+ media, we hypothesized that the complementation of growth of B31 expressing Kir2.1 on high K^+ media would reflect the trafficking of functional receptor to the cell surface. In chapter III we explored this possibility, demonstrating that the B31 system can be used to study the function and trafficking of Kir2.1 and other open K^+ channels such as KCNK3 and KCNK9. Moreover, the fact that B31 growth was rescued in high K^+ media when expressing Kir2.1 channel fused to the characterized trafficking motifs known to reduce the surface levels of proteins demonstrated that the B31 screening system could be used for identifying the *cis*-acting peptide sequences that downregulate surface trafficking of the K^+ channels and other membrane proteins in mammalian cells.

Based on our studies with B31 along with the fact that previous studies have demonstrated that the extreme C-terminal tail of Kir2.1 can be modified without having an effect on the function or surface transport of the protein (45,77), we hypothesized that B31 could be used to develop a gain-of-function screening system to identify trafficking signal sequences that reduce the levels of membrane proteins on the cell surface. By fusing a random peptide library to the C-terminal tail of Kir2.1, expressing the library

in B31 and screening on high K^+ media, we hypothesized that the signals that reduced the surface levels of Kir2.1 would be enriched on the screening plates. Furthermore, as our initial studies on B31 demonstrated that the B31 growth was rescued both by the fusion of ER retrieval motifs, as well as an endocytosis motif, we predicted that the B31 screening system would offer a platform to screen for trafficking motifs functioning through many distinct pathways.

Here, in Chapter two, we developed and carried out the B31 screening. As hypothesized, the B31 screening system was able to select for trafficking signal sequences that reduced the surface levels of Kir2.1. Upon characterization of the identified hit sequences we determined that our system identified trafficking motifs functioning to reduce the surface levels of Kir2.1 through at least four distinct trafficking pathways: (1) sequences containing large patches of hydrophobic residues which leads to the ERAD (represented by clone E3), (2) sequences containing the di-Arg motif mediating COPI-mediated ER retrieval (represented by clones E6 and J77), (3) sequences which mediate clathrin-mediated endocytosis (represented by clones J47, J55, A8, and A9) and (4) a sequence (clone K20) matching the PPXY motif that causes ubiquitination and subsequent degradation probably in the post-ER stage of trafficking (fig. 36). Additionally, the fact that many of hit sequences functioned when transplanted to CD8 demonstrates the screening systems ability to identify autonomous trafficking motifs not limited to the Kir2.1 protein context.

The most commonly identified signal sequences from the screen were sequences involved with protein folding quality control. Hit sequences containing large patches of strong hydrophobic residues (represented by hit sequence E3), which are recognized as a sign of protein misfolding in the ER and induces ERAD, were the most abundantly identified signals obtained from the screen. The next most abundant signals in the screen were di-Arg signals (represented by sequences E6 and J77), which act as a signal of misfolded proteins that have escaped the ER and induces COPI mediated ER retrieval. It is perhaps not surprising that these sequences would be the most common in the screening. The escape of

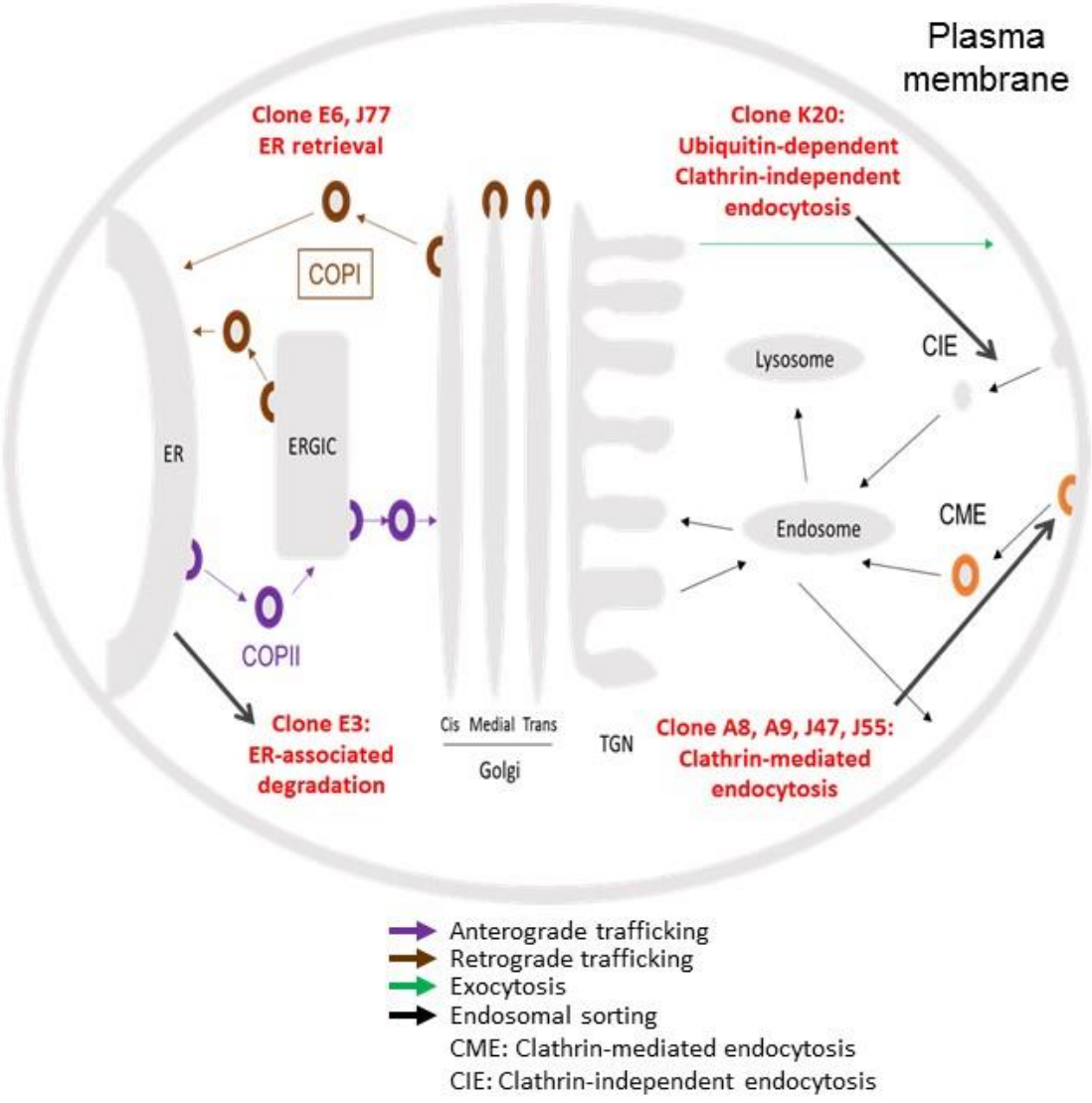

Figure 36. Overview of hit sequence function in the context of Kir2.1 identified from the B31 screening system.

misfolded proteins from the ER is associated with many diseases including cancers and neurodegenerative diseases (4). It is therefore logical that the cellular systems associated with identifying protein misfolds in the ER and beyond would be very robust. In fact, the abundance of strong hydrophobic signals that caused the ERAD of Kir2.1 were so high that it was necessary to optimize the screening system to reduce the number of these sequences from appearing on the screening so that we could identify other signals.

ER-retrieval of proteins is both an essential cellular process and critical process for membrane protein quality control, yet to date there remains only the two well characterized ER retrieval motifs in a relatively limited number of membrane proteins, the di-Lys (KKXX-COOH or KXKXX-COOH) and di-Arg (RXR) motifs (97). Hence, we were somewhat surprised that our screening did not identify more novel ER-retrieval motifs. Of the two known motifs we knew our screening system would be unable to detect di-Lys motifs, since our fusion of C-terminal KKXX motif to Kir2.1 did not rescue B31 growth in the 600 mM K^+ screening plate and also minimally reduced the surface expression of Kir2.1 in HEK293 cell (data not shown). The C-terminal di-Lys motif has been characterized to be less functional when placed distally from the transmembrane region, as opposed to the di-Arg signal that is less effective when placed proximally to the transmembrane region (83). Being that the C-terminal tail of Kir2.1 is 249 amino acids, the di-Lys motif will not function optimally in the context of Kir2.1. However thus far, the B31 screening system only identified the di-Arg motif and did not yet identify any novel ER retrieval motif. While we did demonstrate that Kir2.1 fused with the A8 sequence associates with COPI by co-IP assay and also the A8 sequence alone can pull-down COPI *in vitro*, the Kir2.1-A8 channel was not localized to the ER, and we were unable to clearly prove or disprove the functional significance of that binding in the trafficking pathways. CD8-A8 was localized to the ER at the steady-state, although pulse-chase analysis did not provide evidence of the ER retrieval from the Golgi for this construct. Nevertheless, in light of

Kir2.1-A8 binding COPI, and CD8-A8 being localized to the ER, it is possible that sequence A8 in different protein contexts might function as a novel ER retrieval motif.

We hypothesize that our current lack of novel ER retrieval motif is at least partly due to the high numbers of false positive clones and previously characterized motifs that appeared in our screening, limiting our ability to screen enough diversity space to identify a novel ER-retrieval motif. This issue of the "background noise" in the B31 screening system is perhaps the greatest challenge of the system. This issue, and further strategies to combat this issue will be discussed further in the discussion and future studies section. Resolving this issue will increase the likelihood of identifying novel trafficking motifs functioning through ER retrieval as well as other trafficking pathways.

In addition to the above motifs our screening also identified signals enriched for Leu residues, which, in the context of Kir2.1, we characterized as promoting endocytosis. We hypothesized that these motifs could be functioning as di-Leu endocytosis motifs. Indeed, our Ala mutation studies suggest that, of the four representative Leu rich motifs characterized, at least two, J47 and J55, are functioning as a classic di- Leu motif. The two other representative motifs, A8 and A9, while they may be also functioning as the classic motif, had some additional curious attributes that suggest other mechanisms could be involved. Firstly, Kir2.1-A8 and A9 bind COPI, the coat protein involved in retrograde trafficking, in co-IP assays. Additionally, synthetic peptides containing the A8 sequence were able to pull-down COPI *in vitro* as well, implying the direct interaction with the COPI complex. Despite binding, Kir2.1-A8 did not show typical localization in the ER at the steady-state. While as of current we have been unable to prove the functional relevance of the binding, the other motifs did not bind COPI. If the A8 and A9 COPI binding proves to be functionally relevant it might indicate that these sequences are functioning through a novel mechanism. While COPI has been best characterized as the coat protein mediating retrograde trafficking from the Golgi to the ER (97), there have been reports of COPI having a cryptic role in the post-endocytic sorting of proteins, although no distinct mechanism for this pathway has been elucidated (98,99). Thus it

is possible that A8 and A9 sequences play a role in the post-endocytic intracellular sorting of Kir2.1 through a COPI interaction, e.g., by regulating the plasma membrane recycling, to reduce the steady-state surface expression level.

An additional curiosity of Kir2.1-A8 and A9 is the fact that the additional downstream hydrophobic residue from the di-Leu or Leu-Val, separated by a single amino acid, seemed to contribute to a surface reduction phenotype similarly to the di-Leu or Leu-Val. Downstream hydrophobic residues playing a role in the di-Leu motif is not currently established. Based on the characterized classic di-Leu motif we expected that mutating any of the critical di-Leu or Leu-Val residues would result in total loss of surface reduction. Rather, what we observed was a single deletion of any of the di-Leu or Leu-Val residues as well as the downstream hydrophobic caused a partial restoration of the protein on the surface. These results could suggest that Kir2.1-A8 and A9 is functioning through a novel mechanism rather than the established di-Leu motif. Alternatively, they could indicate a novel role of additional downstream hydrophobic residues in enriching the di-Leu, motif which would also be a novel finding.

CD8-A8 and -A9 require further investigation as well. Unlike with Kir2.1, A8 and A9 sequences fused to CD8 localized the protein to the ER, at the steady-state, indicating these sequences were functioning through a different mechanism in the context of CD8 when compared with Kir2.1. In light of CD8-A8's ER localization and the fact that synthetic A8 peptides are able to pull-down COPI, we hypothesized that in the context of CD8 sequences A8 and A9 might function as an ER retrieval signal. However, by pulse-chase analysis we could not see the early maturation of CD8-A8 that we would expect of a protein undergoing retrieval, rather it appeared as retention in the ER. If CD8-A8 and A9 are truly retained in the ER, further work will be necessary to determine the mechanism of action. Of course, it is not possible to completely rule out the possibility of a mechanism of ER retrieval with this CD8 pulse-chase assay, as the CD8 protein could be rapidly retrieved from the ERGIC where early O-glycosylation enzymes are absent,

as has been reported for another receptor (13). Delineating the mechanism of CD8-A8 and A9 ER localization has the potential to identify novel mechanisms of ER retrieval/retention.

Finally, we obtained one hit sequence that we characterized as functioning as a PPxY ubiquitin ligase binding domain. However, the exact mechanism of Kir2.1 surface reduction remains elusive. Being that Kir2.1-K20 functioned similarly in both B31 and B31 *Δdoa10*, we ruled out ERAD for the reduced protein expression of this construct. Furthermore, the fact that our Ab feeding assay did not show a change in the endocytosis rate between Kir2.1-WT and Kir2.1-K20 indicates that the increased rate of endocytosis itself is not the mechanism either. It is curious that the fusion of the K20 sequence to Kir2.1 seemed to change the mechanism of endocytosis from the clathrin-mediated to clathrin-independent one, although that alone also cannot explain the surface reduction phenotype. Previous studies have suggested that the PPxY motif in ENaC induces the clathrin-independent endocytosis of the channel (94), however there remains conflicting evidence (93), and a clear consensus has not been made (92). Based on our current data, we speculate that the K20 peptide recruits the WW domain-containing ubiquitin E3 ligase that ubiquitinates Kir2.1, and this induces clathrin-independent endocytosis, which eventually leads to the degradation of the channel in the lysosome and/or proteasome. Additional studies on Kir2.1-K20 are required to determine where the ubiquitination is occurring, where the degradation is occurring, and the specific CIE pathway to fully elucidate the trafficking mechanism. Kir2.1-K20 will offer an interesting model that provides a better understanding of the PPxY motif's role in membrane protein trafficking.

IV.4.5a The B31 screening system requires the screening of many clones to identify potentially novel sequences:

The biggest challenge of the B31 screening system is the high amount of false positive clones that must be screened to identify hit sequences. In the screening system, the factor that determines B31 survival is

the lack of Kir2.1 channel on the cell surface. Therefore, as hypothesized, the trafficking signal motifs that reduce the cell surface levels of Kir2.1 are enriched on the screening plate. However, by the nature of the screen, any non-trafficking related factor that results in a reduction of Kir2.1 on the B31 surface are enriched as well. These false positive sequences act as “background noise” that increases the number of clones that need to be screened to identify true hit sequences.

The problem of false positive clones due to erroneous homologous recombination perhaps best illustrates the issue. In gap repair cloning by homologous recombination in yeast there is a small percentage of vector plasmid that undergoes erroneous homologous recombination in which the vector recombines with itself, losing the insert sequence but maintaining the selection marker. The percentage of erroneous homologous recombination is very low, reported to be below 1% (55). However, B31 containing these plasmids will survive the screening condition. Even an error rate of 0.5% would result in an additional 5000 false positive clones per million clones.

Of course, false positive clones due to erroneous homologous recombination are only one type of false positive that can appear in the screening system. Factors that inhibit ion conductance through the channel, Kir2.1 elongation clones, and yeast specific mechanisms all can appear as false positive clones in the screen. As discussed earlier, we developed a number of technical strategies to reduce the prevalence of false hit clones to a manageable range and systematically evaluated surviving clones to eliminate false positives, however false positive clones continued to remain throughout the screen reducing the throughput of the screens.

Additionally, as the screen progressed the high number of clones containing the established trafficking motifs became problematic as well. Our success in isolating the established trafficking motifs from the surviving hit clones demonstrated the screening system’s ability to enrich trafficking motifs from a random peptide library. Even better, we identified many trafficking signals functioning through multiple

distinct pathways. However, the high number of hits bearing the established strong trafficking signals eventually required screening of many clones to identify potentially novel sequences.

For example, the most commonly identified sequence type from the screen was sequences containing a patch of strong hydrophobic residues (e.g., clone E3), which both reduced the surface levels of Kir2.1 when fused to its C-terminal tail and also showed a much lower levels of overall expression by western blot analysis. We experimentally determined that these sequences were acting as a substrate for ERAD. These sequences were true, biologically relevant, hit sequences, however the high incidence of these sequences in the screen made identifying other types of sequence motifs very inefficient. As one strategy to combat this, we performed the screen with an oligonucleotide in which the random region was encoded by an NVK sequence; where N could encode any nucleotide, V could encode A, C, or G, and K could encode G or T. This sequence still permitted the encoding of all 20 amino acid residues however it now discriminated against strong hydrophobic residues and still eliminates the TAA and TGA stop codons.

While this approach did reduce the number of hit clones containing the strong hydrophobic sequences, it was an imperfect solution. As previously described, a weakness of oligonucleotides, and particularly oligonucleotides containing random sequences is the low prevalence of congeneric species containing one or more deleted nucleotide (78). In our case, any such congeneric species in the oligonucleotide pool would eliminate the desired effect of the NVK sequence, and hit clones containing the strong hydrophobic signals that caused the ERAD of Kir2.1 continued to appear throughout the screening.

In addition to the strong hydrophobic sequences, we also obtained a large number of clones containing di-Arg type motifs and, to a lesser extent, di-Leu type motifs. Again these motifs are *bona fide* trafficking signals that we would expect the screen to pick up, but their prevalence on the screening plate reduced the diversity space we could reasonably screen through. In the future studies chapter we propose

optimization strategies that, if successful, will greatly reduce the number of false positive clones appearing in the screen. We also propose strategies for reducing the known trafficking motifs from appearing on the screen.

V. Conclusions:

Here, the main findings and conclusions of this doctoral work are summarized:

- B31 growth assay reflects the functional surface expression levels of Kir2.1 and other inward rectifying K^+ channels.
- Developed the B31-based screening system to systematically identify sequence motifs that down-regulate surface expression of membrane proteins.
- Identified sequence motifs that reduced surface levels of Kir2.1 through at least four distinct trafficking pathways:
    - ERAD
    - COPI-mediated ER retrieval
    - Clathrin-mediated endocytosis
    - Ubiquitin ligase binding motif
    - Some identified signals are potentially functioning through novel mechanisms
- The B31 system requires the screening of many clones to identify novel sequences due to the high number of false positive and established motifs that appear on the screen
    - Additional technological and genetic optimization can eliminate false positives and established motifs:

VI. Future Studies:

VI.1 Optimizations to the B31 screening system:

We have demonstrated that our newly developed B31 yeast based screening system is able to be used to screen a random peptide library to identify trafficking motifs that reduce the surface levels of membrane proteins. However, the biggest challenge of the B31 screening system is the high amount of false positive clones and previously characterized motifs that appear on the screening plate, which reduces the throughput of the screening, and prohibited us from screening through the diversity space needed to identify more of the novel sequences. Despite the high amount of screening the current system requires, we believe that with sufficient resources and automation, the necessary diversity space could be screened. However, further optimizing the screen to reduce the false hits and known motifs would greatly improve the efficacy of the screening. Here, we propose optimization strategies that if successful will greatly reduce the number of false positive clones appearing in the screen.

VI.1.1 A fluorescent cell sorting strategy to eliminating false hit clones and rapidly degraded clones

False positive hit clones due to erroneous homologous repair that retain the auxotrophic marker but do not express Kir2.1 was the most abundant false positive hit appearing on the screen. Additional false positive clones such as Kir2.1 tail elongation causes the rapid degradation of Kir2.1. The most abundant true hit sequences were patches of strong hydrophobic residues, which caused ERAD of Kir2.1. The abundance of these Kir2.1 non-expressing or rapidly degrading clones greatly reduced the throughput of the screening system. Utilizing an improved fluorescent cell sorting strategy has the potential to screen out these clones before appearing on the screening plate.

During the initial screening optimization, we switched from using untagged Kir2.1 to GFP-tagged Kir2.1. We hypothesized, that by utilizing GFP-Kir2.1 we could perform an initial screening of the B31 growth phenotype on the high K^+ media, then a secondary screening by FCM to determine the Kir2.1 total

expression level by GFP levels. We compared the GFP levels in B31 expressing GFP tagged Kir2.1-WT, as well as the degrading E3 sequence and non-degrading J77 sequence by FCM analysis. Indeed, we could see a clear reduction in GFP expression in GFP-Kir2.1-E3 compared to both GFP-Kir2.1-WT and J77 (data not shown). Screening the yeast from the selection plate for GFP expression was a slow process being that the yeast needed to be individually picked and diluted for FCM analysis. However, utilizing fluorescent cell sorting, B31 expressing a GFP-Kir2.1 C-terminal fusion library could first be screened in high K^+ liquid media, followed by a secondary screening utilizing fluorescent cell sorting to exclude the population of cells with no or low GFP expression. Sorted cells could then be plated pre-cleared of clones lacking Kir2.1 expression or expressing Kir2.1 undergoing rapid degradation. This approach would simultaneously eliminate the most abundant false positive population, as well as the large population of ERAD inducing strong hydrophobic sequences. Indeed, a very similar approach is commonly used for screening yeast surface display libraries (55), and such protocols are likely amenable to the B31 screening system.

VI.1.2 Further mutations of the yeast protein trafficking machinery in B31 can be generated to potentially reduce the established trafficking sequences from appearing in the screen:

Completely eliminating the previously characterized trafficking motifs from appearing on the screen is impossible as the B31 screening system is designed to enrich such sequences. However, through further deletion and mutation of genes involved with protein trafficking in B31 the presence of certain signals can be reduced. For example, in this work we have shown that deleting the Doa10 gene in B31 selectively eliminated the growth of B31 *Δdoa10* on high K^+ media when expressing Kir2.1 constructs which undergo ERAD. Screening using B31 *Δdoa10* would likely result in much fewer clones in that Kir2.1 is degraded through ERAD. Similarly, Michelson *et. al*. developed a yeast mutant with mutated β and δ subunits of COPI that selectively inhibits COPI binding the di-Arg ER retrieval motif but not the di-Lys motif (38). Generating these mutations in B31 could eliminate di-Arg signals, which were the second

most abundant signal in the screen, from appearing on the screening plate. This COPI mutation could be particularly useful in the B31 system considering there are only the two well characterized ER retrieval motifs in membrane proteins, the di-Lys and di-Arg motifs. Given that the di-Lys motif does not function in the context of Kir2.1 due to the length of the C-terminal tail, utilizing a B31 mutant deficient in binding the di-Arg motif would mean any ER-retrieval motif identified would likely be novel.

The exact binding sites between some of the trafficking motifs and transport machinery have been determined (36-38) and mutating those residues in B31 could lead to the selective exclusion of other characterized signal motifs from the screening system. Additionally, less specific yeast mutants have been generated that cause generalized deficiencies in various trafficking pathways. For example, yeast with mutated dsl1 genes have been reported to partially reduce the efficacy of COPI-dependent ER retrieval (100) . There have also been many mutant yeast generated in which endocytosis has been disrupted (101). Generating additional strategic mutations in B31 could serve as a powerful tool for eliminating characterized sequences, or further focusing the B31 screening system to identify signals functioning on a specific pathway. Of course, many of these additional mutations are reported to slow the growth and/or reduce the viability of the yeast. Candidate B31 mutants would need to be tested to ensure that (1) the mutation is causing the desired results and (2) the transformation efficiency of the mutant B31 remains high enough to screen the necessary diversity space.

CITED LITERATURE

1. Savage, N. (2015) Proteomics: High-protein research. *Nature* **527**, S6-7
2. Hoeijmakers, J. H. (2009) DNA damage, aging, and cancer. *N Engl J Med* **361**, 1475-1485
3. Amara, J. F., Cheng, S. H., and Smith, A. E. (1992) Intracellular protein trafficking defects in human disease. *Trends Cell Biol* **2**, 145-149
4. Howell, G. J., Holloway, Z. G., Cobbold, C., Monaco, A. P., and Ponnambalam, S. (2006) Cell biology of membrane trafficking in human disease. *Int Rev Cytol* **252**, 1-69
5. Sampson, H. M., Thomas, D. Y., and Begley, T. P. (2007) Protein Trafficking Diseases: Small Molecule Approaches. in *Wiley Encyclopedia of Chemical Biology*, John Wiley & Sons, Inc. pp
6. Scheinost, J. C., Boldt, G. E., and Wentworth, P. (2012) Protein Misfolding and Disease. in *Chemical Biology*, John Wiley & Sons, Inc. pp 379-400
7. Tokarev, A. A., Alfonso, A., and Segev, N. (2009) Overview of Intracellular Compartments and Trafficking Pathways. in *Trafficking Inside Cells: Pathways, Mechanisms and Regulation*, Springer New York, New York, NY. pp 3-14
8. Okamoto, Y., Bernstein, J. D., and Shikano, S. (2013) Role of C-terminal membrane-proximal basic residues in cell surface trafficking of HIV coreceptor GPR15 protein. *J Biol Chem* **288**, 9189-9199
9. Szul, T., and Sztul, E. (2011) COPII and COPI traffic at the ER-Golgi interface. *Physiology (Bethesda)* **26**, 348-364
10. Vembar, S. S., and Brodsky, J. L. (2008) One step at a time: endoplasmic reticulum-associated degradation. *Nat Rev Mol Cell Biol* **9**, 944-957
11. Brandizzi, F., and Barlowe, C. (2013) Organization of the ER-Golgi interface for membrane traffic control. *Nat Rev Mol Cell Biol* **14**, 382-392
12. Michelsen, K., Yuan, H., and Schwappach, B. (2005) Hide and run. Arginine-based endoplasmic-reticulum-sorting motifs in the assembly of heteromultimeric membrane proteins. *EMBO Rep* **6**, 717-722
13. Hermosilla, R., Oueslati, M., Donalies, U., Schonenberger, E., Krause, E., Oksche, A., Rosenthal, W., and Schulein, R. (2004) Disease-causing V(2) vasopressin receptors are retained in different compartments of the early secretory pathway. *Traffic* **5**, 993-1005
14. Jackson, C. L. (2009) Mechanisms of transport through the Golgi complex. *J Cell Sci* **122**, 443-452
15. Banfield, D. K. (2011) Mechanisms of protein retention in the Golgi. *Cold Spring Harb Perspect Biol* **3**, a005264
16. Guo, Y., Sirkis, D. W., and Schekman, R. (2014) Protein sorting at the trans-Golgi network. *Annu Rev Cell Dev Biol* **30**, 169-206
17. Wieffer, M., Maritzen, T., and Haucke, V. (2009) SnapShot: endocytic trafficking. *Cell* **137**, 382 e381-383
18. Mayor, S., and Pagano, R. E. (2007) Pathways of clathrin-independent endocytosis. *Nat Rev Mol Cell Biol* **8**, 603-612
19. Doherty, G. J., and McMahon, H. T. (2009) Mechanisms of endocytosis. *Annu Rev Biochem* **78**, 857-902
20. Mellman, I. (2006) Endosomes Come of Age. in *Endosomes*, Springer New York, New York, NY. pp 1-13
21. Pattni, K., and Stenmark, H. (2006) Protein Sorting in Endosomes. in *Endosomes*, Springer New York, New York, NY. pp 76-88

22. McMahon, H. T., and Boucrot, E. (2011) Molecular mechanism and physiological functions of clathrin-mediated endocytosis. *Nat Rev Mol Cell Biol* **12**, 517-533
23. Cai, H., Reinisch, K., and Ferro-Novick, S. (2007) Coats, tethers, Rabs, and SNAREs work together to mediate the intracellular destination of a transport vesicle. *Dev Cell* **12**, 671-682
24. Rothnie, A., Clarke, A. R., Kuzmic, P., Cameron, A., and Smith, C. J. (2011) A sequential mechanism for clathrin cage disassembly by 70-kDa heat-shock cognate protein (Hsc70) and auxilin. *Proc Natl Acad Sci U S A* **108**, 6927-6932
25. Sato, K., and Nakano, A. (2007) Mechanisms of COPII vesicle formation and protein sorting. *FEBS Lett* **581**, 2076-2082
26. Teasdale, R. D., and Jackson, M. R. (1996) Signal-mediated sorting of membrane proteins between the endoplasmic reticulum and the golgi apparatus. *Annu Rev Cell Dev Biol* **12**, 27-54
27. Barlowe, C. (2003) Signals for COPII-dependent export from the ER: what's the ticket out? *Trends Cell Biol* **13**, 295-300
28. Mancias, J. D., and Goldberg, J. (2005) Exiting the endoplasmic reticulum. *Traffic* **6**, 278-285
29. Pandey, K. N. (2010) Small peptide recognition sequence for intracellular sorting. *Curr Opin Biotechnol* **21**, 611-620
30. Hurley, J. H., and Stenmark, H. (2011) Molecular mechanisms of ubiquitin-dependent membrane traffic. *Annu Rev Biophys* **40**, 119-142
31. Kurten, R. C. (2003) Sorting motifs in receptor trafficking. *Adv Drug Deliv Rev* **55**, 1405-1419
32. Traub, L. M. (2009) Tickets to ride: selecting cargo for clathrin-regulated internalization. *Nat Rev Mol Cell Biol* **10**, 583-596
33. Sobhy, H. (2016) A Review of Functional Motifs Utilized by Viruses. *Proteomes* **4**
34. Nyfeler, B., Zhang, B., Ginsburg, D., Kaufman, R. J., and Hauri, H. P. (2006) Cargo selectivity of the ERGIC-53/MCFD2 transport receptor complex. *Traffic* **7**, 1473-1481
35. Ma, D., Taneja, T. K., Hagen, B. M., Kim, B. Y., Ortega, B., Lederer, W. J., and Welling, P. A. (2011) Golgi export of the Kir2.1 channel is driven by a trafficking signal located within its tertiary structure. *Cell* **145**, 1102-1115
36. Kelly, B. T., McCoy, A. J., Spate, K., Miller, S. E., Evans, P. R., Honing, S., and Owen, D. J. (2008) A structural explanation for the binding of endocytic dileucine motifs by the AP2 complex. *Nature* **456**, 976-979
37. Ma, W., and Goldberg, J. (2013) Rules for the recognition of dilysine retrieval motifs by coatomer. *EMBO J* **32**, 926-937
38. Michelsen, K., Schmid, V., Metz, J., Heusser, K., Liebel, U., Schwede, T., Spang, A., and Schwappach, B. (2007) Novel cargo-binding site in the beta and delta subunits of coatomer. *J Cell Biol* **179**, 209-217
39. Bonifacino, J. S., and Traub, L. M. (2003) Signals for sorting of transmembrane proteins to endosomes and lysosomes. *Annu Rev Biochem* **72**, 395-447
40. Zarei, M. M., Eghbali, M., Alioua, A., Song, M., Knaus, H. G., Stefani, E., and Toro, L. (2004) An endoplasmic reticulum trafficking signal prevents surface expression of a voltage- and Ca2+-activated K+ channel splice variant. *Proc Natl Acad Sci U S A* **101**, 10072-10077
41. Parmar, H. B., Barry, C., Kai, F., and Duncan, R. (2014) Golgi complex-plasma membrane trafficking directed by an autonomous, tribasic Golgi export signal. *Mol Biol Cell* **25**, 866-878
42. Preuss, M. L., Weidman, P., and Nielsen, E. (2009) How We Study Protein Transport. in *Trafficking Inside Cells: Pathways, Mechanisms and Regulation*, Springer New York, New York, NY. pp 15-41
43. Kozik, P., Francis, R. W., Seaman, M. N., and Robinson, M. S. (2010) A screen for endocytic motifs. *Traffic* **11**, 843-855

44. Hurt, C. M., Ho, V. K., and Angelotti, T. (2013) Systematic and quantitative analysis of G protein-coupled receptor trafficking motifs. *Methods Enzymol* **521**, 171-187
45. Shikano, S., Coblitz, B., Sun, H., and Li, M. (2005) Genetic isolation of transport signals directing cell surface expression. *Nat Cell Biol* **7**, 985-992
46. Grishin, A., Li, H., Levitan, E. S., and Zaks-Makhina, E. (2006) Identification of gamma-aminobutyric acid receptor-interacting factor 1 (TRAK2) as a trafficking factor for the K+ channel Kir2.1. *J Biol Chem* **281**, 30104-30111
47. Kozik, P., Hodson, N. A., Sahlender, D. A., Simecek, N., Soromani, C., Wu, J., Collinson, L. M., and Robinson, M. S. (2013) A human genome-wide screen for regulators of clathrin-coated vesicle formation reveals an unexpected role for the V-ATPase. *Nat Cell Biol* **15**, 50-60
48. Kolb, A. R., Needham, P. G., Rothenberg, C., Guerriero, C. J., Welling, P. A., and Brodsky, J. L. (2014) ESCRT regulates surface expression of the Kir2.1 potassium channel. *Mol Biol Cell* **25**, 276-289
49. Kuryshev, Y. A., Ficker, E., Wang, L., Hawryluk, P., Dennis, A. T., Wible, B. A., Brown, A. M., Kang, J., Chen, X. L., Sawamura, K., Reynolds, W., and Rampe, D. (2005) Pentamidine-induced long QT syndrome and block of hERG trafficking. *J Pharmacol Exp Ther* **312**, 316-323
50. Kim Chiaw, P., Huan, L. J., Gagnon, S., Ly, D., Sweezey, N., Rotin, D., Deber, C. M., and Bear, C. E. (2009) Functional rescue of DeltaF508-CFTR by peptides designed to mimic sorting motifs. *Chem Biol* **16**, 520-530
51. Amaral, M. D. (2005) Processing of CFTR: traversing the cellular maze--how much CFTR needs to go through to avoid cystic fibrosis? *Pediatr Pulmonol* **39**, 479-491
52. Gietz, R. D., and Schiestl, R. H. (2007) High-efficiency yeast transformation using the LiAc/SS carrier DNA/PEG method. *Nat Protoc* **2**, 31-34
53. Kushnirov, V. V. (2000) Rapid and reliable protein extraction from yeast. *Yeast* **16**, 857-860
54. Gibson, D. G. (2009) Synthesis of DNA fragments in yeast by one-step assembly of overlapping oligonucleotides. *Nucleic Acids Res* **37**, 6984-6990
55. Chao, G., Lau, W. L., Hackel, B. J., Sazinsky, S. L., Lippow, S. M., and Wittrup, K. D. (2006) Isolating and engineering human antibodies using yeast surface display. *Nat Protoc* **1**, 755-768
56. Gera, N., Hussain, M., and Rao, B. M. (2013) Protein selection using yeast surface display. *Methods* **60**, 15-26
57. Cheng, T. H., Chang, C. R., Joy, P., Yablok, S., and Gartenberg, M. R. (2000) Controlling gene expression in yeast by inducible site-specific recombination. *Nucleic Acids Res* **28**, E108
58. Feyder, S., De Craene, J. O., Bar, S., Bertazzi, D. L., and Friant, S. (2015) Membrane trafficking in the yeast Saccharomyces cerevisiae model. *Int J Mol Sci* **16**, 1509-1525
59. Sychrova, H. (2004) Yeast as a model organism to study transport and homeostasis of alkali metal cations. *Physiol Res* **53 Suppl 1**, S91-98
60. Kolacna, L., Zimmermannova, O., Hasenbrink, G., Schwarzer, S., Ludwig, J., Lichtenberg-Frate, H., and Sychrova, H. (2005) New phenotypes of functional expression of the mKir2.1 channel in potassium efflux-deficient Saccharomyces cerevisiae strains. *Yeast* **22**, 1315-1323
61. Bendahhou, S., Donaldson, M. R., Plaster, N. M., Tristani-Firouzi, M., Fu, Y. H., and Ptacek, L. J. (2003) Defective potassium channel Kir2.1 trafficking underlies Andersen-Tawil syndrome. *J Biol Chem* **278**, 51779-51785
62. Ma, D., Tang, X. D., Rogers, T. B., and Welling, P. A. (2007) An andersen-Tawil syndrome mutation in Kir2.1 (V302M) alters the G-loop cytoplasmic K+ conduction pathway. *J Biol Chem* **282**, 5781-5789
63. Schwarzer, S., Kolacna, L., Lichtenberg-Frate, H., Sychrova, H., and Ludwig, J. (2008) Functional expression of the voltage-gated neuronal mammalian potassium channel rat ether a go-go1 in yeast. *FEMS Yeast Res* **8**, 405-413

64. Goldstein, S. A., Bockenhauer, D., O'Kelly, I., and Zilberberg, N. (2001) Potassium leak channels and the KCNK family of two-P-domain subunits. *Nat Rev Neurosci* **2**, 175-184
65. Boulkroun, S., Samson-Couterie, B., Golib-Dzib, J. F., Amar, L., Plouin, P. F., Sibony, M., Lefebvre, H., Louiset, E., Jeunemaitre, X., Meatchi, T., Benecke, A., Lalli, E., and Zennaro, M. C. (2011) Aldosterone-producing adenoma formation in the adrenal cortex involves expression of stem/progenitor cell markers. *Endocrinology* **152**, 4753-4763
66. Pei, L., Wiser, O., Slavin, A., Mu, D., Powers, S., Jan, L. Y., and Hoey, T. (2003) Oncogenic potential of TASK3 (Kcnk9) depends on K+ channel function. *Proc Natl Acad Sci U S A* **100**, 7803-7807
67. Barel, O., Shalev, S. A., Ofir, R., Cohen, A., Zlotogora, J., Shorer, Z., Mazor, G., Finer, G., Khateeb, S., Zilberberg, N., and Birk, O. S. (2008) Maternally inherited Birk Barel mental retardation dysmorphism syndrome caused by a mutation in the genomically imprinted potassium channel KCNK9. *Am J Hum Genet* **83**, 193-199
68. O'Kelly, I., Butler, M. H., Zilberberg, N., and Goldstein, S. A. (2002) Forward transport. 14-3-3 binding overcomes retention in endoplasmic reticulum by dibasic signals. *Cell* **111**, 577-588
69. Clarke, C. E., Veale, E. L., Green, P. J., Meadows, H. J., and Mathie, A. (2004) Selective block of the human 2-P domain potassium channel, TASK-3, and the native leak potassium current, IKSO, by zinc. *J Physiol* **560**, 51-62
70. Okamoto, Y., and Shikano, S. (2011) Phosphorylation-dependent C-terminal binding of 14-3-3 proteins promotes cell surface expression of HIV co-receptor GPR15. *J Biol Chem* **286**, 7171-7181
71. Zerangue, N., Schwappach, B., Jan, Y. N., and Jan, L. Y. (1999) A new ER trafficking signal regulates the subunit stoichiometry of plasma membrane K(ATP) channels. *Neuron* **22**, 537-548
72. Holton, K. L., Loder, M. K., and Melikian, H. E. (2005) Nonclassical, distinct endocytic signals dictate constitutive and PKC-regulated neurotransmitter transporter internalization. *Nat Neurosci* **8**, 881-888
73. Zaks-Makhina, E., Kim, Y., Aizenman, E., and Levitan, E. S. (2004) Novel neuroprotective K+ channel inhibitor identified by high-throughput screening in yeast. *Mol Pharmacol* **65**, 214-219
74. Baldwin, T. A., and Ostergaard, H. L. (2002) The protein-tyrosine phosphatase CD45 reaches the cell surface via golgi-dependent and -independent pathways. *J Biol Chem* **277**, 50333-50340
75. Dupont, N., Jiang, S., Pilli, M., Ornatowski, W., Bhattacharya, D., and Deretic, V. (2011) Autophagy-based unconventional secretory pathway for extracellular delivery of IL-1beta. *EMBO J* **30**, 4701-4711
76. Tang, W., Ruknudin, A., Yang, W. P., Shaw, S. Y., Knickerbocker, A., and Kurtz, S. (1995) Functional expression of a vertebrate inwardly rectifying K+ channel in yeast. *Mol Biol Cell* **6**, 1231-1240
77. Ma, D., Zerangue, N., Lin, Y. F., Collins, A., Yu, M., Jan, Y. N., and Jan, L. Y. (2001) Role of ER export signals in controlling surface potassium channel numbers. *Science* **291**, 316-319
78. Temsamani, J., Kubert, M., and Agrawal, S. (1995) Sequence identity of the n-1 product of a synthetic oligonucleotide. *Nucleic Acids Res* **23**, 1841-1844
79. Bass, J. J., Wilkinson, D. J., Rankin, D., Phillips, B. E., Szewczyk, N. J., Smith, K., and Atherton, P. J. (2017) An overview of technical considerations for Western blotting applications to physiological research. *Scand J Med Sci Sports* **27**, 4-25
80. Ciechanover, A. (2005) Intracellular protein degradation: from a vague idea thru the lysosome and the ubiquitin-proteasome system and onto human diseases and drug targeting. *Cell Death Differ* **12**, 1178-1190
81. Ruggiano, A., Foresti, O., and Carvalho, P. (2014) Quality control: ER-associated degradation: protein quality control and beyond. *J Cell Biol* **204**, 869-879

82. Gassmann, M., Haller, C., Stoll, Y., Abdel Aziz, S., Biermann, B., Mosbacher, J., Kaupmann, K., and Bettler, B. (2005) The RXR-type endoplasmic reticulum-retention/retrieval signal of GABAB1 requires distant spacing from the membrane to function. *Mol Pharmacol* **68**, 137-144
83. Shikano, S., and Li, M. (2003) Membrane receptor trafficking: evidence of proximal and distal zones conferred by two independent endoplasmic reticulum localization signals. *Proc Natl Acad Sci U S A* **100**, 5783-5788
84. Jackson, M. R., Nilsson, T., and Peterson, P. A. (1993) Retrieval of transmembrane proteins to the endoplasmic reticulum. *J Cell Biol* **121**, 317-333
85. Gomez-Navarro, N., and Miller, E. (2016) Protein sorting at the ER-Golgi interface. *J Cell Biol* **215**, 769-778
86. Heffernan, L. F., and Simpson, J. C. (2014) The trials and tubule-ations of Rab6 involvement in Golgi-to-ER retrograde transport. *Biochem Soc Trans* **42**, 1453-1459
87. Dutta, D., and Donaldson, J. G. (2012) Search for inhibitors of endocytosis: Intended specificity and unintended consequences. *Cell Logist* **2**, 203-208
88. Varkevisser, R., Houtman, M. J., Waasdorp, M., Man, J. C., Heukers, R., Takanari, H., Tieland, R. G., van Bergen En Henegouwen, P. M., Vos, M. A., and van der Heyden, M. A. (2013) Inhibiting the clathrin-mediated endocytosis pathway rescues K(IR)2.1 downregulation by pentamidine. *Pflugers Arch* **465**, 247-259
89. Salah, Z., Alian, A., and Aqeilan, R. I. (2012) WW domain-containing proteins: retrospectives and the future. *Front Biosci (Landmark Ed)* **17**, 331-348
90. Lecker, S. H., Goldberg, A. L., and Mitch, W. E. (2006) Protein degradation by the ubiquitin-proteasome pathway in normal and disease states. *J Am Soc Nephrol* **17**, 1807-1819
91. Clague, M. J., and Urbe, S. (2010) Ubiquitin: same molecule, different degradation pathways. *Cell* **143**, 682-685
92. Butterworth, M. B., Edinger, R. S., Frizzell, R. A., and Johnson, J. P. (2009) Regulation of the epithelial sodium channel by membrane trafficking. *Am J Physiol Renal Physiol* **296**, F10-24
93. Wang, H., Traub, L. M., Weixel, K. M., Hawryluk, M. J., Shah, N., Edinger, R. S., Perry, C. J., Kester, L., Butterworth, M. B., Peters, K. W., Kleyman, T. R., Frizzell, R. A., and Johnson, J. P. (2006) Clathrin-mediated endocytosis of the epithelial sodium channel. Role of epsin. *J Biol Chem* **281**, 14129-14135
94. Lee, I. H., Campbell, C. R., Song, S. H., Day, M. L., Kumar, S., Cook, D. I., and Dinudom, A. (2009) The activity of the epithelial sodium channels is regulated by caveolin-1 via a Nedd4-2-dependent mechanism. *J Biol Chem* **284**, 12663-12669
95. Malik, B., Price, S. R., Mitch, W. E., Yue, Q., and Eaton, D. C. (2006) Regulation of epithelial sodium channels by the ubiquitin-proteasome proteolytic pathway. *Am J Physiol Renal Physiol* **290**, F1285-1294
96. Lv, Y., Zhang, K., and Gao, H. (2014) Paip1, an effective stimulator of translation initiation, is targeted by WWP2 for ubiquitination and degradation. *Mol Cell Biol* **34**, 4513-4522
97. Popoff, V., Adolf, F., Brugger, B., and Wieland, F. (2011) COPI budding within the Golgi stack. *Cold Spring Harb Perspect Biol* **3**, a005231
98. Daro, E., Sheff, D., Gomez, M., Kreis, T., and Mellman, I. (1997) Inhibition of endosome function in CHO cells bearing a temperature-sensitive defect in the coatomer (COPI) component epsilon-COP. *J Cell Biol* **139**, 1747-1759
99. Gabriely, G., Kama, R., and Gerst, J. E. (2007) Involvement of specific COPI subunits in protein sorting from the late endosome to the vacuole in yeast. *Mol Cell Biol* **27**, 526-540
100. Reilly, B. A., Kraynack, B. A., VanRheenen, S. M., and Waters, M. G. (2001) Golgi-to-endoplasmic reticulum (ER) retrograde traffic in yeast requires Dsl1p, a component of the ER target site that interacts with a COPI coat subunit. *Mol Biol Cell* **12**, 3783-3796

101. Boettner, D. R., Chi, R. J., and Lemmon, S. K. (2011) Lessons from yeast for clathrin-mediated endocytosis. *Nat Cell Biol* **14**, 2-10

APPENDICES

Parts of this thesis have been previously published in:

Bernstein, J. D., Okamoto, Y., Kim, M., and Shikano, S. (2013) Potential use of potassium efflux-deficient yeast for studying trafficking signals and potassium channel functions. FEBS Open Bio 3, 196-203

FEBS PRESS
science publishing by scientists

FEBS Open Bio

FEBS Open Bio - Open Access License and Copyright

UIC GRADUATE COLLEGE
UNIVERSITY OF ILLINOIS AT CHICAGO
606 University Hall, 601 S Morgan St (MC 192), Chicago, IL 60607-7106, http://grad.uic.edu

iThenticate Report Form

Information should be typed and then saved as a pdf. The completed form must be submitted to the defense committee with your thesis/dissertation. This form will also be submitted to the Graduate College with the final thesis/dissertation document and after successful defense.

The student is the sole author of their thesis or dissertation, and it is the student's responsibility to ensure that all information in their document is correctly cited and attributed, and that proper copyright permissions have been obtained. The *iThenticate* screening process should be only one part of their effort towards this end. For example, *iThenticate* cannot detect images and figures taken from other sources, texts in languages other than English, and user error (e.g. inappropriate exclusions).

Student Name (Last, First M.): **Brenstein, Joshua D.**
Student UIN: **651485371**
Student Email Address: **jberns4@uic.edu**
Graduate Program Name (e.g., Biological Sciences): **Biochemistry and Molecular Genetics**
Degree Sought: **PhD**
Program Code (see http://catalog.uic.edu/gcat/degree-programs/grad-prof-degree-programs/): 20FS**4050PHD**
Thesis/Dissertation Title (must match title as submitted on the *Committee Recommendation Form* and the title page of the thesis/dissertation – use mixed case): **Identification and Characterization of Signal Motifs that Regulate Surface Levels of Membrane Proteins**

- Percent overlap in the initial *iThenticate* report -- before any review (e.g., 50%): **19**
- Percent overlap in the *iThenticate* report -- after manual review to exclude trivial phrase overlaps and quoting/paraphrasing with proper citation (this is before editing your manuscript by adding citations, quote marks, correctly paraphrasing, etc.): **0**

If actual edits to the manuscript are required (such as adding citations, quote marks, rephrasing, etc.), the new version of the manuscript is uploaded to *iThenticate*.

- Percent overlap in the *iThenticate* report -- after manual review, and after trivial overlaps were excluded, following edits to exclude overlaps of concern, i.e. adding citations, quote marks, correctly paraphrasing, etc. (if no edits to the manuscript were required, type "not applicable"): **not applicable**
- Have you included your own previously published work (Yes/No)? **yes**
- If you have included your own previously published work, have you referenced it correctly according to the publisher's guidelines (Yes/No/Not Applicable)? **yes**
- If you have included your own previously published work, did you include the publisher's copyright permission statement or written permission as an appendix (Yes/No/Not Applicable)? **yes**
- Have you included collaborative work in your thesis/dissertation (Yes/No)? **yes**
- If you have included collaborative work in your thesis/dissertation, have you included a "Contribution of Authors" paragraph as described in the *Introduction to Screening Your Thesis or Dissertation* (Yes/No/Not Applicable)? **yes**

- Provide a brief statement to indicate what was changed in the editing of your manuscript including what you added to clarify contributions, previous publication and what you did to ensure proper citation and attribution (if no edits to the manuscript were required, type "not applicable"): **Dissertation uploaded with the references removed and received an initial iThenticate report of 19% overlap. Set the word limit to 15 and selected to exclude methods reducing overlap to 14%. I then excluded my publication reducing overlap to 4%. The remaining overlaps were either references/citations to my publication or matching phrases in the materials and methods. I excluded these overlaps and achieved a 0% overlap score**

VITA

NAME: Joshua D. Bernstein

EDUCATION: PhD, Biochemistry and Molecular Genetics, University of Illinois at Chicago College of Medicine, Chicago, IL, 2017

B.A., Biology, Yeshiva University, New York, NY, 2009

RESEARCH EXPERIENCE: Graduate Research Assistant, Laboratory of Dr. Sojin Shikano, Department of Biochemistry and Molecular Genetics, University of Illinois at Chicago, Chicago, Illinois, May 2011 – September 2016

Associate Researcher, Laboratory of Dr. Shoshana Yakar, Department of Endocrinology, Diabetes and Bone Diseases, Mount Sinai School of Medicine, New York, NY, August 2010 – August 2011

Research Assistant, Laboratory of Dr. Sumanta Goswami, Department of Biology, Yeshiva University, New York, NY, June 2009 – August 2010

PUBLICATIONS: **Bernstein, J. D.**, Okamoto, Y., Kim, M. & Shikano, S. Potential use of potassium efflux-deficient yeast for studying trafficking signals and potassium channel functions. FEBS Open Bio 3, 196–203 (2013).

Okamoto, Y., **Bernstein, J. D.** & Shikano, S. Role of C-terminal Membrane-proximal Basic Residues in Cell Surface Trafficking of HIV Coreceptor GPR15 Protein. Journal of Biological Chemistry 288, 9189–9199 (2013).

Song, Y., Aglipay, J. A., **Bernstein, J. D.**, Goswami, S. & Stanley, P. The Bisecting GlcNAc on N-Glycans Inhibits Growth Factor Signaling and Retards Mammary Tumor Progression. Cancer Research 70, 3361–3371 (2010).

POSTERS: **Joshua Bernstein**, Yukari Okamoto, Sojin Shikano. A Novel Yeast-Based Screening System Identifies Signal Motifs That Regulate Membrane Protein Trafficking. Presented at Experimental Biology Meeting, April 2017, Chicago

Joshua Bernstein, Yukari Okamoto, Sojin Shikano. A Yeast-Based Screening for Signal Motifs That Regulate Membrane Protein Trafficking. Presented at Chicago Symposium on Cell Signaling, May 2015, Northwestern University

Joshua Bernstein, Yukari Okamoto, Sojin Shikano. A Yeast-Based Screening for Signal Motifs That Regulate Membrane Protein Trafficking. Poster to be presented at Student Research Forum, April 2015, UIC

Joshua Bernstein, Yukari Okamoto, Sojin Shikano. A Yeast-Based Screening for Signal Motifs That Regulate Membrane Protein Trafficking. Poster to be presented at Experimental Biology Meeting, March 2015, Boston

Joshua Bernstein, Yukari Okamoto, Sojin Shikano. Development of a New Yeast-Based Screen to Identify Membrane Trafficking Signals. Poster presented at Department Retreat, Biochemistry and Molecular Genetics, Aug 2013, Lake Geneva

Yukari Okamoto, **Joshua Bernstein**, Sojin Shikano. Role of Membrane-Proximal Basic Residues in Cell Surface Trafficking of GPR15. Poster presented at Experimental Biology Meeting, April 2013, Boston

Joshua Bernstein, Yukari Okamoto, Sojin Shikano. Role of Membrane-Proximal Basic Residues in Cell Surface Trafficking of GPR15. Poster presented at Department Retreat, Biochemistry and Molecular Genetics, Aug 2012, Lake Geneva

TEACHING: Rotation student mentor, Department of Biochemistry and Molecular Genetics, University of Illinois at Chicago, Chicago, Illinois, 2012-2017

Undergraduate student mentor, Department of Biochemistry and Molecular Genetics, University of Illinois at Chicago, Chicago, Illinois, 2014

` Teaching Assistant – Medical Biochemistry and Nutrition (BMS648) Department of Biochemistry and Molecular Genetics, University of Illinois at Chicago, Chicago, Illinois, 2013